

# Technical Program for Long-Term Management of Canada's Used Nuclear Fuel – Annual Report 2020

NWMO-TR-2021-01

December 2021

**Nuclear Waste Management Organization (S. Briggs, ed.)**

**nwmo**

NUCLEAR WASTE  
MANAGEMENT  
ORGANIZATION

SOCIÉTÉ DE GESTION  
DES DÉCHETS  
NUCLÉAIRES



**Nuclear Waste Management Organization**  
22 St. Clair Avenue East, 4<sup>th</sup> Floor  
Toronto, Ontario  
M4T 2S3  
Canada

Tel: 416-934-9814  
Web: [www.nwmo.ca](http://www.nwmo.ca)

**Technical Program for Long-Term Management of  
Canada's Used Nuclear Fuel – Annual Report 2020**

**NWMO-TR-2021-01**

December 2021

**Nuclear Waste Management Organization (S. Briggs, ed.)**

**Document History**

Title:	Technical Program for Long-Term Management of Canada's Used Nuclear Fuel – Annual Report 2020		
Report Number:	NWMO-TR-2021-01		
Revision:	R000	Date:	December 2021
Nuclear Waste Management Organization			
Authored by:	NWMO (S. Briggs, ed.)		
Reviewed by:	P. Gierszewski		
Approved by:	C. Boyle		



**ABSTRACT**

**Title:** Technical Program for the Long-Term Management of Canada's Used Nuclear Fuel – Annual Report 2020  
**Report No.:** NWMO-TR-2021-01  
**Author(s):** NWMO (S. Briggs, ed.)  
**Company:** Nuclear Waste Management Organization  
**Date:** December 2021

**Abstract**

This report is a summary of activities and progress in 2020 for the Nuclear Waste Management Organization's Technical Program. The primary purpose of the Technical Program is to support the implementation of Adaptive Phased Management (APM), Canada's approach for the long-term management of used nuclear fuel.

The work continued to develop the repository design; to understand the engineered barrier, geological and other processes important to the safety case; and to assess the candidate siting areas.

NWMO continued to participate in international research activities, including projects associated with the Mont Terri Underground Rock Laboratory, the SKB Äspö Hard Rock Laboratory, the Greenland ICE Project, the OECD (Organisation for Economic Co-operation and Development) Nuclear Energy Agency and BIOPROTA.

NWMO's technical program supported technical presentations at national and international conferences, issued 7 NWMO technical reports and published 27 journal articles.



**TABLE OF CONTENTS**

	<b><u>Page</u></b>
<b>ABSTRACT .....</b>	<b>iv</b>
<b>1 INTRODUCTION.....</b>	<b>1</b>
<b>2 OVERVIEW OF NWMO TECHNICAL PROGRAMS .....</b>	<b>3</b>
<b>3 REPOSITORY ENGINEERING AND DESIGN.....</b>	<b>5</b>
<b>3.1 USED FUEL TRANSPORTATION.....</b>	<b>5</b>
3.1.1 Used Fuel Transportation System Development.....	5
<b>3.2 USED FUEL PACKAGING PLANT .....</b>	<b>6</b>
3.2.1 Receipt of UFTP/BTP and Used Fuel Module/Basket Unloading.....	7
3.2.2 Used Fuel Inspection and UFC Loading.....	8
3.2.3 UFC Welding Cell.....	9
3.2.4 UFC Decontamination Cell.....	11
3.2.5 UFC Copper Application and Machining Cell .....	11
3.2.6 UFC Copper Annealing / NDE Work Cell .....	12
3.2.7 Buffer Box Storage, Handling & Dispatch Area .....	13
<b>3.3 MINING AND REPOSITORY ENGINEERING .....</b>	<b>14</b>
3.3.1 Emplacement Equipment .....	14
3.3.2 Emplacement Plan .....	14
3.3.3 Thermal Modeling of the UFCs when placed in the DGR Base Case .....	21
3.3.4 Preliminary Construction Plan for an APM DGR .....	23
3.3.5 Excavated Rock Management Area.....	23
3.3.6 Sealing for Decommissioning and Closure.....	24
3.3.7 Reference DGR Cost Update for Shafts, Headframes and Hoisting Systems ....	24
<b>4 ENGINEERED BARRIER SYSTEM .....</b>	<b>25</b>
<b>4.1 CONTAINER DURABILITY .....</b>	<b>25</b>
4.1.1 UFC Design.....	26
4.1.2 UFC Serial Production Campaign .....	27
4.1.3 UFC Welding Technology Development .....	28
4.1.4 UFC Copper Coating Development.....	31
4.1.5 UFC Non-Destructive Examination.....	38
4.1.6 UFC Material Testing .....	42
<b>4.2 COPPER DURABILITY .....</b>	<b>42</b>
4.2.1 Used Fuel Container Corrosion Studies.....	42
4.2.2 Internal Corrosion of UFC.....	47
4.2.3 Microbial Studies .....	48
4.2.4 Field Deployments.....	49
4.2.5 Corrosion Modelling .....	51
<b>4.3 PLACEMENT ROOM SEALS AND OTHERS .....</b>	<b>51</b>
4.3.1 Reactive Transport Modelling of Concrete-Bentonite Interactions .....	51
4.3.2 Gas-Permeable Seal Test (GAST).....	52
4.3.3 DECOVALEX .....	52
4.3.4 Shaft Seal Properties .....	57
4.3.5 Thermo-hydro-mechanical Modelling of NWMO Placement Room.....	58
4.3.6 Coupled Thermo-hydro-mechanical Benchtop Experiments.....	58

<b>5</b>	<b>GEOSCIENCE .....</b>	<b>61</b>
<b>5.1</b>	<b>GEOSPHERE PROPERTIES.....</b>	<b>61</b>
5.1.1	Geological Setting and Structure.....	61
5.1.2	Hydrogeological Properties .....	65
5.1.3	Hydrogeochemical Conditions.....	69
5.1.4	Transport Properties of the Rock Matrix.....	75
5.1.5	Geomechanical and Thermal Properties.....	78
<b>5.2</b>	<b>LONG-TERM GEOSPHERE STABILITY .....</b>	<b>86</b>
5.2.1	Long Term Climate Change – Glaciation .....	86
5.2.2	Groundwater System Stability and Evolution .....	87
5.2.3	Seismicity .....	88
5.2.4	Geomechanical Stability of the Repository.....	90
<b>6</b>	<b>REPOSITORY SAFETY .....</b>	<b>93</b>
<b>6.1</b>	<b>WASTE INVENTORY.....</b>	<b>93</b>
6.1.1	Physical Inventory .....	93
6.1.2	Radionuclide Inventory .....	94
6.1.3	Chemical Composition .....	94
6.1.4	Irradiation History .....	94
<b>6.2</b>	<b>WASTEFORM DURABILITY .....</b>	<b>94</b>
6.2.1	Used Fuel Dissolution .....	94
6.2.2	Solubility .....	95
<b>6.3</b>	<b>BIOSPHERE .....</b>	<b>97</b>
6.3.1	General Approach – Post-closure Biosphere Modelling and Data .....	97
6.3.2	Participation in BIOPROTA .....	97
<b>6.4</b>	<b>SAFETY ASSESSMENT .....</b>	<b>98</b>
6.4.1	Pre-closure Safety .....	98
6.4.2	Post-closure Safety .....	101
<b>6.5</b>	<b>MONITORING .....</b>	<b>103</b>
6.5.1	Knowledge Management.....	103
<b>7</b>	<b>SITE ASSESSMENT .....</b>	<b>105</b>
<b>7.1</b>	<b>IGNACE .....</b>	<b>105</b>
7.1.1	Geological Investigation .....	105
7.1.2	Environmental Assessment.....	105
<b>7.2</b>	<b>SOUTH BRUCE .....</b>	<b>106</b>
7.2.1	Geological Investigation .....	106
7.2.2	Environmental Assessment.....	107
	<b>REFERENCES .....</b>	<b>109</b>
	<b>APPENDIX A: NWMO TECHNICAL REPORTS AND REFEREED JOURNAL ARTICLES ...</b>	<b>123</b>
<b>A.1</b>	<b>NWMO TECHNICAL REPORTS.....</b>	<b>124</b>
<b>A.2</b>	<b>REFEREED JOURNAL ARTICLES.....</b>	<b>125</b>

**LIST OF TABLES**

	<b><u>Page</u></b>
Table 4-1: 2020 UFC Serial Production Results .....	27
Table 6-1: Typical Physical Attributes Relevant to Long-term Safety .....	93

**LIST OF FIGURES**

	<b><u>Page</u></b>
Figure 1-1: Illustration of a Deep Geological Repository Reference Design.....	2
Figure 1-2: Interested Community Status as of 31 December 2020 .....	2
Figure 3-1: Interim Storage Facilities and Potential Siting Areas.....	5
Figure 3-2: Concept Layout of the Used Fuel Packaging Plant (UFPP). The Key Acronyms Denoting Processing Areas and Components Are: CCA (Contamination-controlled Area), Non-CCA (non-contaminated control area), BB (Buffer Box), BTP (Basket Transportation Package), UFTP (Used Fuel Transportation Package), UFC (Used Fuel Container), NDE (Non-destructive Examination), and RMSA (Radioactive Material Storage Area) .....	7
Figure 3-3: The Used Fuel Transportation Package (UFTP)/Basket Transportation Package (BTP) Shipping & Receiving Area .....	8
Figure 3-4: Fuel Transfer into a Used Fuel Container (Top View): (a) Equipment to Operate the Push Ram that Penetrates the Work Cell Shielding Wall, (b) A Used Fuel Module on Positioning Table in Shielded Work Cell and (c) Bundles pushed by Ram into the UFC Located in the Shielded Work Cell. ....	9
Figure 3-5: Typical Work Cell Arrangement with Various Process Worktables .....	10
Figure 3-6: (a)The Welding and Preheat Worktable and (b) Weld Non-Destructive Examination Worktable .....	10
Figure 3-7: Used Fuel Container Decontamination Cell (Top View) .....	11
Figure 3-8: Copper Cold Spray and Copper Annealing Worktable .....	12
Figure 3-9: Copper Annealing Worktable.....	12
Figure 3-10: Buffer Box (BB) Storage, Handling and Dispatch Area .....	13
Figure 3-11: Highly Compacted Bentonite (HCB) Block .....	15
Figure 3-12: Shaped Highly Compacted Bentonite (HCB) Block.....	15
Figure 3-13: Buffer Box Assembly .....	16
Figure 3-14: Vacuum Lift Highly Compacted Bentonite (HCB) .....	16
Figure 3-15: Vacuum Lift Used Fuel Container (UFC).....	17
Figure 3-16: Simulated Emplacement Room with Faux Rock Walls Simulated Drill and Blast Profile: (a) Exterior Steel Frame Approximately 3m x 3m x 15m in Size, (b) Interior with Faux Rock Walls and (c) Actual Blast Profile from Underground Research Laboratory .....	18
Figure 3-17: Buffer Box Attachment Installed on Versa Lift 25/35 .....	19
Figure 3-18: Fork Pocket Brick Delivery Equipment .....	20
Figure 3-19: Gapfill Delivery Equipment (Auger System) .....	21
Figure 3-20: Isometric View of the Used Fuel Container Layout in a Sedimentary Rock Deep Geological Repository (DGR).....	22
Figure 3-21: Example Buffer Box Assembly for the Used Fuel Container .....	23
Figure 4-1: Illustration of the Used Fuel Container Reference Design .....	25
Figure 4-2: Prototype Used Fuel Container Reference Design .....	26
Figure 4-3: Prototype 2018 Used Fuel Container (UFC) Insert Design .....	26
Figure 4-4: Fabricated Dummy Cast Iron Insert.....	28
Figure 4-5: Dummy Insert Being Loaded into Used Fuel Container (UFC) Lower Assembly Using a Custom Handling Tool at Welding Contractor Novika Solutions .....	28

Figure 4-6: Weld Cross-section of LP-GMAW Sample .....	29
Figure 4-7: Comparison of (a) Hybrid Laser Arc Welding (HLAW) and (b) Laser Preheated-Gas Metal Arc Weld (LP-GMAW) .....	30
Figure 4-8: Weld Cross-section of LP-GMAW Sample .....	30
Figure 4-9: Hardness (HV) Map Performed on Cross-section of Laser Preheated g-Gas Metal Arc Welding Partial Penetration Weld. Hardness Indent Spacing 0.5 mm. Hardness Levels on Weld, Heat Affected Zone and Base Metal All Meet Specification Requirements .....	31
Figure 4-10: Equiaxed Microstructure of Acid Copper Deposit – Growth Direction from Left to Right.....	32
Figure 4-11: Mechanical (Tensile) Testing: (a) 1 mm Thick Tensile Specimens Showing Fracture in the Gauge Length and (b) Example Stress Strain Curves .....	32
Figure 4-12: Tube Trials Evaluated the Effect of Steel Substrate Surface Finishes: (a) Turned – 3.2 $\mu\text{m Ra}$ , (b) Turned – 1.6 $\mu\text{m Ra}$ , and (c) Abrasively Polished.....	33
Figure 4-13: Upper Hemi-head Optimization Run Results with Machined (turned) 1.6 $\mu\text{m Ra}$ Steel Finish: (a) with “Outer” Shield Design and (b) with “Inner” Shield Design After “Outer” Shield Removal .....	34
Figure 4-14: Development of Laser Ablation Technique on Short Pipe Segments Using the Pulsed Laser Technique: (a) Short Pipe Segment Showing Heavy Oxidation and (b) Cleaned Surface Using Laser Ablation .....	35
Figure 4-15: Demonstration Trial of Laser Ablation Technique on the Lower Assembly: (a) In Process and (b) Final Surface After Laser Ablation and Before Laser Assisted Bond Layer Application.....	36
Figure 4-16: Demonstration Copper Coating Trial on the Lower Assembly: (a) Application of the Laser Assisted Bond Layer and (b) Final Coating After Build-up to Approximately 5 mm .....	36
Figure 4-17: Scanning Electron Microscopy (SEM)-Electron Back Scattered Diffraction (EBSD) Images of Cold Sprayed Copper Grain Orientation (top) and Grain Boundary Character Distribution (bottom): (a) As-sprayed and (b) After Heat Treatment at 350°C for 1 hr (Li et al., 2020).....	37
Figure 4-18: Optical Images of the Electrodeposited (ED) and Cold Spray (CS) Copper Junction: (a) As-sprayed and (b) After Heat Treatment at 350°C for 1 hr (Tam et al., 2020).....	38
Figure 4-19: Finite Element Analysis (FEA) Modelling of Plastic Zones (Colored Areas) Between the Partial Penetration Weld Root and Pores: Subsurface Pores in Case 1, 2 and 3, and Surface Breaking Pores in Case 4 and 5.....	39
Figure 4-20: Hemi-head Scanning Mechanism with Eddy Current Probe Attached. ....	40
Figure 4-21: Lower Assembly/Used Fuel Container (UFC) Scanning Mechanism with Ultrasonic Probe Attached .....	41
Figure 4-22: Brittle-to-Ductile Transition Curve (Percent Shear vs. Temperature) of the As- Deposited Weld Material in the Used Fuel Container (UFC) .....	42
Figure 4-23: (a) Schematic of Test Cells for Anoxic Copper Corrosion Investigations at CanmetMATERIALS; (b) Photo of Copper Specimens in a Test Cell During an Experiment; (c) Calculated Copper Corrosion Rates Based on Hydrogen Measurements for Two Deionised Cells and One Concentrated Brine Cell Over Approximately Four and a Half Years (Senior et al. 2020b) .....	45
Figure 4-24: Copper Corrosion Mechanism: a) In the Absence of Ionizing Radiation with Chemically Added $\text{H}_2\text{O}_2$ , and b) In the Presence of Radiation (white arrows indicate electron transfer reactions) .....	47
Figure 4-25: (a) Components of a Pressure Vessel for Ex-situ Microbiological and Corrosion Analyses; (b) A Cored Bentonite Plug Following Water Exposure in a Pressure Vessel	

and Prior to Sample Extraction for Analysis; (c) Schematic of a Pressure Vessel Indicating the Location of Copper Samples and Bentonite Samples Extracted for Microbiological and Water Analysis .....	49
Figure 4-26: (a) Photos of the Test Modules Containing Copper Embedded in Bentonite Clay on the Immersion Platform; (b) Recovery of Modules Following a 6-month Test Immersion in the Pacific Ocean .....	50
Figure 4-27: (a) External View of Borehole Test Module Measuring Approximately 50 cm in Length; (b) Internal View of Test Module Showing Sintered Steel Mesh Which Lines the Modules; (c) Custom Made Packers (black) and Supporting Equipment to Install the Borehole Experiments.....	50
Figure 4-28: Three-dimensional Layout of the TED Experiment Indicating Heaters and Instrument Boreholes (Armand et al. 2017) .....	53
Figure 4-29: Three-dimensional Layout of the ALC Experiment Indicating Heaters and Instrument Boreholes (Armand et al. 2017) .....	54
Figure 4-30: Pressure Evolution at the Sensor TED1253_PRE_01 .....	55
Figure 4-31: Diagram of the Facilities of the Cigéo Project .....	55
Figure 4-32: Temperature Evolution at Points A) P1 and B) P2 .....	56
Figure 4-33: Pore Pressure Evolution at Points A) P1 and B) P2.....	56
Figure 4-34: Heating Only Apparatus .....	58
Figure 4-35: Rendering of the Wetting Cell Design (A) Is the Water Reservoir, (B) Is the Test Cell, and (C) Is the Water Pump .....	59
Figure 4-36: Capacitive Based Moisture Sensor .....	60
Figure 5-1: Updated 3-D Lithostratigraphic Model of the Paleozoic Bedrock of Southwestern and Southcentral Ontario, Surficial Sediment Cover Removed (Carter et al. <i>in press</i> ) .....	62
Figure 5-2: Outcrop Locations Where the Hydrothermal Alteration and Deformation of Plutons Have Been Studied. Green Stars Represent 1 Outcrop, Red Stars Represent 2 Outcrops, Yellow Stars Represent 3 Outcrops and Purple Stars Represent 5 Outcrops .....	64
Figure 5-3: (left) “Heat” Map Representation of Normal Versus Tangential Stress on the Fracture Planes of the Baseline DFN and (right) $\sigma_{nn}$ Probability Density without (top) and with (bottom) Stress Fluctuations.....	67
Figure 5-4: Illustration of Numerical Methodology and Setup to Derive Directional Equivalent Permeabilities. From Left to Right: DFN and Stress Conditions Provided as Input, Normal Stresses Computed Accounting for Stress Fluctuations, Fracture Aperture Transmissivity Relationship, Flow Simulations in Specific Directions and Finally Equivalent Directional Permeabilities. The Last Process is Repeated 80 Times to get 80 “Directional Permeabilities” and, When Relevant, a Permeability Tensor is Defined.....	67
Figure 5-5: Ionic Strength Dependency of Sorption of Se(-II) on Shale, Bentonite, and Illite .....	77
Figure 5-6: Blocks Before of Final Cutting Stage of the 35 x 60 mm and 70 x 100 mm with Tensile Induced Joints .....	80
Figure 5-7: Results from Direct Shear Tests on Rock Joint (N1-CNL) and Replicas of the Surface (RNM-N1-CNL). The Average Geometrical Aperture Deviation of the Replicated Surfaces Versus the Parent Rock Joint is Shown by the Images and the Scale to the Right (From Larsson et al. 2020) .....	81
Figure 5-8: (top left) Image Showing Base of Triaxial Cell with the Micro Fibre Optic Pressure Sensor; (top right) Image of Triaxial Cell Design Created in AutoCAD Inventor; and (bottom) Image Showing the Size of the Micro Fibre Optic Sensors Compared to a Standard Pen .....	84
Figure 5-9: Earthquakes in Northern Ontario, 2019. Events in 2019 Have Black Outlines, while Events from 1900–2018 are Plotted Semi-transparently and Have Grey Outlines. Events and Stations are Plotted in the Study Area Only. The Study Area is Outlined with a Dash-dotted Line. Only Stations with Data Available in 2019 are Shown .....	89

Figure 6-1: High Level Stepwise Approach in Climate Change Impacts Study ..... 100  
Figure 6-2: paLINK-ISM Configuration..... 102  
Figure 7-1: 2-D Seismic Source Vehicle, November 2020 ..... 105  
Figure 7-2: South Bruce Borehole Access and Pad Construction Underway, December 2020 107

## 1 INTRODUCTION

The Nuclear Waste Management Organization (NWMO) is implementing Adaptive Phased Management (APM) for the long-term management of used nuclear fuel. This is the approach recommended in *“Choosing a Way Forward: The Future Management of Canada’s Used Nuclear Fuel”* (NWMO 2005) and selected by the Government of Canada in 2007.

The technical objective of the APM approach is a Deep Geological Repository (DGR) that provides long-term isolation and containment, to ensure safety of people and the environment while the radioactivity in the used fuel decays.

The deep geological repository is a multiple-barrier system designed to safely contain and isolate used nuclear fuel over the long term. It will be constructed at a depth of approximately 500 metres, depending upon the geology of the site, and consist of a series of tunnels leading to a network of placement rooms where the used nuclear fuel will be contained using a multiple-barrier system. A conceptual design for a DGR is illustrated in Figure 1-1 for a generic rock setting (the design will be varied for actual crystalline or sedimentary rock conditions).

The NWMO is presently in the Site Selection phase. No site has been selected to host the DGR. The process for selecting a host community is described in *Moving Forward Together: Process for Selecting a Site for Canada’s Deep Geological Repository for Used Nuclear Fuel* (NWMO 2010). The steps for evaluating the geological suitability of willing and informed host communities consists of a) initial screenings to evaluate the suitability of candidate sites against a list of preliminary screening criteria, using readily available information; b) preliminary assessments to further determine if candidate sites may be suitable for developing a safe used fuel repository; and c) detailed field investigations to confirm suitability of one site.

Initially, 22 communities had expressed interest in the program. In 2020 the number of communities engaged in the site selection process had been narrowed to two, the Ignace area and the South Bruce area, based on preliminary desktop assessments of potential geological suitability and potential for the project to contribute to community well-being. The status of each community as of December 2020 is shown in Figure 1-2. All reports completed are published on the NWMO’s site selection website ([http://www.nwmo.ca/sitingprocess\\_feasibilitystudies](http://www.nwmo.ca/sitingprocess_feasibilitystudies)).

The NWMO continues to conduct technical work to support design, site assessment and safety case for a DGR, in parallel with work to engage with and establish a partnership with communities. This report summarizes technical work conducted in 2020. In the near term, this information will support selection of a preferred site by 2023. In the longer term, this will support an impact assessment and licence application at the selected site. NWMO’s overall implementation plan is described in *Implementing Adaptive Phased Management 2019-2023* (NWMO 2019a).

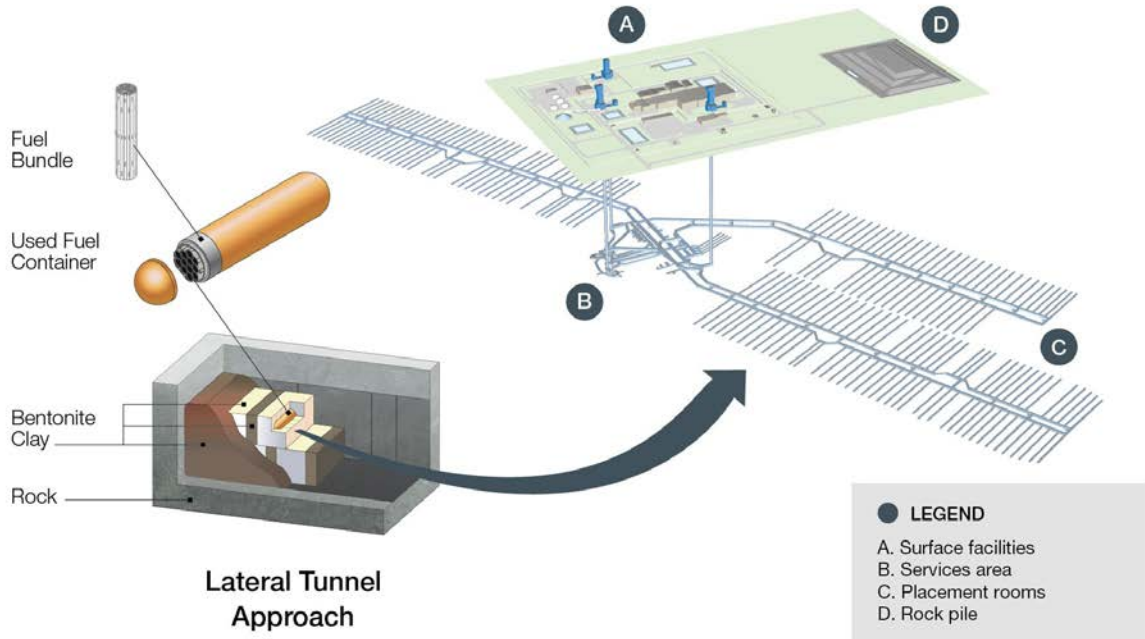


**Figure 1-1: Illustration of a Deep Geological Repository Reference Design**

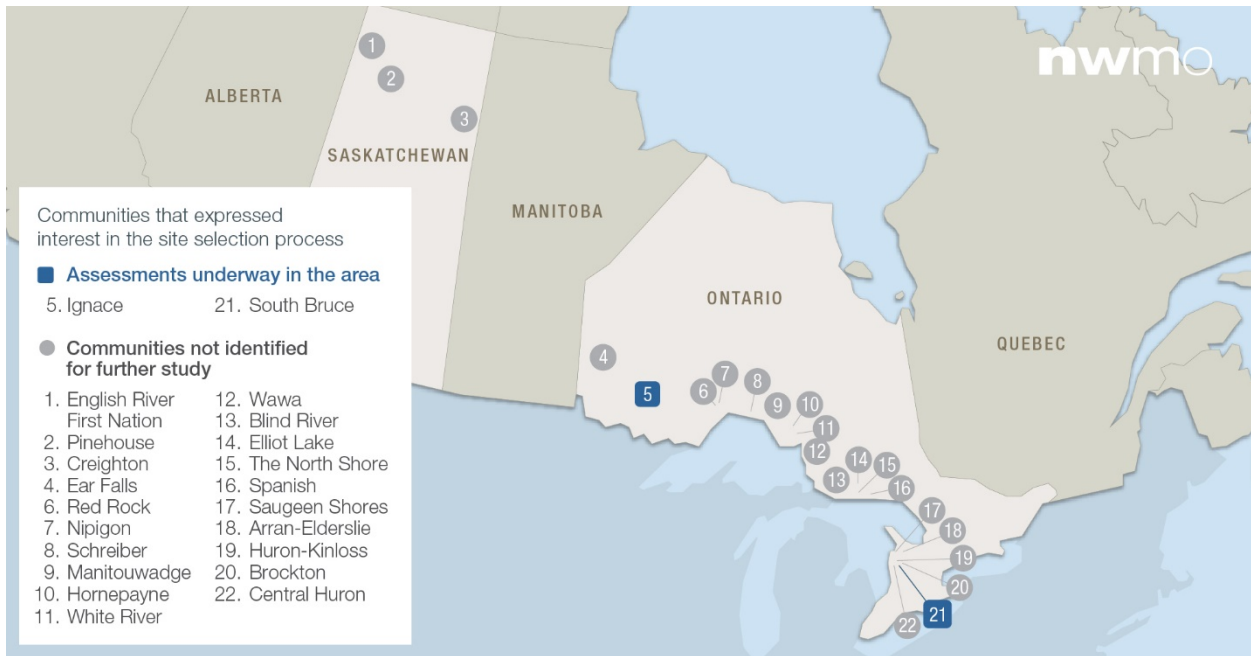


**Figure 1-2: Interested Community Status as of 31 December 2020**

## 2 OVERVIEW OF NWMO TECHNICAL PROGRAMS

The APM Technical Program includes site investigations, preliminary design and proof testing, and developing the safety case for a used fuel DGR. Work conducted during 2020 is summarized in this report. Prior year work is summarized in Chen et al. 2020.

The work is summarized in the following sections divided into Engineering, Geoscience, Repository Safety, and Site Assessment.

This work involved 17 universities (including 15 Canadian universities), as well as a variety of industrial and governmental research partners. A list of the 2020 technical reports produced by NWMO is provided in Appendix A.1. Appendix A.2 provides a list of journal articles on work supported by NWMO.

An important aspect of the NWMO's technical program is collaboration with radioactive waste management organizations in other countries. In 2020, the NWMO had formal agreements with ANDRA (France), INER (Taiwan), KORAD (South Korea), Nagra (Switzerland), NDA (United Kingdom), NUMO (Japan), ONDRAF (Belgium) and SKB (Sweden) to exchange information arising from their respective national programs to develop a deep geologic repository for nuclear waste.

Some of this collaboration is work undertaken at underground research facilities. In 2020, NWMO supported projects at the Mont Terri Underground Rock Laboratory in Switzerland, the SKB Äspö Hard Rock Laboratory in Sweden, the ONKALO facility in Finland, and the Grimsel Test Site (GTS) in Switzerland. These provide information in both crystalline (Äspö, ONKALO, GTS) and sedimentary (Mont Terri) geological environments.

NWMO was involved with the following joint experimental projects in 2020:

- POST Project (Fracture Parameterization for Repository Design & Post-closure Analysis) at Äspö and ONKALO,
- Full-scale In-Situ System Test (FISST/EBBO) demonstration project at ONKALO,
- The Mont Terri Project and Rock Laboratory including:
  - Diffusion across 10-year-old concrete/claystone interface (CI, CI-D),
  - Long-term Diffusion experiment (DR-B),
  - Analysis of Geochemical Data (GD)
  - Geomechanical in-situ Characterization of Opalinus Clay (GC-A)
  - Full Scale Emplacement Experiment (FE-G, FE-M),
  - Hydrogen Transfer (HT) test,
  - Iron Corrosion – Bentonite (IC-A) test,
  - Long-term Pressure Monitoring (LP-A),
  - Microbial Activity (MA),
  - Porewater Gas-characterisation Methods for Reactive and Noble Gases (PC-D),
  - Seismic imaging ahead of and around underground infrastructure (SI-A)
  - Permanent nanoseismic monitoring (SM-C), and
  - Large-scale Sandwich seal experiment (SW-A).
- Materials Corrosion Test (MaCoTe) at GTS.
- Gas-Permeable Seal Test (GAST) at GTS.
- Enhanced Sealing Project (ESP) at Whiteshell Labs, Canada,
- MICA Michigan International Copper Analogue project, and
- International Bentonite Longevity project.

NWMO was involved with the following joint modelling projects in 2020:

- DECOVALEX thermal-hydraulic-mechanical modelling,
- Aspo Groundwater Modelling Task Force,
- Post-closure criticality working group,
- CatchNET cold climate hydrology modelling,
- BIOPROTA biosphere modelling, and
- Joint projects with SKB on modelling fractured rock, including HM coupling; Skempton/Biot coefficient, fracture statistics.

The NWMO also collaborated with Nagra, SKB and POSIVA on a Greenland ice drilling project (ICE) to establish constraints on the impact of ice sheets on groundwater boundary conditions at the ice-bed contact.

The NWMO continued to participate in the international radioactive waste management program of the Organisation for Economic Co-operation and Development (OECD) Nuclear Energy Agency (NEA). Members of this group include the major nuclear energy countries, including waste owners and regulators. NWMO participated in the following NEA activities:

- Radioactive Waste Management Committee (RWMC),
- Integration Group for the Safety Case (IGSC),
- Working Group on the Characterization, the Understanding and the Performance of Argillaceous Rocks as Repository Host Formations (i.e., Clay Club),
- Expert Group on Geological Repositories in Crystalline Rock Formations (i.e., Crystalline Club),
- Expert Group on Operational Safety (EGOS),
- Thermodynamic/Sorption Database Development (TDB) Project, and
- Working Party on Information, Data and Knowledge Management (WP-IDKM).

This report aligns with the RD2019 - NWMO's Program for Research and Development for Long Term Management of Used Nuclear Fuel (NWMO 2019b). This report describes the major technical research and development activities of the NWMO. It is complementary to NWMO activities in site selection, site characterization, design and engineering proof testing, and considers the full lifecycle of the repository. A key point is that underlying science studies will continue throughout the repository phases in order to support future licence decisions. The report reviews the general status of understanding of used nuclear fuel properties, used fuel containers, sealing materials, geological processes, and safety assessment. It identifies directions for future research and development.

### 3 REPOSITORY ENGINEERING AND DESIGN

Despite the pandemic, research and development progressed in the Engineering Program during 2020. Primary areas of work included: used fuel transportation system development, used fuel container design and manufacturing, buffer and sealing systems, mining and repository engineering and the development of the Used Fuel Packaging Plant (UFPP). Summaries of these activities are provided in the following sections.

#### 3.1 USED FUEL TRANSPORTATION

##### 3.1.1 Used Fuel Transportation System Development

Canada's used nuclear fuel is currently safely managed in facilities licensed for interim storage. These facilities are located at nuclear reactor sites in Ontario, Quebec and New Brunswick, as well as Atomic Energy of Canada's sites at Whiteshell Laboratories in Manitoba and Chalk River Laboratories in Ontario. Managing all of Canada's used nuclear fuel in a single repository location will require the transport of used nuclear fuel from these interim storage facilities to the central location of the DGR.

NWMO is currently in a site selection process for the repository and has narrowed its focus to two potential siting areas: the Ignace area in Northwestern Ontario and the South Bruce area in Southern Ontario. The map illustrates the locations of the interim storage facilities as well as identifies the potential siting areas (see Figure 3-1).



**Figure 3-1: Interim Storage Facilities and Potential Siting Areas**

As part of its responsibility for the long-term management of Canada's used nuclear fuel, the NWMO will be responsible for transporting used fuel to the selected repository site. Technical, operational and cost evaluations of options for used fuel transportation systems for these two potential siting areas are ongoing. Key components of the used fuel transportation system include:

- transportation packages,
- transportation modes,
- conveyances and fleets,
- routing,
- transportation infrastructure,
- interfacing facility infrastructure at interim storage facilities and at the DGR,
- nuclear security/escort requirements,
- emergency response and recovery requirements,
- logistics, i.e., shipment scheduling, cycle times including transit times and non-transit times for on- and off- loading of transport packages,
- operations, i.e., operations at facilities, operations during transport for modes of transport, escort operations, communication, tracking and monitoring.

Analysis of these key components was performed during 2018 to 2020. The objective was to compare options for transportation systems including transportation modes (i.e. all-road, and road-rail combination), package designs, and operational considerations taking into account two potential siting areas. This work will support and provide the basis for the 2021 Transportation Lifecycle Cost Estimate, which will support NWMO's reference design and cost estimate for the overall APM project.

The reference transportation system is an all-road system transporting an estimated 5.5 million fuel bundles (Gobien and Ion, 2020) to a DGR, located in either of two distinct geological settings: crystalline rock in Northwestern Ontario; and sedimentary rock in Southern Ontario. The reference transportation system assumes that fuel is transported using: Used Fuel Transportation Packages (UFTPs) for OPG owned fuel; and Basket Transportation Packages (BTPs) for non-OPG owned fuel.

### **3.2 USED FUEL PACKAGING PLANT**

The Used Fuel Packaging Plan (UFPP) is a key facility at the DGR site for the long-term storage of used fuel. The UFPP will have all the provisions required for receiving the transportation casks known as Used Fuel Transportation Packages (UFTP) for fuel being transported in storage modules or Basket Transportation Packages (BTP) for fuel in sealed baskets, equipment for fuel handling, designated facilities for the encapsulation of the fuel in Used Fuel Containers (UFCs) and their dispatching for emplacement in the DGR.

The NWMO is currently furthering the details of the conceptual design phase of the UFPP based on previous work performed in 2014. Substantial work was completed in 2020 leading to an updated conceptual design. The overall conceptual layout of the UFPP is shown in Figure 3-2. Process operations required for handling the fuel and its encapsulation in the UFCs were scoped and are described below.

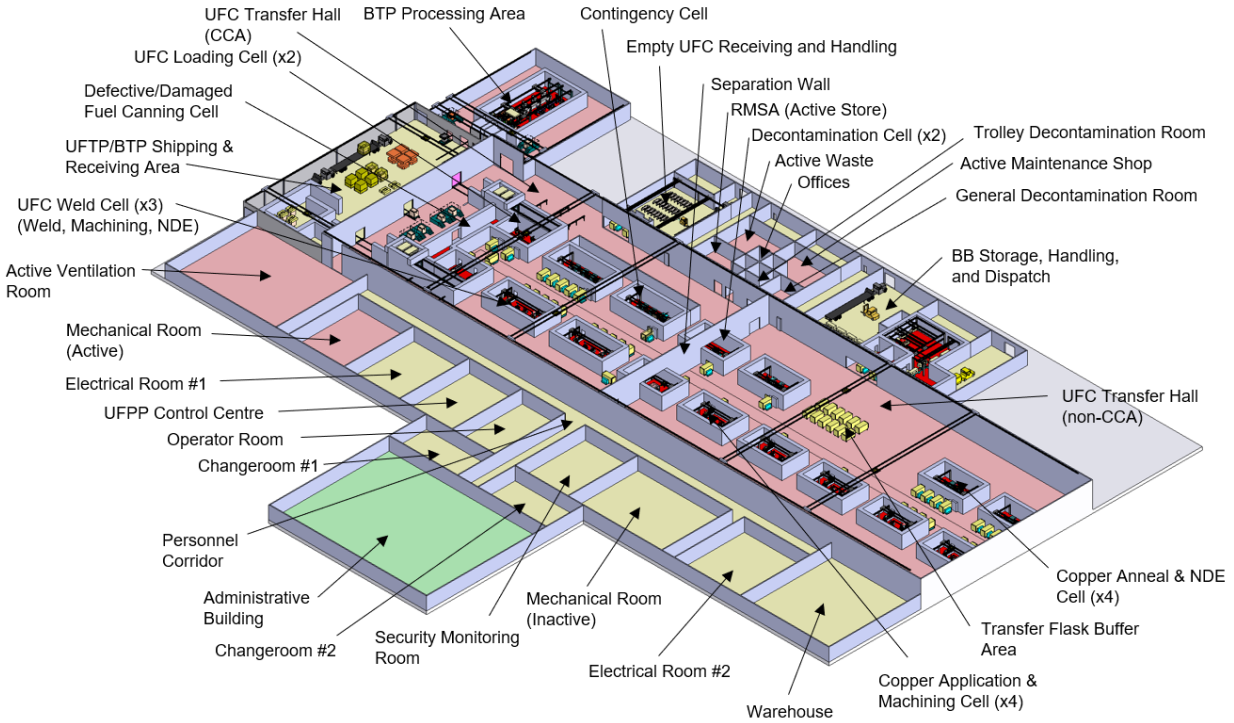


**Figure 3-2: Concept Layout of the Used Fuel Packaging Plant (UFPP). The Key Acronyms Denoting Processing Areas and Components Are: CCA (Contamination-controlled Area), Non-CCA (non-contaminated control area), BB (Buffer Box), BTP (Basket Transportation Package), UFTP (Used Fuel Transportation Package), UFC (Used Fuel Container), NDE (Non-destructive Examination), and RMSA (Radioactive Material Storage Area)**

### 3.2.1 Receipt of UFTP/BTP and Used Fuel Module/Basket Unloading

The UFTP/BTPs containing used fuel modules/baskets are first received at the shipping and receiving area of the UFPP. This shipping and receiving area have space and lifting equipment for unpacking the UFTP/BTPs from arriving cask transportation tractor trailers, and for staging the UFTP/BTPs for unloading their fuel inside a shielded area of the UFPP. Additional temporary buffer shielded storage space for the UFTP/BTPs is available in the event the facility is not ready to unload the transportation packages. Once the unloading of the UFTP/BTPs is complete, the shipping area is also used to reload the transportation casks onto the tractor trailers with empty storage modules or baskets for shipment off-site. A transfer interface for baskets in BTP to fuel modules is also present in the Receipt Area Annex in preparation for used fuel unloading. A preliminary layout of the Receipt Area of the UFTP/BTP Facility is shown in Figure 3-3.

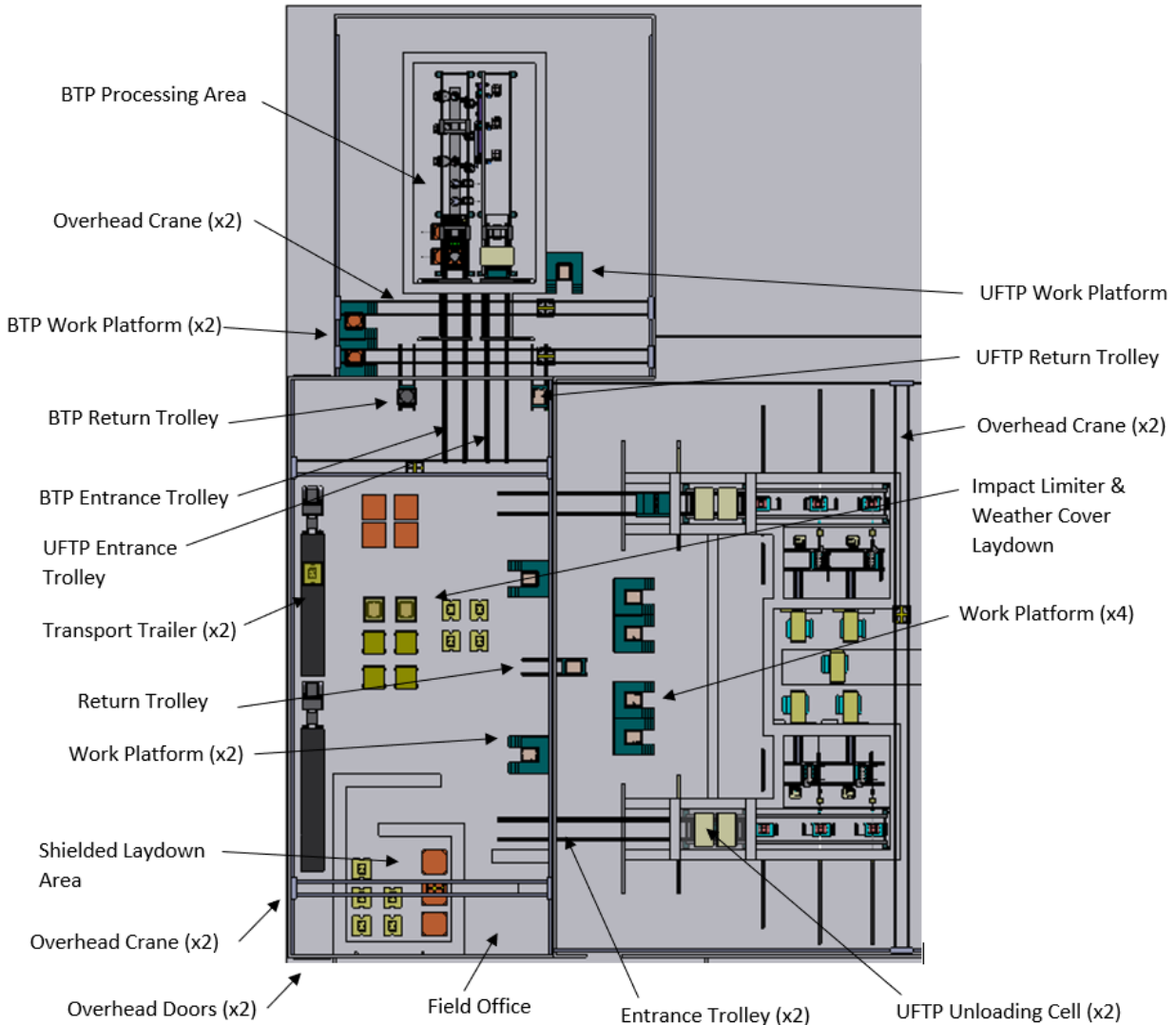


**Figure 3-3: The Used Fuel Transportation Package (UFTP)/Basket Transportation Package (BTP) Shipping & Receiving Area**

### 3.2.2 Used Fuel Inspection and UFC Loading

The used fuel bundles are inspected inside a shielded area after they have been removed from the UFTP. Individual bundles are inspected and their identifications confirmed. This is followed by inserting the bundles into the UFC in an adjacent cell. See Figure 3-4 for the layout of the used fuel inspection and adjoining UFC loading system. When a UFC is filled, the hemi-head as depicted in Figure 4-1 is placed onto the UFC base and transferred for processing to the Used Fuel Welding Cell.

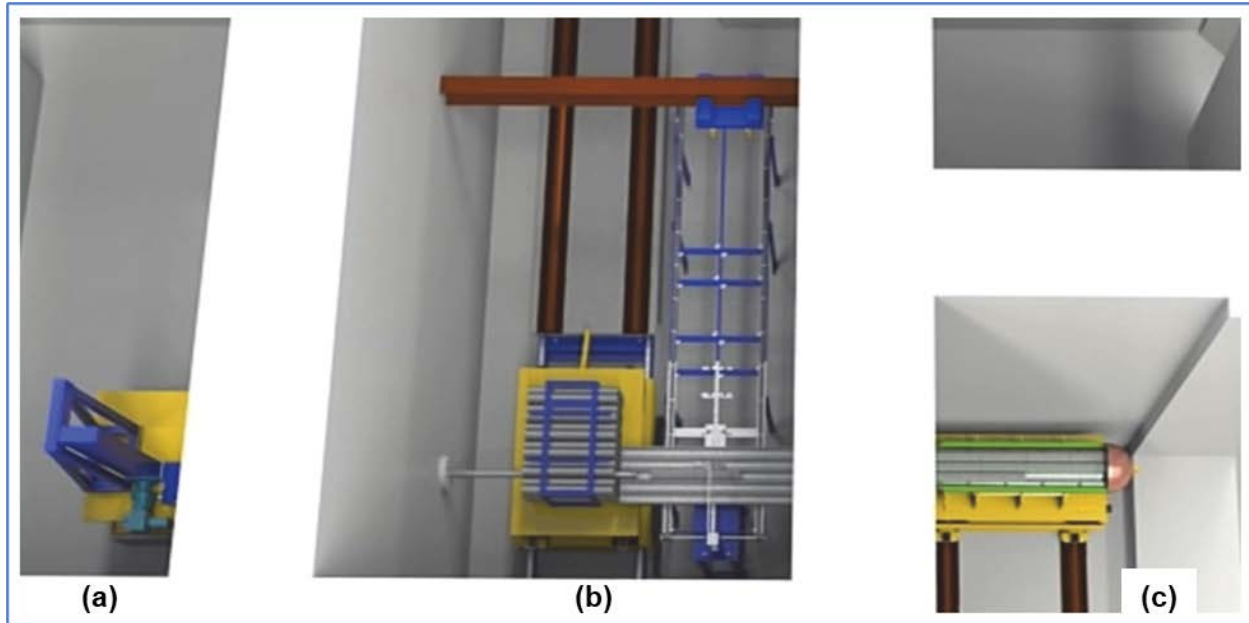


**Figure 3-4: Fuel Transfer into a Used Fuel Container (Top View): (a) Equipment to Operate the Push Ram that Penetrates the Work Cell Shielding Wall, (b) A Used Fuel Module on Positioning Table in Shielded Work Cell and (c) Bundles pushed by Ram into the UFC Located in the Shielded Work Cell.**

Description of Figure 3-4:

- a) Equipment to operate the push ram that penetrates the work cell shielding wall.
- b) A used fuel module loaded with fuel bundles is located on a positioning table in the shielded work cell.
- c) Bundles are pushed by the ram into the UFC located in the shielded work cell. The UFC is shown in a cut-way view with top half of the UFC removed for the purpose of this illustration.

### 3.2.3 UFC Welding Cell

UFCs loaded with fuel are welded shut in the UFC Welding Cell. The welding process attaches the hemispherical head to the container base and consists of the following four stages: pre-heat, circumferential welding of the hemi-head to the UFC base, excess weld material removal, weld inspection and verification through non-destructive examination. This process is completed in a shielded area with a controlled environment. While welding, the UFC is rotated with the weld tools hovering over the joint line between the hemi-head and lower assembly. See Figure 3-5 and Figure 3-6 for typical arrangements.

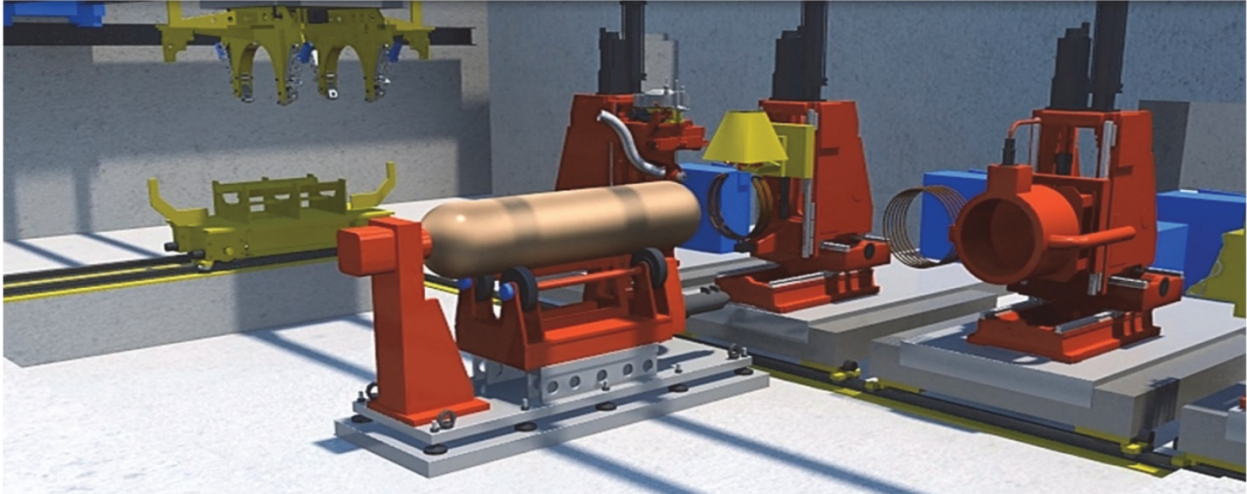


**Figure 3-5: Typical Work Cell Arrangement with Various Process Worktables**

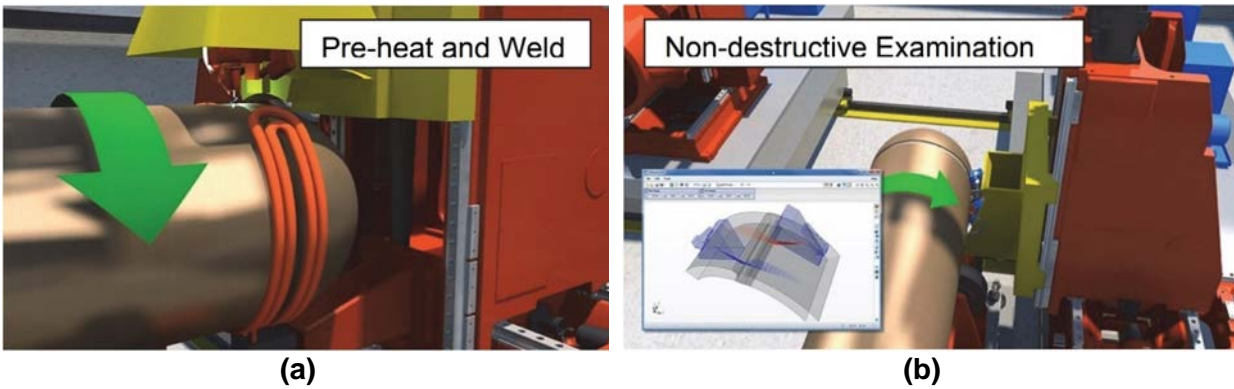


**Figure 3-6: (a) The Welding and Preheat Worktable and (b) Weld Non-Destructive Examination Worktable**

### 3.2.4 UFC Decontamination Cell

The UFC Decontamination cell is located as an interface between the UFC Welding Cell and the UFC Copper Application and Machining Cell. The UFC decontamination cell removes potential contaminants from the outer surface of the UFC prior to the application of the copper coating to the UFC joint weld area. See Figure 3-7 for its layout.

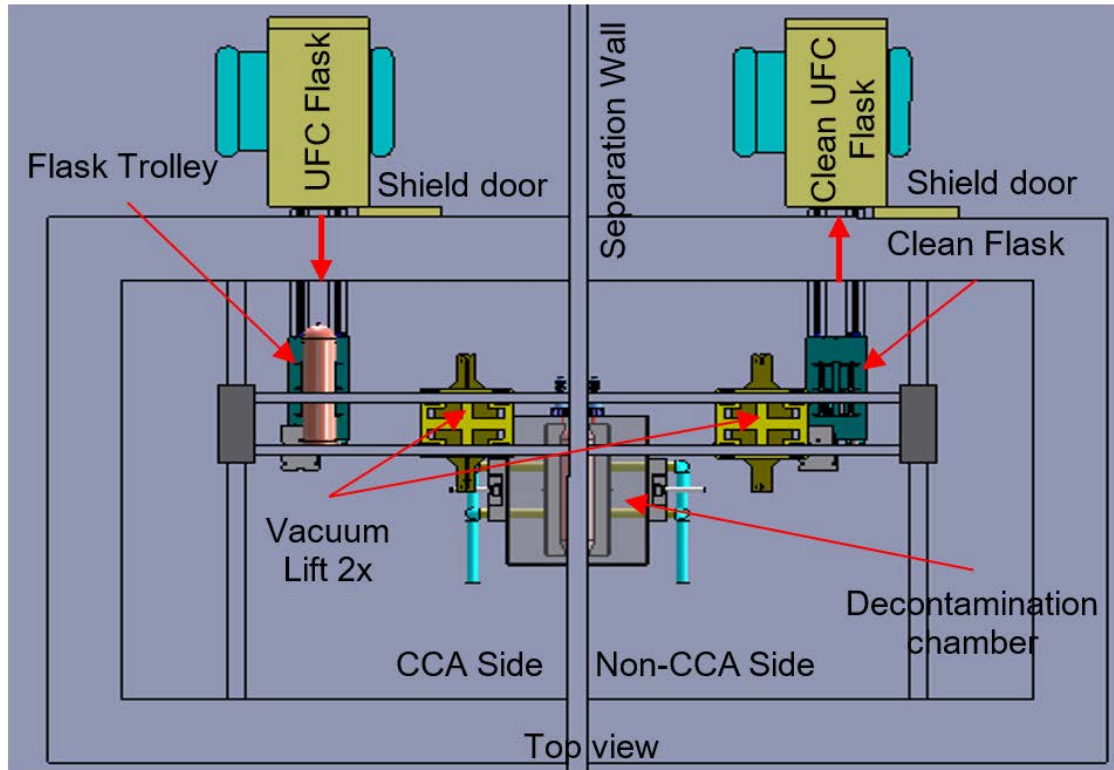
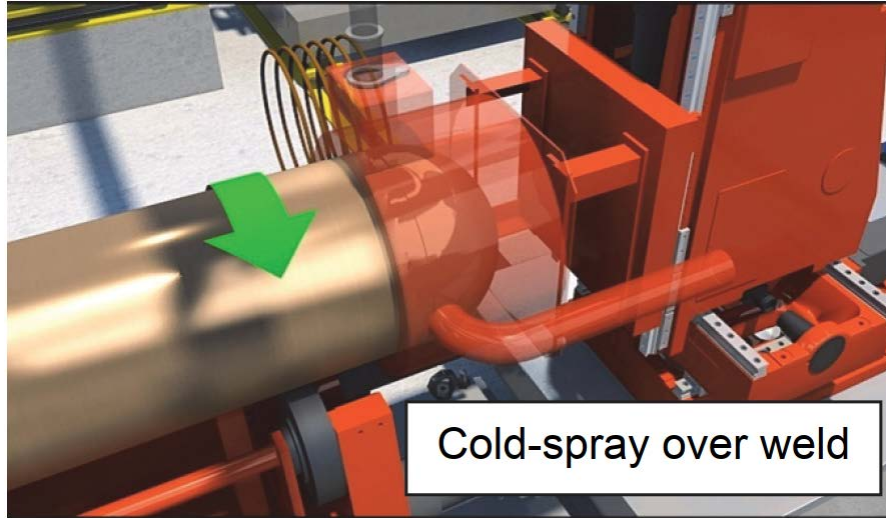


Figure 3-7: Used Fuel Container Decontamination Cell (Top View)

### 3.2.5 UFC Copper Application and Machining Cell

In the UFC Copper Application and Machining Cell, the welded UFC is subjected to a full circumferential copper coating process for the uncoated welding joint area of the UFC. This process consists of pre-heating, copper coating and copper machining. It is performed in a shielded area with a controlled environment. The UFC is rotated while the cold-spray copper application tools hover over the uncoated region between the hemi-head and lower assembly to deposit the copper coating. See Figure 3-8 for typical arrangement.



**Figure 3-8: Copper Cold Spray and Copper Annealing Worktable**

### **3.2.6 UFC Copper Annealing / NDE Work Cell**

When the copper application and machining process is complete, heat is applied to the UFC at the copper annealing worktable to soften the copper that has previously been applied by cold spray. After completion, the copper is cooled and the surface integrity is verified through non-destructive examination. The copper annealing setup is shown in Figure 3-9.

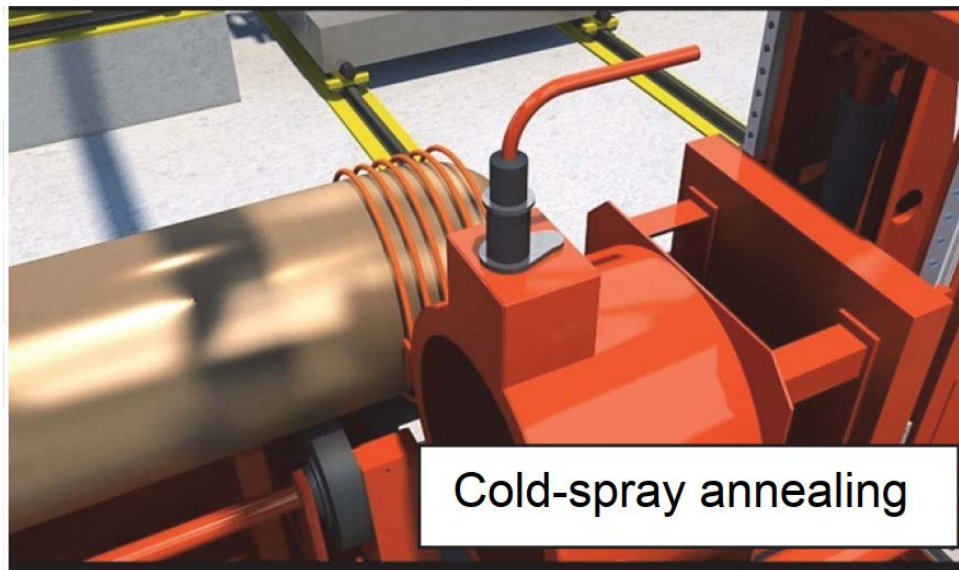


**Figure 3-9: Copper Annealing Worktable**

### 3.2.7 Buffer Box Storage, Handling & Dispatch Area

UFCs that have been welded, copper coated, and had their welds inspected and verified are transferred to the DGR dispatch area of the UFPP. The UFCs are loaded into buffer storage boxes and loaded onto the dispatch vehicle. The facility has provision for temporary buffer storage of empty buffer boxes in a temperature and humidity-controlled environment. A preliminary layout of the buffer box storage, handling and dispatch area is shown in Figure 3-10.

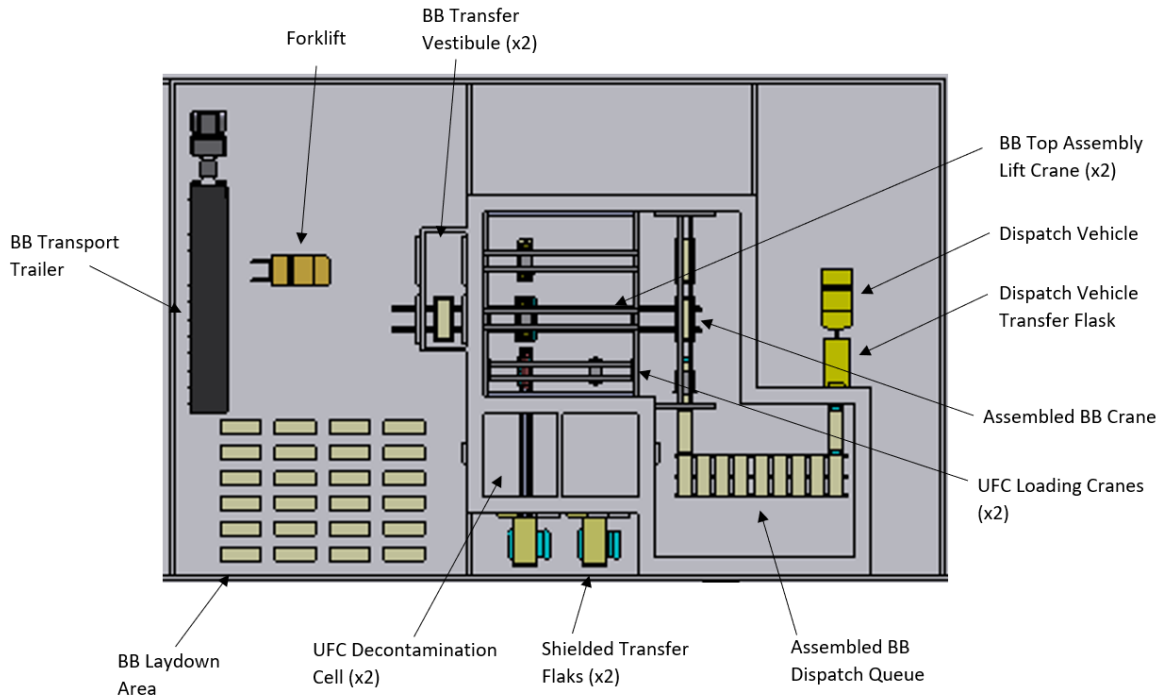


**Figure 3-10: Buffer Box (BB) Storage, Handling and Dispatch Area**

### 3.3 MINING AND REPOSITORY ENGINEERING

The NWMO continues to support the development of the buffer and sealing systems including optimized manufacturing, storage, and emplacement technology for the Highly Compacted Bentonite (HCB) blocks that are placed directly around the UFCs.

The gapfill material delivery equipment was designed and fabrication initiated. An emplacement plan for a large-scale demonstration trial was produced, defining the scope of the emplacement plan as well as schedule and expected costs. A delivery system for smaller HCB bricks was designed and built.

#### 3.3.1 Emplacement Equipment

The prototype emplacement equipment was designed and built by Medatech Engineering Services (Collingwood, Canada) to NWMO requirements, and tested at the NWMO's proof testing facility in Oakville, Ontario. Further enhancements will be implemented for the emplacement equipment to increase forward visibility and provide enhancements to the steering system for fine control.

#### 3.3.2 Emplacement Plan

The purpose of this work was to define the scope of the emplacement demonstration. The plan was reviewed internally and by a third party for a comprehensive benchmarking review against their own experience in demonstration programs. The review identified some opportunities to obtain more quantitative data with enhancements to equipment. The opportunities were adopted in the test plan and are being reflected in updates to the equipment.

##### 3.3.2.1 Background

###### 3.3.2.1.1 Bentonite

The NWMO has continued to accept large volumes of unprocessed and fabricated bentonite materials into NWMO's proof testing facility in Oakville, Ontario, as a component of the Proof Test Plan. These materials consist of:

- (i) Granular MX-80 bentonite;
- (ii) HCB Blocks delivered from the Penn State compression facility for shaping; and
- (iii) Crushed granular MX-80 based Gap Fill Material (GFM).

Given the volume of material, there is a need to conduct a testing program in order to identify sub-standard material, and further refine the frequency of testing as well as material specifications for future Quality Control programs. In 2020, the NWMO initiated a testing program based on ASTM methods on delivered bentonite materials as follows: (i) moisture content, (ii) grain size analysis, (iii) consistency limits, (iv) methylene blue tests, (v) free swell, (vi) mineralogical and chemical composition, and (vii) dry density.

###### 3.3.2.1.2 HCB Blocks

HCB blocks are pressed from raw MX-80 sodium bentonite. The raw bentonite is sourced from the United States at a moisture content of 10-12% ( $m_{\text{water}}/m_{\text{dry solid}}$ ). It is then up blended with water to bring the moisture content up to 20%. This blending work is performed by a local food blending company in a large industrial blender. The blended bentonite returns to the NWMO proof test facility in tote bags where it is loaded into an isostatic pressing bag and form assembly. Once the bag is filled, air is withdrawn and the bag sealed, it is sent to Pennsylvania State University to be cold isostatically pressed at their High-Pressure Test Facility. The

bentonite is pressed at 100 MPa in their 1.5 m diameter pressure vessel which results in a HCB block with a dry density  $\geq 1.74 \text{ g/cm}^3$  (Figure 3-11). To date, over twenty full size blocks have been pressed using cold isostatic hydraulic press technology. Block yield has been approximately 90%.



**Figure 3-11: Highly Compacted Bentonite (HCB) Block**

The isostatic pressing produces a block that is “near net shaped”, meaning it is close to the final desired shape. The blocks are machined to final dimensions for the Buffer Box assembly in the robotic milling cell at NWMO’s proof testing facility in Oakville, Ontario (Figure 3-12).



**Figure 3-12: Shaped Highly Compacted Bentonite (HCB) Block**

### **3.3.2.1.3 Used Fuel Container**

The engineered barrier closest to the fuel is the used fuel container. Its safety function is containment and isolation. It fulfills the safety function by incorporating the corrosion barrier and the structural vessel to meet performance requirements. The used fuel container is a mid-sized capacity (12 bundle/layer x 4 layers= 48 bundle) vessel which incorporates a steel core for structural strength and a 3 mm exterior copper coating for corrosion resistance. The weight of the container loaded with fuel is approximately 2,800 kg.

### 3.3.2.1.4 Buffer Box and Assembly

The buffer box assembly (Figure 3-13) is two highly compacted bentonite blocks containing a used fuel container.



**Figure 3-13: Buffer Box Assembly**

The HCB blocks and Used Fuel Containers have no lifting features and generally cannot be handled with conventional equipment without damage. The Buffer Box is therefore assembled with vacuum lifting equipment. The vacuum lift is capable of lifting the HCB (Figure 3-14 on either the bottom flat surface or on the top cavity surface, and with a vacuum pad change, it can pick up the UFC (Figure 3-15). The unit is purpose built and battery powered. The vacuum lift is fabricated by the Vacuum Lifting Company SF4KB unit with a safe working load rating of 4200 kg with the HCB vacuum pad.



**Figure 3-14: Vacuum Lift Highly Compacted Bentonite (HCB)**



**Figure 3-15: Vacuum Lift Used Fuel Container (UFC)**

#### **3.3.2.1.5 HCB Block Storage**

HCB blocks are sensitive to humidity. Once the HCB blocks are removed from the pressing bag, if not used immediately they need to be stored in a location where the vapour pressure of water in air is in equilibrium with the vapour pressure of the water in the block. This is accomplished by storing the HCB blocks in a humidity-controlled room and maintaining the relative humidity above 70% at 20°C.

#### **3.3.2.1.6 Mock Emplacement Room**

The NMWO has fabricated a mock emplacement room at NWMO's proof testing facility in Oakville, Ontario (Figure 3-16). The mock emplacement room simulates the anticipated dimensions, as well as the drill and blast profile of underground excavation. The resulting rock surface is rough with near 90-degree angles at the "look outs" (i.e. sharp profile changes due to the drill and blast process).



**Figure 3-16: Simulated Emplacement Room with Faux Rock Walls Simulated Drill and Blast Profile: (a) Exterior Steel Frame Approximately 3m x 3m x 15m in Size, (b) Interior with Faux Rock Walls and (c) Actual Blast Profile from Underground Research Laboratory**

### **3.3.2.1.7 Buffer Box Delivery Tooling**

The buffer box delivery tooling, or buffer box attachment, is a custom engineered forklift attachment that is used with the electric Versa Lift 25/35 lift truck at NWMO's proof testing facility in Oakville, Ontario (Figure 3-17). It was designed specifically to lift and place Buffer Box assemblies. It features:

1. Three 16 inch wide, adjustable/removable tines with independent hydraulic load levelling.
2. Inflatable air bags to apply a compressive load to the ends of the buffer box assembly
3. Five cameras and three alignment lasers to allow remote placement of the buffer box assembly using the Versa Lift's remote-control pendant.

The attachment was designed and built as a research tool; as such, it has many features that can be changed including, adjustable/removal of tines to allow test flexibility, adjustable bag pressure, different tine configurations, etc. Buffer boxes with 2 or 3 pockets can be used and the tines can be repositioned along the width of the buffer box. This feature allows testing of several different configurations before settling on a 'reference' design. The inflatable airbags apply a compressive load of up to 1000 kg to each end of the buffer box assembly. These loads help prevent sagging of the buffer box, depending on the position of the tines. They also prevent the HCB from separating should there be a crack or a break. Since in the future this equipment will have to be remotely operated due to the high radiation fields, it is important to demonstrate that the buffer boxes can be placed remotely. The cameras and lasers help the operator drive the vehicle and correctly position it to place the buffer box. With the success of the initial demonstrations, enhancements in fine steering control will be performed as well as improvements to the vision system necessary for the emplacement activities.



**Figure 3-17: Buffer Box Attachment Installed on Versa Lift 25/35**

### **3.3.2.2 Fork Pocket Brick Delivery Equipment**

To fill the voids left to accommodate the buffer box delivery equipment, HCB bricks must be inserted into the fork pocket void. This will be performed by a custom-built cart capable of lifting the bricks and pushing them into the space with an electric screw (see Figure 3-18). The equipment has been designed, built and placed in service.



**Figure 3-18: Fork Pocket Brick Delivery Equipment**

### **3.3.2.3 Gapfill Delivery Equipment (Auger System)**

The final major component necessary for the full-scale emplacement demonstration is an auger system to deliver the gapfill to the residual space between the rock face and the emplaced

buffer boxes. The system was designed in 2020 and will be fabricated during 2021 for a demonstration trial in 2022. See Figure 3-19 for an illustration of the auger system.

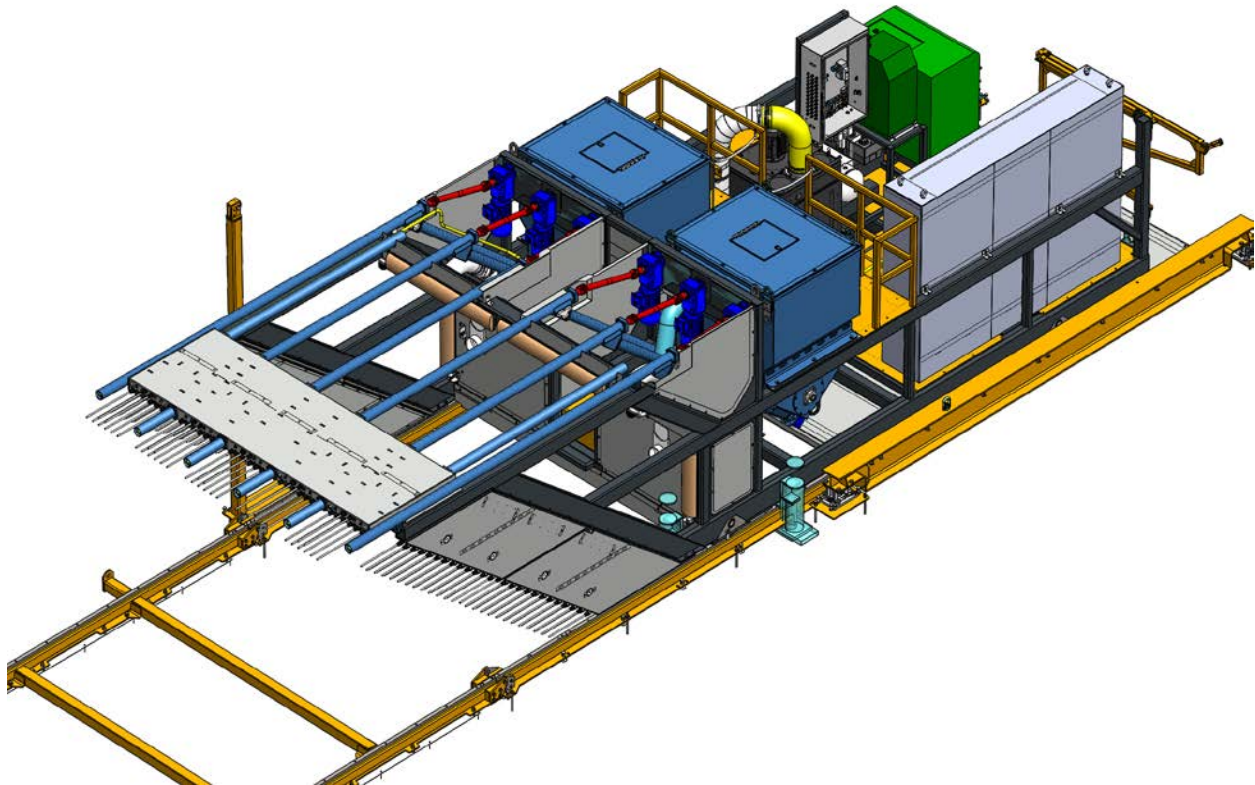


**Figure 3-19: Gapfill Delivery Equipment (Auger System)**

### 3.3.3 Thermal Modeling of the UFCs when placed in the DGR Base Case

In Canada, the Used Fuel Container (UFC) spacing in the Deep Geological Repository is selected to keep the container surface temperature below 100°C. Hence, the thermal analysis of the DGR is important both for DGR design and its safety. During 2020, near-field modelling of the UFCs emplacement configuration was performed to study the impact that various design characteristics and material properties will have on the container surface temperature. These factors included:

1. gaps in the placement room,
2. buffer thermal conductivity,
3. model geometry simplification,
4. repository depth, and
5. placement room layout.

The analysis considered two geological settings: crystalline and sedimentary rock, and it focused on the base case DGR layout design which has the following characteristics:

1. Stacking of two buffer boxes with one UFC each as shown in Figure 3-20 and Figure 3-21,
2. 25 m spacing between emplacement rooms or tunnels, and
3. 0.3 m wide spacer block for crystalline rock and 0.7 m wide for sedimentary rock

The analysis considers various air gaps between the bentonite blocks and the rock. NWMO is aiming to minimize/eliminate these gaps; the numbers below are expected to be lower during actual emplacement; however, they are assumed for the analysis as they lead to higher temperatures (e.g., conservative). The assumed gaps are:

1. 10 mm gap between buffer box and spacer block,
2. 7.5 mm container/buffer box gap, and
3. 10 mm roof/gap fill gap

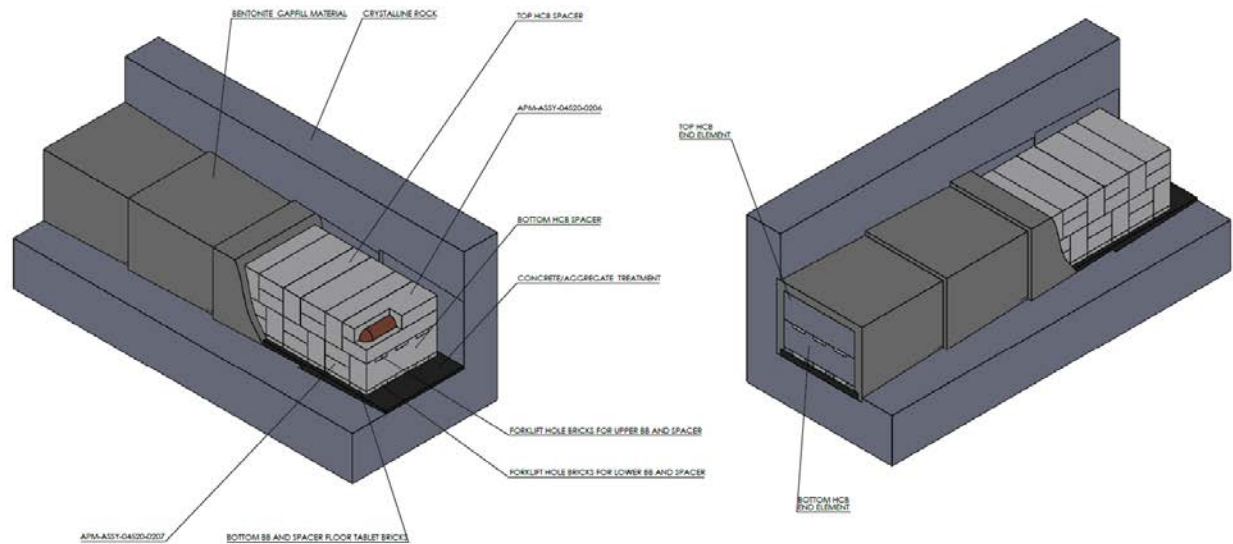


**Figure 3-20: Isometric View of the Used Fuel Container Layout in a Sedimentary Rock Deep Geological Repository (DGR)**

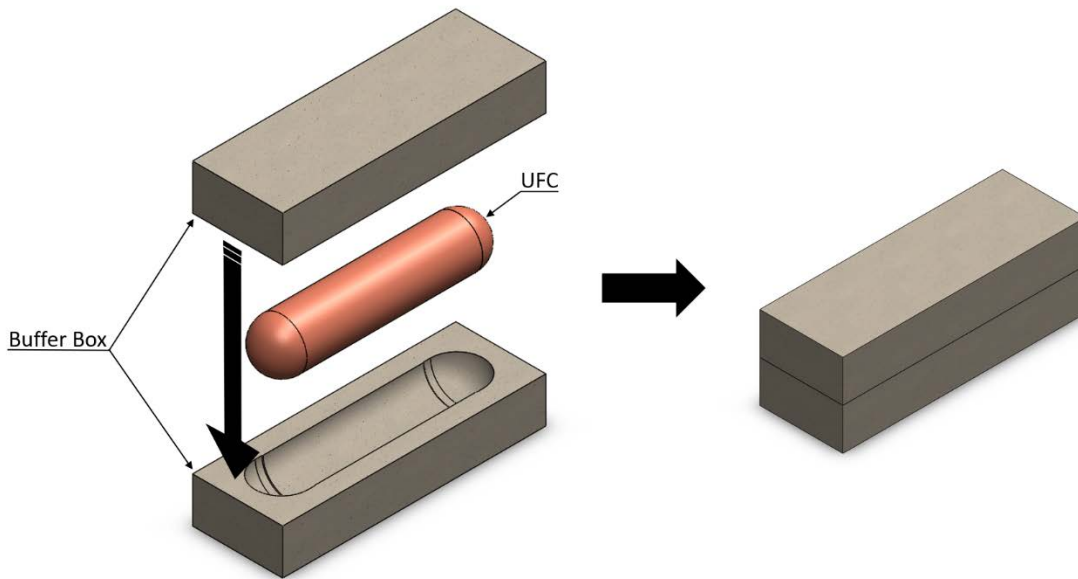


**Figure 3-21: Example Buffer Box Assembly for the Used Fuel Container**

The thermal analysis of the DGR containers layout for the Base Case found that the maximum bounding container surface temperature is approximately 92°C in either crystalline or sedimentary geological settings. This study also showed that there is no benefit from using offsetting layout between the upper and lower layers of the buffer boxes. It also demonstrated that the temperature of the surrounding rock is not significantly impacted by the presence of gaps in the container/buffer box, the buffer box/spacing gaps, and the fill/tunnel roof gaps.

The findings of this study are also being used to conduct experimental tests as part of the Proof Test Program at NWMO's proof testing facility in Oakville, Ontario. Drawings were prepared to show the latest concepts for Buffer Box emplacement for different emplacement schemes along with modelling detailed solutions to be used for verification and validation during the tests.

### 3.3.4 Preliminary Construction Plan for an APM DGR

A high-level construction strategy and preliminary Construction Plan for building the APM Deep Geological Repository (DGR) facility in site-specific crystalline and in generic sedimentary geospheres were also developed in 2020. The Preliminary Construction Plan describes the sequencing of work and the construction methodologies to be used for constructing the entire APM DGR facility, including surface facilities and infrastructure, underground development and facilities, and key off-site facilities. This plan is based on the Adaptive Underground Repository Layout for site-specific crystalline and generic sedimentary geospheres and includes an updated surface facility layout and the Ventilation, Main, and Service Shafts. More detailed construction planning will be performed in the future to validate the current plan in parallel with progress with the design and planning for the APM DGR facility and as site-specific details become available. This will offer an opportunity to further optimize the site-specific execution details and improve cost effectiveness.

### 3.3.5 Excavated Rock Management Area

Work on a geochemical characterization of borehole IG-BH01 located at the Ignace project site in a crystalline geological setting was started during the reporting period. The primary objective

is to gather geochemical information of the site through rock sampling gathering at the borehole. The findings will be used to update the current hypothetical reference design for a Deep Geological Repository (DGR). In particular, the results will be used to further technical studies related to waste rock management. It is expected that as the work progresses at the project site, additional testing will be performed to detail more specific characteristics of the geochemical properties of the rock.

### **3.3.6 Sealing for Decommissioning and Closure**

An update of the previous plan for the decommissioning and closure of a reference hypothetical Mark II APM DGR facility was begun in 2020. The emphasis is on updating the conceptual design information for the sealing systems for both crystalline and sedimentary settings. In particular, updating the seals and plug concepts for the following DGR components:

- placement rooms,
- main shaft (for the sedimentary geosphere only due to its more demanding requirements),
- access tunnels, and
- boreholes

The update will address current APM DGR geometries requirements and site-specific details with recent developments affecting materials and technologies

### **3.3.7 Reference DGR Cost Update for Shafts, Headframes and Hoisting Systems**

The basis for the earlier capital estimate of shafts, headframes and hoisting systems is being updated from the 2014 study. The update addresses major scope changes caused by modifications to the 2014 reference DGR design based on the findings of on-going geotechnical characterization work that affects shaft ventilation design, additional 250 m level cut out, and shaft station layouts.

## 4 ENGINEERED BARRIER SYSTEM

The Engineered Barrier System (EBS) is a major component of the underground design. It includes the wasteform, container, buffer and sealing systems. Summaries of these activities are provided in the following sections. A summary of wasteform durability is provided in Section 6.2.

### 4.1 CONTAINER DURABILITY

In 2020, the NWMO continued the execution of the Proof Test Program to validate the reference design of the Used Fuel Container (UFC) (shown in Figure 4-1 and Figure 4-2). Despite challenges and work delays associated with the global pandemic, progress was made on the UFC Serial Production campaign under which continued manufacturing optimizations and design refinements were advanced based on feedback from UFC manufacture. These developments are summarized in the subsections below.

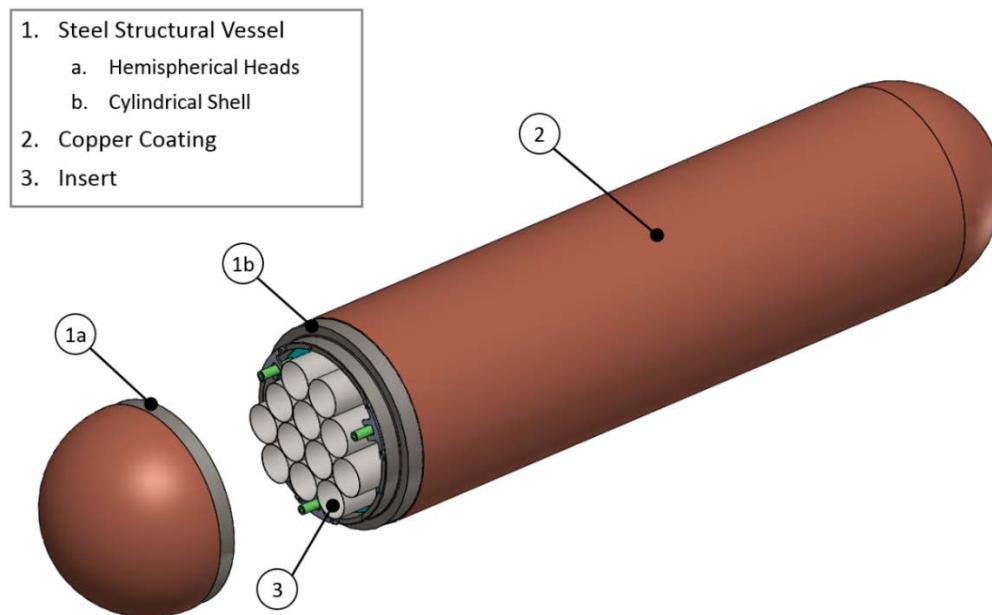


**Figure 4-1: Illustration of the Used Fuel Container Reference Design**

However, one important aspect of the ongoing design program is the participation of international partner organizations that are considering similar strategies for the management of their own nuclear materials. In 2020, the Japanese program co-authored a peer-reviewed article with NWMO staff that favourably identified aspects of the Canadian copper-coated container that may be applicable to their own solutions (Suzuki et al. 2020). While preliminary, the conclusion is that these technologies appear to be suitable for the Japanese program, and further collaborative work is ongoing.



**Figure 4-2: Prototype Used Fuel Container Reference Design**

#### **4.1.1 UFC Design**

The Insert is the internal structure of the UFC and is made of an array of 12 long tubes with capacity for up to 48 used fuel bundles. A conceptual design was fabricated in 2018, as shown in Figure 4-3. This design meets the design requirements but during development opportunities for improvement were identified. A review of its design was initiated in 2019 to improve its constructability and reduce manufacturing costs without affecting functionality and performance.

In 2020, several alternate UFC Insert designs were developed and reviewed by two manufacturing/design organizations focusing on ease of manufacturing and cost savings. The findings are being assessed for incorporation into a future iteration of the Insert design.



**Figure 4-3: Prototype 2018 Used Fuel Container (UFC) Insert Design**

## 4.1.2 UFC Serial Production Campaign

### 4.1.2.1 Fabrication of Used Fuel Containers Prototypes

In 2020, the NWMO continued the execution of its UFC Serial Production campaign. The objective of this program is to fabricate 15 UFCs using reference materials, fabrication and inspection technologies to verify the product against the reference design requirements and quality acceptance standards. During the execution of this work, further design refinements and manufacturing optimizations will be applied as necessary based on feedback from testing, inspection, and validation programs. Refer to Sections 4.1.3, 4.1.4 and 4.1.5 for advancements in welding, copper coating and NDE processes that will be incorporated in the UFC Serial Production campaign.

Throughout the Serial Production campaign in 2020, drawings, manufacturing, inspection & test plans, and related documentation such as procedures and inspection report templates were created and revised to support machining, welding, copper coating, and NDE work on UFC components. The quantity of UFC components manufactured and processed in 2020 are documented in Table 4-1.

**Table 4-1: 2020 UFC Serial Production Results**

UFC Component	2020 Quantity				
	Steel Machining	Welding & Weld NDE	Copper Coating	Copper Coating Machining	Copper NDE
Upper Hemispherical Head	5	N/A	5	2	5
Lower Hemispherical Head	5	N/A	N/A	N/A	N/A
Shell	5	N/A	N/A	N/A	N/A
Lower Assembly (i.e., shell welded to lower head)	N/A	5	0	1	N/A
Closure Zone	N/A	0	0	0	0

Moving forward into 2021, a significant effort will be spent in completing the first 5 UFCs. The remaining 10 UFC's will be in various stages of component manufacture with completion of all UFC's targeted by the end of 2022.

### 4.1.2.2 Design and Fabrication of Dummy Insert and Tooling

As part of the Proof Test Program, a need was identified to demonstrate using a fully loaded UFC during key UFC manufacturing processes (i.e., closure welding, cold spray copper coating and machining, NDE) and emplacement handling operations. To achieve this, a dummy insert was designed to simulate the weight of a UFC Insert fully loaded with 48 fuel bundles. The dummy insert, manufactured from cast iron (ASTM A48 Gr. 25) is shown in Figure 4-4. The insert is inserted into the UFC lower assembly prior to welding using an insertion tool shown in Figure 4-5.

Serial Production UFC's will all contain dummy inserts. These vessels will be available for future buffer box emplacement trials within a mock-up emplacement room at NWMO's proof testing facility in Oakville, Ontario.



**Figure 4-4: Fabricated Dummy Cast Iron Insert**



**Figure 4-5: Dummy Insert Being Loaded into Used Fuel Container (UFC) Lower Assembly Using a Custom Handling Tool at Welding Contractor Novika Solutions**

#### **4.1.3 UFC Welding Technology Development**

In 2020, the use of Hybrid Laser Arc Welding (HLAW) for the UFCs was replaced with laser preheated gas metal arc welding (LP-GMAW) to increase weld quality and process robustness. HLAW and LP-GMAW are similar in that both use GMAW for weld filler deposition but are different in the use of their laser capability. In HLAW, the laser is used to melt and fuse the

base metal at the root (lower portion) of the weld. In LP-GMAW, the laser is used to “pre-heat” the material close to the steel melting point just prior to the weld filler metal being deposited in the weld joint. Development work on LP-GMAW welding (see Figure 3-6) demonstrated sufficient penetration (>8 mm) and fewer defects (such as porosity) compared to HLAW. LP-GMAW has also proven to be a simpler process to implement than HLAW, owing to less interaction between the laser and GMAW arc in the weld volume. This process change required a significant change to the joint geometry in order to increase the weld filler metal volume. The prior weld joint (Figure 3-7a) contained a small 1.5 mm chamfer while the new weld joint (Figure 3-7b) contains a larger “double-J” or “U-groove” type design with a 6 mm depth and 40° opening angle. In 2020, the LP-GMAW process was qualified for use in Serial Production welding. Weld qualification involves non-destructive examination (NDE), mechanical testing, and hardness testing of representative coupons (pipe sections of the exact UFC diameter and joint design in this case). The test coupons passed all required testing. A metallographic cross-section and hardness map of a test coupon is shown in Figure 3-8 and Figure 3-9, respectively. Following qualification, five Serial Production lower assembly welds were completed with no rejectable defects. Moving forward, the LP-GMAW process will be adopted for UFC lower assembly and closure welding.

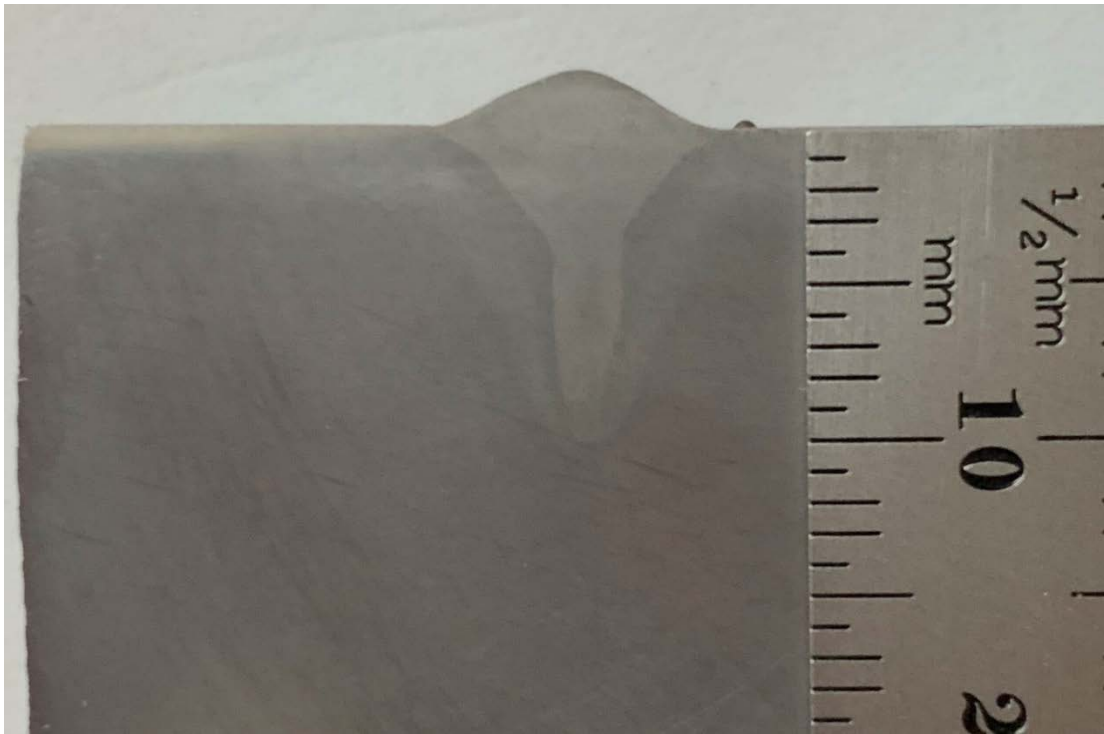


**Figure 4-6: Weld Cross-section of LP-GMAW Sample**

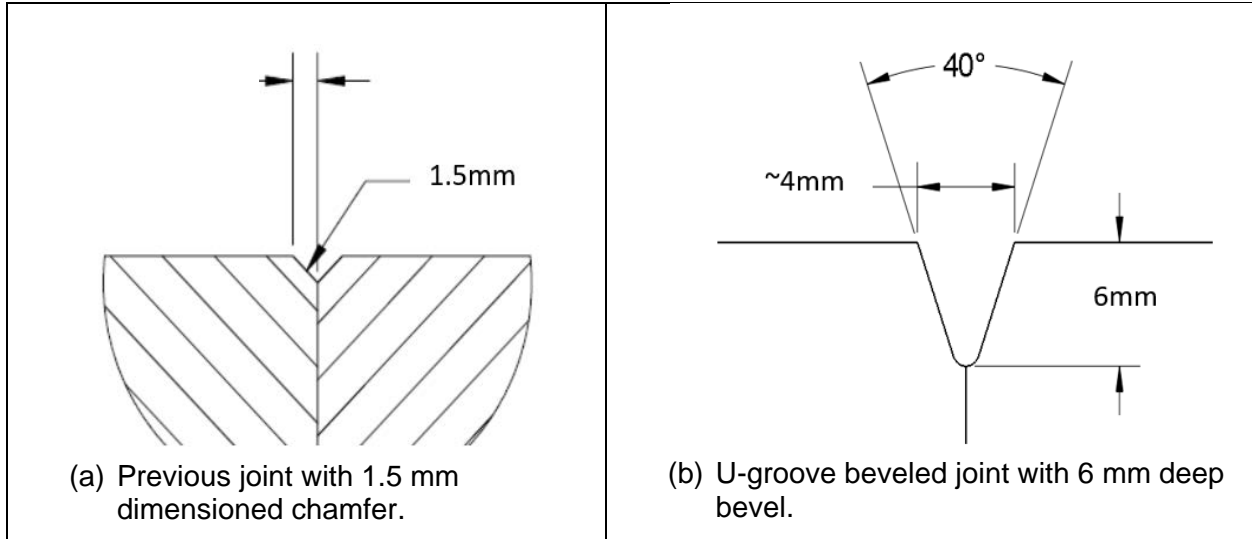


**Figure 4-7: Comparison of (a) Hybrid Laser Arc Welding (HLAW) and (b) Laser Preheated-Gas Metal Arc Weld (LP-GMAW)**

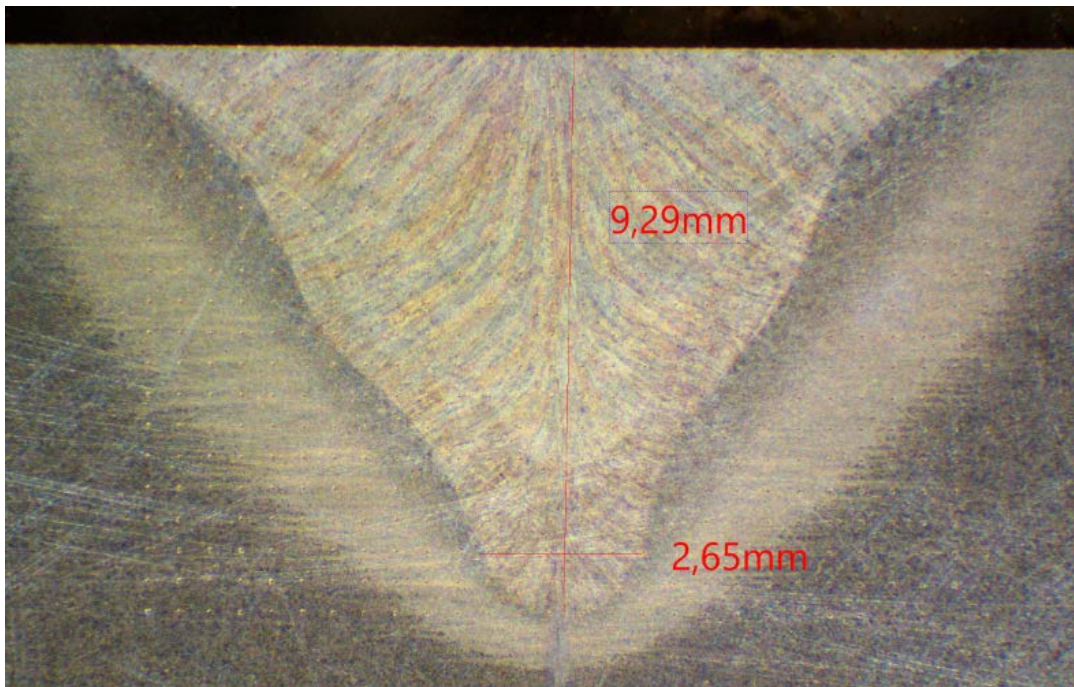


**Figure 4-8: Weld Cross-section of LP-GMAW Sample**

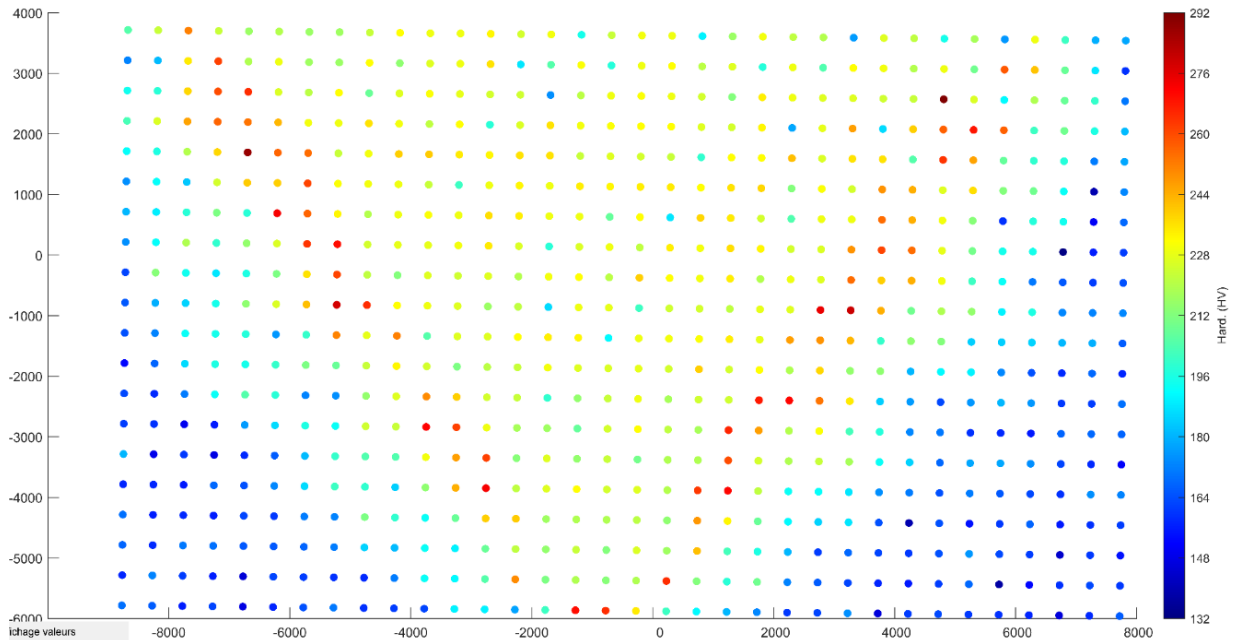


**Figure 4-9: Hardness (HV) Map Performed on Cross-section of Laser Preheated g-Gas Metal Arc Welding Partial Penetration Weld. Hardness Indent Spacing 0.5 mm. Hardness Levels on Weld, Heat Affected Zone and Base Metal All Meet Specification Requirements**

#### 4.1.4 UFC Copper Coating Development

##### 4.1.4.1 Electrodeposition Process Development

Since 2012, the NWMO has engaged prime contractor Integran Technologies, Inc. (“Integran”, Mississauga, Ontario, Canada) for the development of a copper electrodeposition technology via the use of an ultra-pure pyrophosphate (solution chemistry) system. The process was successfully scaled and demonstrated on hemi-heads. Six Serial Production hemi-heads were completed meeting all specification requirements with margin. However, challenges were encountered when applying this system consistently to lower assemblies. This is due to complexities related to the pyrophosphate chemistry, the size/geometry of the lower assembly, steel surface finish requirements and electroplating tank characteristics (e.g., flow/current density).

In 2020, a new initiative was pursued to evaluate the use of a more robust copper electrodeposition system, namely a copper sulfate/sulfuric acid-based chemistry also known as “acid copper” along with a pulse-reverse applied current. The electrodeposition of copper from an acid-based chemistry has been used extensively and has been in service for many years in the industry. Acid baths have excellent micro-throwing power (the ability of a bath to plate into small surface features) and are thus capable of filling or leveling scratches, grooves, or other undesirable surface conditions. Coupled with the use of a pulse-reverse applied current, the ability to deposit smooth uniform thick copper coatings with good physical properties may be realized.

During 2020, early-stage development to optimize a standard acid copper chemistry was pursued. Three primary processing parameters were explored (i.e., pulse reverse waveform,

current density, and temperature). Variations of these three processing parameters were studied on a small scale leading to a set of conditions capable of meeting the NWMO's two main requirements, namely purity and ductility.

The copper purity for the acid copper was determined to be 99.9+ % which meets the required specification of > 99.9 %. The microstructure of the acid copper was determined to be fine grained equiaxed (Figure 4-10) which meets specification requirements. Further optimization on purity is planned for 2021 to study the effects of processing parameters, chemical constituents and the implementation of process control via analytical techniques.

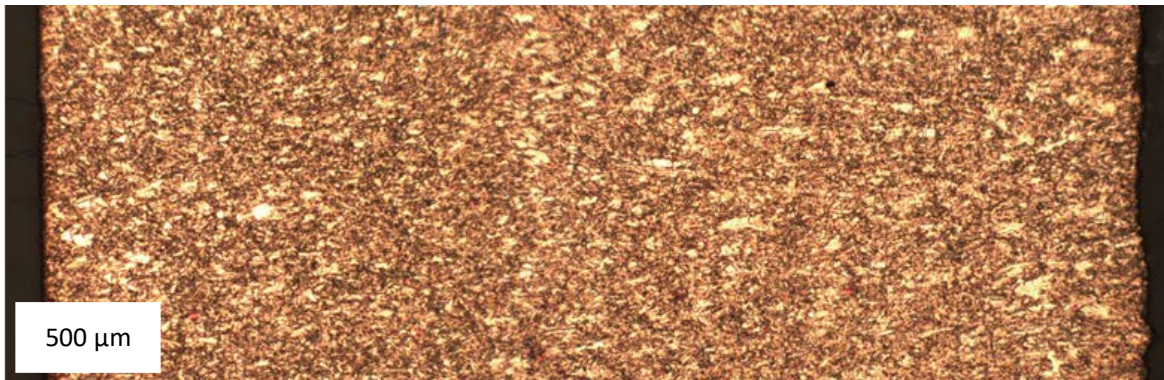
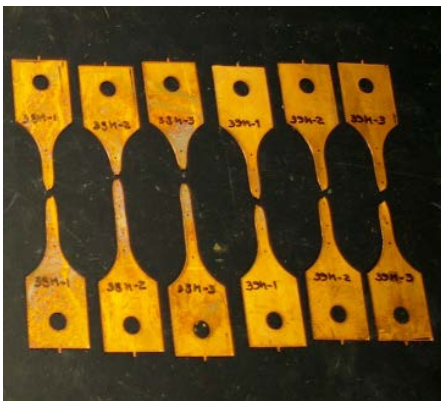
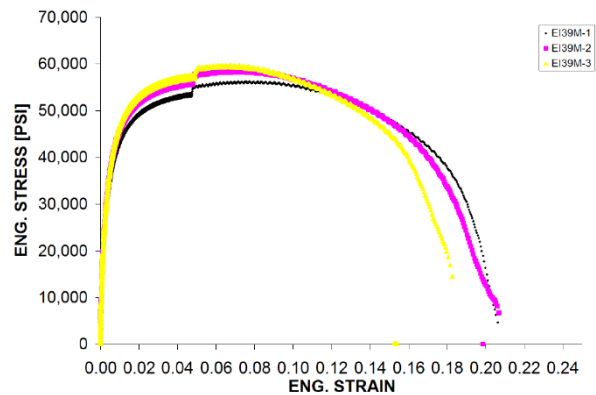


**Figure 4-10: Equiaxed Microstructure of Acid Copper Deposit – Growth Direction from Left to Right**



(a)



(b)

**Figure 4-11: Mechanical (Tensile) Testing: (a) 1 mm Thick Tensile Specimens Showing Fracture in the Gauge Length and (b) Example Stress Strain Curves**

To test copper ductility, mechanical (tensile) testing was performed on 1 mm thick specimens showing elongation values sufficiently greater than the 10 % required and up to 30 %. Figure 4-11 shows representative samples of tensile specimens with their corresponding tensile stress-strain curves.

Since purity and ductility targets were met, the next stage of development aimed to scale-up the process. In this work, long “tube” samples were processed in the component scale plating tanks with varying steel surface finishes. In general, the underlying steel machining lines were visible in the copper coating but were reduced by the action of the applied pulse reverse current;

however, it was evident that a polished steel surface was beneficial, rendering the final finish of the copper uniform and smooth (see Figure 4-12).

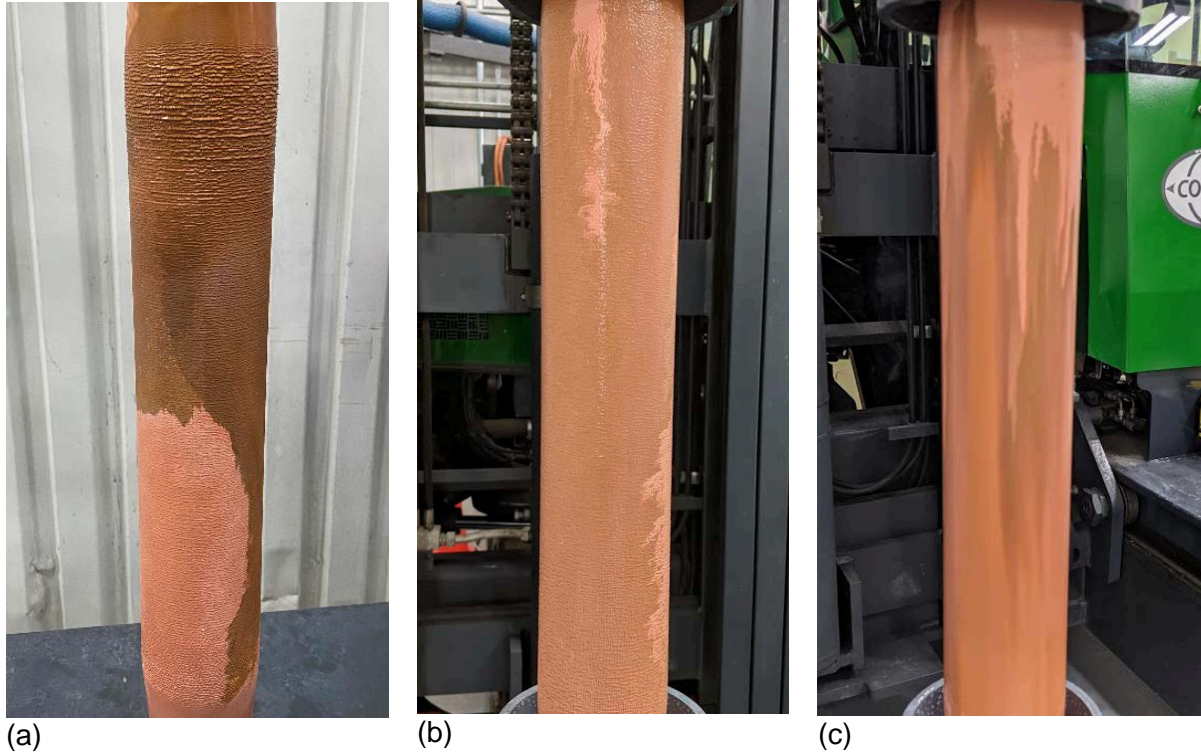


**Figure 4-12: Tube Trials Evaluated the Effect of Steel Substrate Surface Finishes: (a) Turned – 3.2  $\mu\text{m Ra}$ , (b) Turned – 1.6  $\mu\text{m Ra}$ , and (c) Abrasively Polished**

Following this lab-scale work, optimization with UFC components was initiated. With the help of computer modeling, UFC component copper thickness distribution was simulated by varying tank configurations and shielding fixture designs. By the end of 2020, upper hemi-heads were processed and found to respond well to the conditions selected.

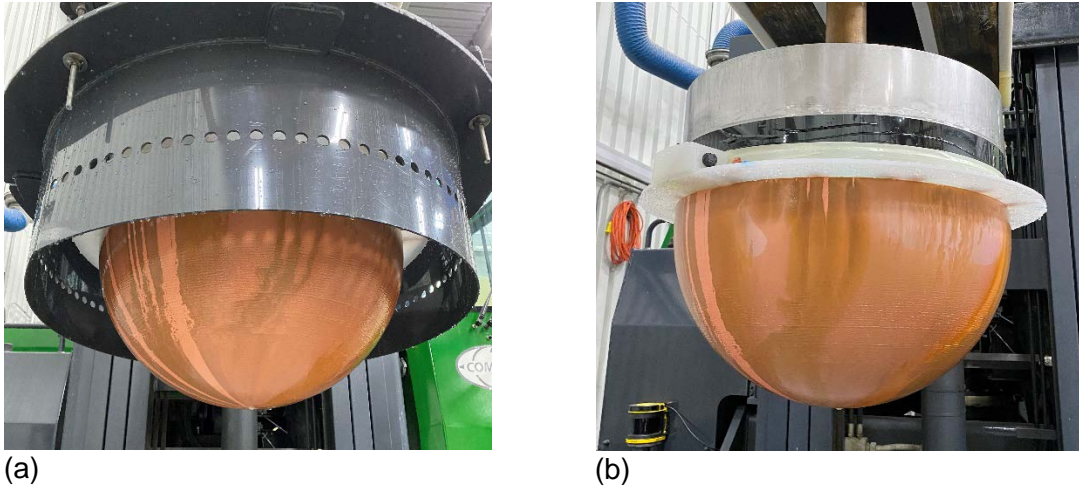


**Figure 4-13: Upper Hemi-head Optimization Run Results with Machined (turned) 1.6  $\mu\text{m}$  Ra Steel Finish: (a) with “Outer” Shield Design and (b) with “Inner” Shield Design After “Outer” Shield Removal**

Figure 4-13 shows the second upper hemi-head optimization run result with a machined (turned) 1.6  $\mu\text{m}$  Ra steel finish. The deposited thickness was found to vary a few millimeters along the arc length of the sphere. Further thickness distribution optimization is required and planned to take place in early 2021. The upper hemi-head also shows some machining line patterns growing with the deposit where the thickness is higher. Given the previous result with the tube trial, abrasive polishing will also be evaluated to help reduce the tendency for the machining line pattern growth. Reducing any substrate effects in the coating such as this will help to reduce any potential coating defects from arising during the process.

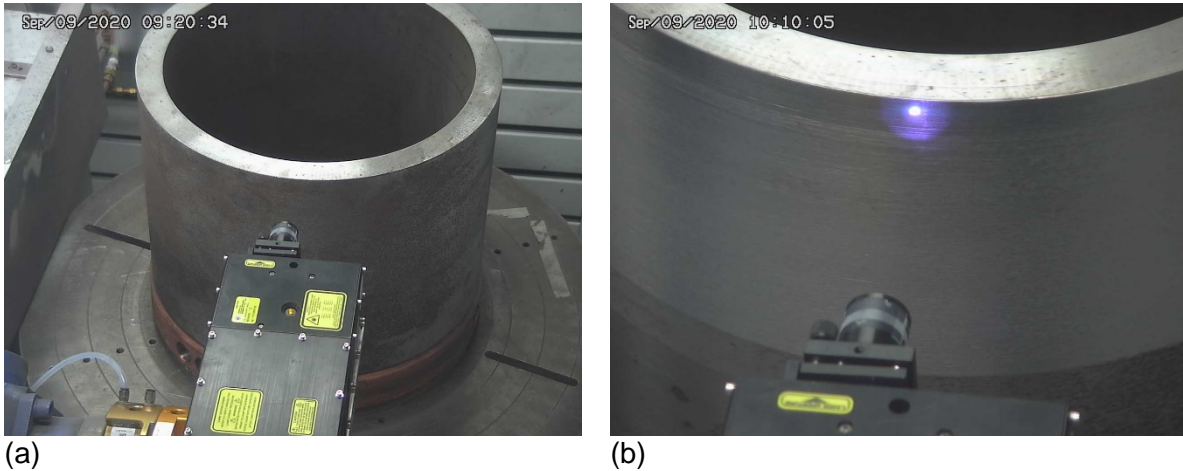
Also planned for 2021 will be process optimization for lower assemblies. In the same manner as the upper hemi-heads, computer modeling will be used to simulate various tank configurations and shielding fixture designs. At the completion of the optimization phase for UFC components, the process will be finalized and demonstrated/validated to produce a coating to the specifications required for Serial Production. In addition to non-destructive examinations, destructive testing will be performed to validate conformance with specifications such as purity, ductility, and adhesion of the coating to the steel substrate. It is expected that Serial Production will re-start to produce copper coated UFC components using the newly developed pulse reverse current acid copper system.

#### **4.1.4.2 Cold Spray Process Development**

The NWMO has engaged with the National Research Council Canada (“NRC”, Boucherville, Quebec, Canada) to develop a cold spray copper coating technology since 2012. Significant progress has been made to develop and optimize the process to meet NWMO requirements where coating application is confined to the closure weld zone of the UFC. In preparation for the Serial Production campaign, the NRC has focused development efforts on “contactless” processing techniques in anticipation of the process taking place in a radioactive hot cell environment where little to no contact with the workpiece is preferred.

In 2020, a new pulsed laser ablation technique was developed (as shown in Figure 4-14) to replace a mechanical abrasive surface preparation operation using a rotary wheel prior to performing the cold spray coating process. The surface preparation step is intended to remove any oxide, scale and/or heat tint from the preceding closure weld process and produce a clean surface to achieve optimal adhesion between the coating and the substrate. Laser ablation is

known to be effective in cleaning steel surfaces and easy to automate in a “contactless” manner.



Note: The laser spot was positioned both to the right and to the top of the of the particle jet considering the dynamics of process.

**Figure 4-14: Development of Laser Ablation Technique on Short Pipe Segments Using the Pulsed Laser Technique: (a) Short Pipe Segment Showing Heavy Oxidation and (b) Cleaned Surface Using Laser Ablation**

To test the effectiveness of the pulsed laser ablation process, several coupons were prepared with various starting surface conditions and processing parameters including surface velocity, step size, laser frequency/power, and power density. The coupons were then copper coated using the laser assisted cold spray technique developed in 2019.

Adhesion testing was performed on these coupons. The measured adhesion strength significantly exceeded the requirement of >20 MPa in all cases and the maximum strength reached approximately four times minimum (a threshold value limited by the strength of the glue used in the testing fixture).

Following completion of this work, demonstration trials using the laser ablation and laser assisted bond layer techniques were performed on lower assemblies. Figure 4-15 and Figure 4-16 show images of the demonstration trials that took place at the NRC.

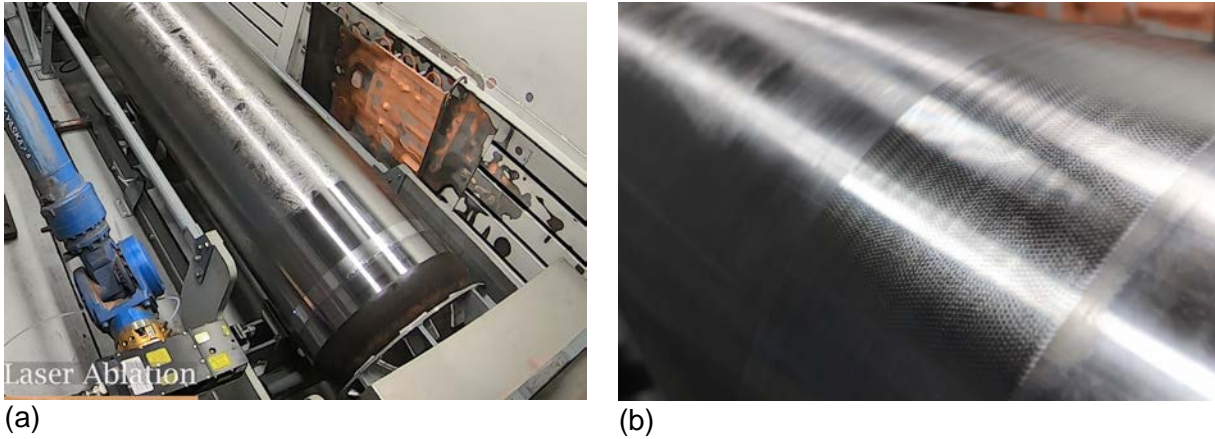


**Figure 4-15: Demonstration Trial of Laser Ablation Technique on the Lower Assembly: (a) In Process and (b) Final Surface After Laser Ablation and Before Laser Assisted Bond Layer Application**

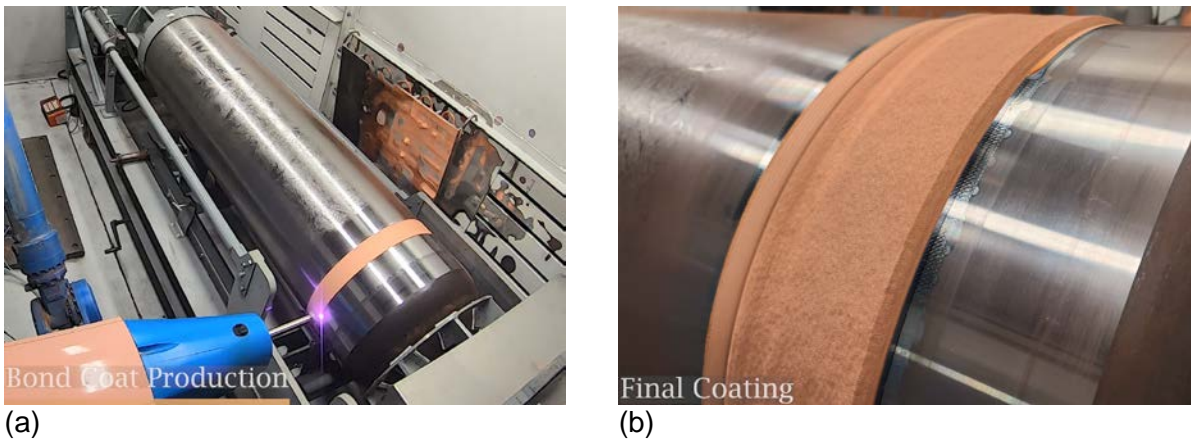


**Figure 4-16: Demonstration Copper Coating Trial on the Lower Assembly: (a) Application of the Laser Assisted Bond Layer and (b) Final Coating After Build-up to Approximately 5 mm**

At the conclusion of the demonstration trials, a reference copper cold spray process will be established in early 2021 to facilitate UFC fabrication in the Serial Production campaign. The Serial Production copper cold spray campaign will be performed in the newly established PolyCSAM Industrialization Centre (Boucherville, QC) located within the NRC facilities and operated by Polycontrols, Inc. (Brossard, QC). Efforts to facilitate technology transfer were initiated in 2020 with the expectation that a full process qualification and demonstration be completed in the first half of 2021 with Serial Production to follow.

#### 4.1.4.3 Technical Research on Copper Coating Materials

In 2020, technical research with focus on the characterization of the copper coating materials was advanced in partnership with the University of Toronto (Toronto, ON). Three journal articles with the following titles were published:

1. Microstructural characterization of copper coatings in development for application to used nuclear fuel containers (Li et al., 2020);

2. Reducing complex microstructural heterogeneity in electrodeposited and cold sprayed copper coating junctions (Tam et al., 2020); and
3. Factors affecting the ductility of cold-sprayed copper coatings (Guerreiro et al., 2020).

The first publication is focused on providing an overview of the specific microstructural characteristics of both the electrodeposited and copper cold sprayed materials. The main technique used to characterize the materials was a combination of scanning electron microscopy (SEM) and electron backscattered diffraction (EBSD). This combined technique yielded critical information such as grain size, grain boundary character distribution and crystallographic texture which all play a role in better understanding of the mechanical and corrosion behavior of these materials (see Figure 4-17).

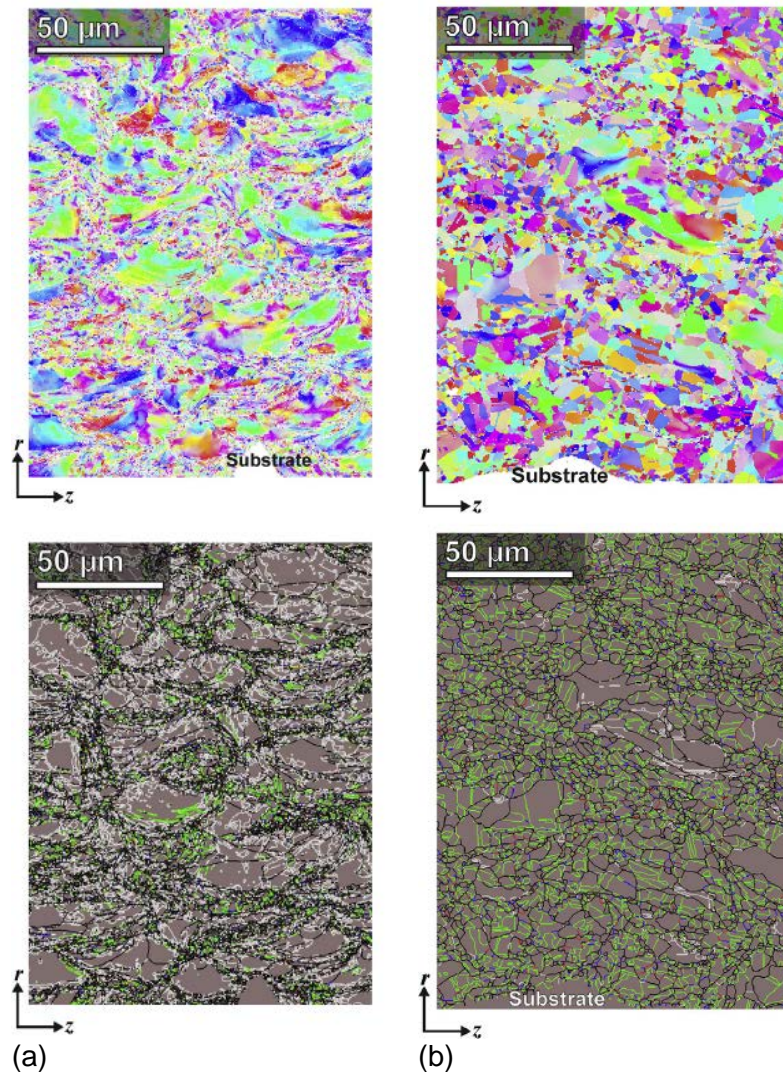


**Figure 4-17: Scanning Electron Microscopy (SEM)-Electron Back Scattered Diffraction (EBSD) Images of Cold Sprayed Copper Grain Orientation (top) and Grain Boundary Character Distribution (bottom): (a) As-sprayed and (b) After Heat Treatment at 350°C for 1 hr (Li et al., 2020)**

Building on this work, the second publication looks at the interaction of both the cold sprayed copper and electrodeposited copper at their junction. With particular emphasis on cold sprayed copper, image analysis revealed that the heterogeneity of the microstructure is significantly reduced after heat treatment (see Figure 4-18). With a more homogeneous microstructure, it is likely that an increasingly uniform mechanical and corrosion behaviour may be expected. This in turn provides a better understanding of how the copper can meet the demands of the UFC's service life and where improvements can be made to optimize the coating's performance. Further investigation on this subject is continuing at the University of Toronto.

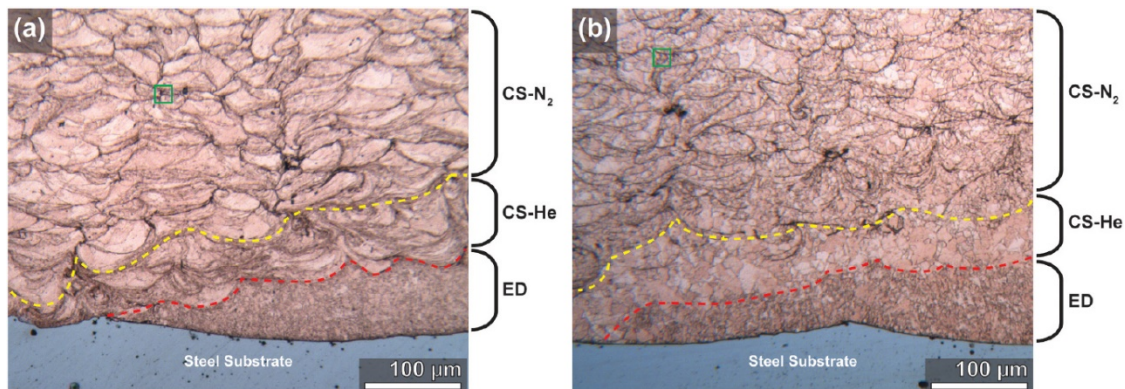


**Figure 4-18: Optical Images of the Electrodeposited (ED) and Cold Spray (CS) Copper Junction: (a) As-sprayed and (b) After Heat Treatment at 350°C for 1 hr (Tam et al., 2020)**

Finally, the third publication focused on specific aspects of the ductility of copper, and specifically effects from the thermal treatment, the powder characteristics and particle size/shape, all as part of the coating optimization. In brief, this effort was focused on quantifying the ductility of copper coatings as these parameters are changed, and the data demonstrated that ductility could range from low values of less than 10% up to nearly 40%.

#### 4.1.5 UFC Non-Destructive Examination

##### 4.1.5.1 Development of Non-Destructive Examination Acceptance Criteria for Closure Weld

The UFC will be inspected using non-destructive examination (NDE) methods at multiple stages of the manufacturing process. Ultrasonic testing and eddy current testing are used to detect volumetric and surface flaws, respectively, in the UFC steel structural vessel and copper coating. Flaw acceptance criteria are used to determine whether an indication detected by the NDE techniques can be acceptable for service.

The UFC weld joint includes a shallow partial penetration weld that is outside the ASME Boiler and Pressure Vessel Code (BPVC) Section III design. As a result, the NDE acceptance criteria in ASME BPVC Section III cannot be directly applied to the UFC weld joint. In the absence of defined ASME acceptance criteria, the weld flaw acceptance criteria for the inspection of earlier UFC prototypes were based on the threshold detection limits of the NDE equipment. This approach, while considered conservative, provided valuable feedback on the types and sizes of indications and aided in continued weld process development. To resolve this issue, a work package was initiated in 2020 to review the basis of the ASME criteria and redefine the flaw acceptance criteria for the UFC partial penetration weld joint based on the approach used by ASME Section III Division 3 Subsection WC (i.e., storage containments). The development work included simulation of container structural performance using finite element analysis (FEA), focusing on porosity and inclusion flaws. The limiting size, shape and orientation of the flaw

were determined based on the stress interaction between the flaw and the root of the partial penetration weld. Figure 4-19 shows the plastic zones (i.e., colored areas) in the weld region with an artificial flaw (e.g., a subsurface pore or a surface breaking pore). A variety of flaw configurations (different sizes and/or locations) were tested to find the limiting case, where a full plastic zone forms penetrating the entire weld thickness. A set of flaw acceptance criteria suitable for the UFC weld joint were then developed by the NWMO team and independently reviewed by third party experts and NWMO's NDE service supplier. The criteria will be adopted in NWMO's UFC inspection procedure and applied in the Serial Production campaign in 2020 and beyond.

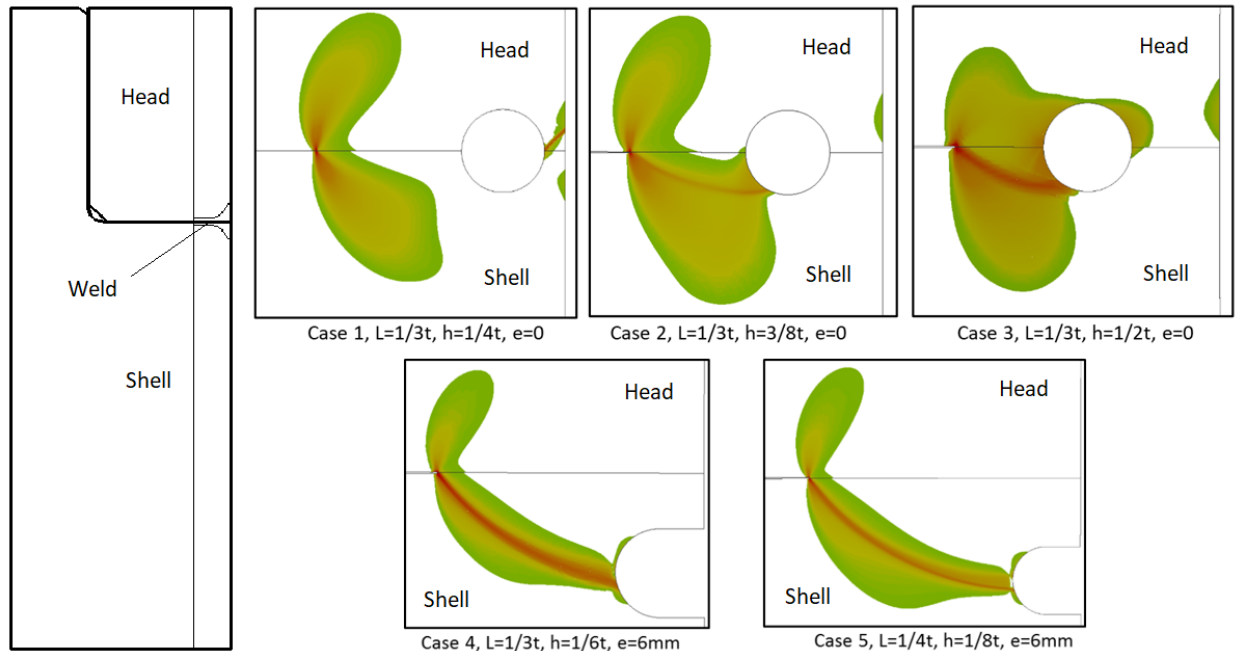


**Figure 4-19: Finite Element Analysis (FEA) Modelling of Plastic Zones (Colored Areas) Between the Partial Penetration Weld Root and Pores: Subsurface Pores in Case 1, 2 and 3, and Surface Breaking Pores in Case 4 and 5**

#### 4.1.5.2 NDE Equipment Development

In 2020, the Non-Destructive Examination (NDE) program focused on equipment upgrades to perform inspection of copper coated UFC components. Previously, ultrasonic and eddy current inspections were conducted by NDE technicians using hand-held probes against a manual grid pattern to ensure coverage. In order to improve repeatability and data quality, NWMO's NDE vendor, Nucleom Inc. (Quebec City, QC) designed and fabricated scanning mechanisms for mounting probes rigidly and accurately against UFC part surfaces. The scanning mechanisms attach to the NDE inspection benches as shown in Figure 4-20 (hemi-head scanning mechanism) and Figure 4-21 (lower assembly/UFC scanning mechanism). These scanning mechanisms allow for high consistency and repeatability, precise positioning of probes, and subsequent locating of defects. In addition, probe-to-surface pressure is kept constant (compared to manual handling), reducing signal variation and increasing inspection quality. These scanning mechanisms shall be used for Serial Production copper coating inspections in 2021.



**Figure 4-20: Hemi-head Scanning Mechanism with Eddy Current Probe Attached.**



**Figure 4-21: Lower Assembly/Used Fuel Container (UFC) Scanning Mechanism with Ultrasonic Probe Attached**

### 4.1.6 UFC Material Testing

In 2020, the NWMO continued mechanical testing of the UFC materials to establish a material property database. Tensile testing of the UFC carbon steel base materials to obtain the strain hardening properties at room and elevated temperatures is ongoing at Cambridge Materials Testing Limited (Cambridge, ON). This testing will be completed in early 2021.

Charpy V-notch impact tests were also conducted by the same vendor for the UFC carbon steel base and weld materials to establish the ductile-to-brittle transition curve under impact loads (see Figure 4-22 for one of the test results). The transition curve will be used to ensure that the UFC will not be subject to brittle fracture at the lowest service temperature. Due to the size of the partial penetration weld joint, sub-size test samples were used. The acceptance criteria for the sub-size tests have been proposed based on linear correlation between the sub-size and full-size specimens. Comparisons between full size and sub-size Charpy V-notch impact tests were also conducted on the base metal to examine the correlation method.

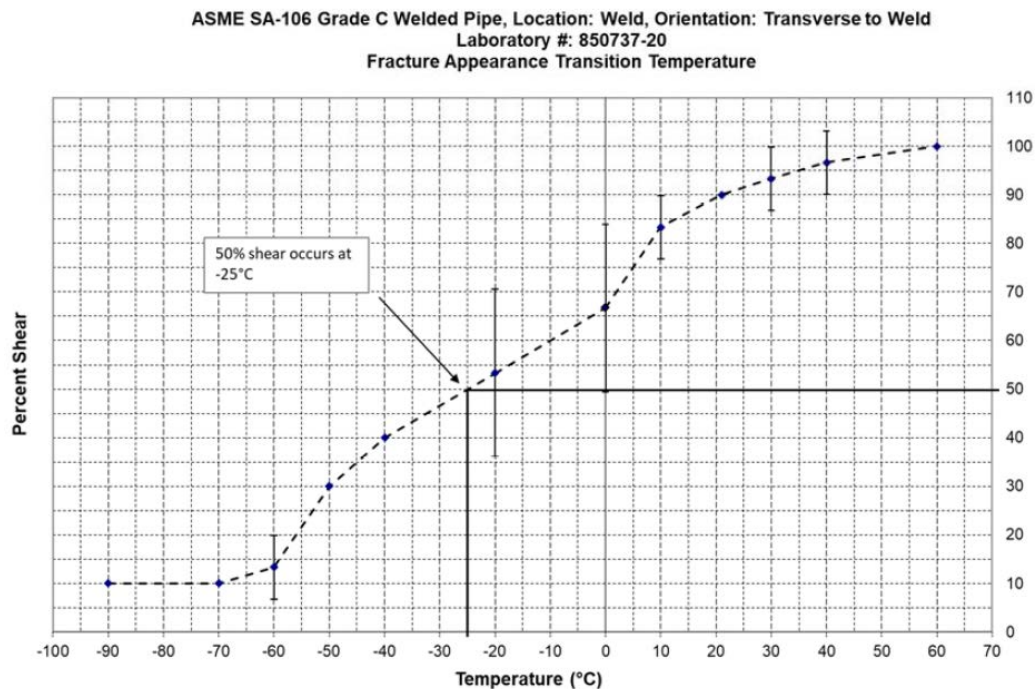


**Figure 4-22: Brittle-to-Ductile Transition Curve (Percent Shear vs. Temperature) of the As-Deposited Weld Material in the Used Fuel Container (UFC)**

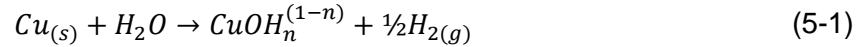
## 4.2 COPPER DURABILITY

### 4.2.1 Used Fuel Container Corrosion Studies

#### 4.2.1.1 Anoxic Corrosion of Copper

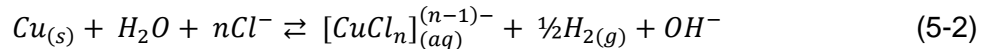
Although oxygen will be present in the DGR for a brief period following closure and decommissioning, anoxic conditions will persist for the majority of the repository's lifetime. Using thermodynamics, it is possible to predict very long lifetimes of copper in these conditions, an assertion supported by natural analogues such as "native" copper, which can be excavated as a metallic species that is millions or even billions of years old. Despite this, in some experiments

where copper is placed in oxygen-free water, trace amounts of hydrogen have been detected, and some researchers have claimed the hydrogen is a corrosion product of Equation (5-1).

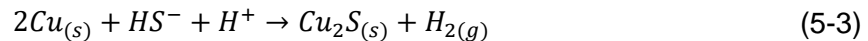


Despite being forbidden by classical thermodynamics and the inability of independent researchers to reproduce experimental results or unequivocally identify the copper corrosion product, “CuOH<sub>n</sub><sup>(1-n)</sup>”, the existence of such a mechanism must be validated or invalidated by the NWMO. In fact, compelling evidence now exists from SKB (Hedin et al. 2018) that the process represented by Equation (5-1) does not occur, but that exposures of copper to water allow for the release of hydrogen trapped during the copper manufacturing process, and this effect can be eliminated by careful pre-treatment of copper before exposure to water.

Equation (5-1) is related to a second, anoxic corrosion of copper that occurs in acidic, highly saline solutions according to Equation (5-2). As per the above example, some observations of hydrogen have been made during immersion of copper in brine; however, in this case trace hydrogen is expected as the system comes to equilibrium. In a DGR, the forward (corrosion) reaction will be suppressed owing to the neutral (i.e., not acidic) pH, the low diffusivity of the copper-chloride reaction products through bentonite clay, and the dissolved hydrogen in the groundwater that is present in the anoxic condition. At extremely high brine concentrations (i.e., 5 to 10 X seawater), there is some question regarding the precise equilibrium conditions, which require characterization and quantification.



The third process of interest, anoxic copper corrosion in the presence of sulphide, Equation (5-3), is afforded the largest UFC copper corrosion allowance (Hall et al. 2021). Although Canadian groundwater contains virtually no sulphide, it is possible that microorganisms existing far away from the UFC could produce sulphide from their metabolic processes, which would enter the groundwater. Due to the presence of the bentonite buffer, diffusion of sulphide inward to the UFC will be slow. However, once the sulphide reaches the container corrosion proceeds quickly; thus, more information is required with respect to the mechanism of this process, as well as the affect other groundwater species may have on the process or the products of the process.



Work being conducted by NWMO at CanmetMATERIALS (Hamilton, Canada) in collaboration with the University of Toronto investigates the individual the combined effects of Equation 5-3 along with pH effects. This work utilizes a specialized corrosion cell, depicted in Figure 4-23 (a) and (b), which maintains an anoxic environment at 75 °C while allowing for the introduction of chemical species (gas or liquid) into the cell. A detailed description of this apparatus was published by Senior et al. (2020a) in 2020. Hydrogen is measured by purging the headspace of the cell and the amount is correlated to a rate of corrosion by assuming the reactions shown in Equation 5-3 take place. Notably, the release of trapped hydrogen from within the copper, or the production of hydrogen from other corrosion reactions within the cell (i.e., through the interaction of steels and water) will be assumed to be copper corrosion using this calculation method, and this will overestimate copper corrosion (Senior et al. 2019). Similarly, hydrogen produced via corrosion that is absorbed by the metal will be missed in a corrosion calculation, although this

process is not expected. Nonetheless, a representative graph of the results is shown in Figure 4-23 (c) which plots the presumed corrosion rate versus time for deionised water cells and a strong brine cell which are periodically dosed with gaseous  $H_2S$  over the course of approximately four and a half years.

The corrosion experiments are ongoing, but some consistent trends are exhibited by the data following the approximately four-and-a-half-year duration of the program. In pure water, hydrogen was evolved, and initial corrosion rates were calculated to be less than 0.5 nm/year before falling below the detection limit of the experiment. Similar results were seen for dilute and strong chloride solutions; that is, an initial small release of hydrogen followed by a gradual decline with time to near or below the detection limit as shown in Figure 4-23 (c). Upon addition of small concentrations of  $H_2S$  to each cell, which simulates the effects of microbially produced sulfide species, small initial releases of hydrogen are observed followed by a return to corrosion rates which near the detection limit of the hydrogen probe. It is also important to note that each cell underwent integrity and leak testing at the end of 2019 to ensure that hydrogen was not escaping the cells. These tests will continue with additional spiking of  $H_2S$  gas, altering electrolyte pH, and increasing chloride concentrations to investigate the behaviour of the copper. When complete, test cells will be disassembled and the copper interrogated for the presence of absorbed hydrogen and the makeup of corrosion products. More detailed results from this program have been published by Senior et al. (2019) and (2020b).

As mentioned above, the introduction of sulfide to either saline or pure water environments did result in hydrogen evolution, producing initial low corrosion rates equivalent to 0.1 and 0.2 nm/year, respectively, which drop to the detection limit of the experiment over several months. However, even if for a damage assessment, it was assumed these rates were sustained, the largest of these miniscule rates would produce less than 0.25 mm of damage in 1,000,000 years and are consistent with the conservative NWMO total corrosion allowance of 1.204 mm over that period of time (Hall et al. 2021).

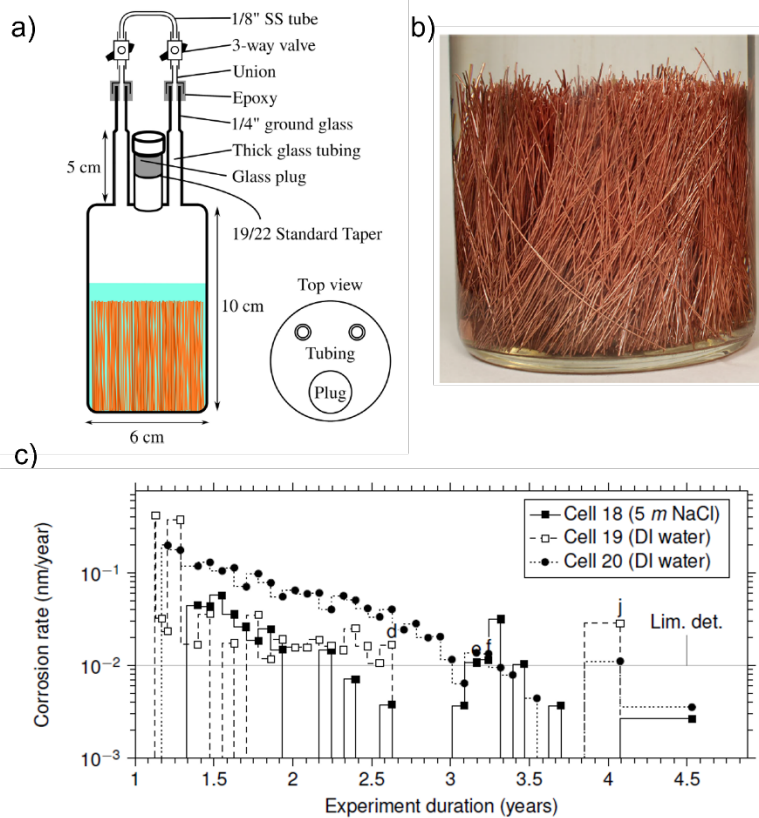


**Figure 4-23: (a) Schematic of Test Cells for Anoxic Copper Corrosion Investigations at CanmetMATERIALS; (b) Photo of Copper Specimens in a Test Cell During an Experiment; (c) Calculated Copper Corrosion Rates Based on Hydrogen Measurements for Two Deionised Cells and One Concentrated Brine Cell Over Approximately Four and a Half Years (Senior et al. 2020b)**

#### 4.2.1.2 Corrosion of Copper Coatings

With the development of copper coatings, it has become necessary to investigate different copper forms to ensure that corrosion does not occur preferentially via mechanisms that do not occur for wrought coppers. Despite many years of effort, little difference has been found among the samples, regardless of test method. Only very slight differences can be seen only where extensive cycles of electrical currents to initiate copper oxidation (i.e., to artificially simulate corrosion) are used. In these experiments, there is some evidence that the copper coatings made by electrodeposition or cold spray undergo a very minor preferential grain etching, such that corrosion depth may be very slightly greater near grain boundaries. Thus, since late 2019, the NWMO has been focusing on identifying or narrowing the chemistry requirements for copper coatings. There is also an intent to create a purity specification for copper coatings that emphasizes corrosion performance which also considers trace chemical species that may be incorporated into the coating during the manufacturing process. Therefore, a new program has been initiated to evaluate copper coatings exhibiting a range of impurities and determine the concentration limits of the individual constituents by which the reference (wrought) corrosion allowance can be maintained. The outcome of this program aims to provide additional information required for the creation of a corrosion-based purity specification for the copper coatings intended for the UFC.

### 4.2.1.3 Corrosion of Copper in Radiolytic Environments

The copper coated UFC will be exposed to a continuous flux of  $\gamma$ -radiation emitted from the decay of radionuclides in the used fuel. Although the  $\gamma$ -radiation does not affect the metal directly, any trapped water or humid air near the UFC will decompose to produce redox-active and acidic species that can affect the corrosion of the copper coating. A fundamental understanding of the copper corrosion behaviour in the presence of  $\gamma$ -radiation is needed to predict the long-term corrosion progression of the copper with confidence and assure its long-term integrity.

An approach was taken to decouple the effects of radiation by performing corrosion experiments in solutions containing the important radiolysis species (i.e.,  $\text{H}_2\text{O}_2$ ,  $\text{H}^+$ , and  $\text{NO}_3^-$ ) and in solutions in the presence of radiation at dose rate of 1.4 kGy/h (Wren et al. 2019). Periodic solution analysis (i.e., pH and copper ions measurements) along with surface oxides characterization allowed for the identification of the stages of corrosion behaviour and how they are influenced by  $\gamma$ -radiation (Figure 4-24). Based on these analyses, the duration of Stage 1 is short due to the production of acidic radiolysis products that decrease the pH very quickly and thereby increase the concentration of copper ions to a higher amount than in the absence of radiation. The elevated concentration of copper in solution leads to earlier formation of  $\text{Cu}(\text{OH})_2$  compared with non-irradiated system. As corrosion progresses, Stage 3 involves the precipitation of  $\text{Cu}_2\text{O}$  which continues to deposit and undergoes conversion to  $\text{Cu}_2(\text{NO}_3)(\text{OH})_3$  under continuous flux of radiation (Stage 4).

Results of corrosion experiment in the presence of chemically added radiolysis species indicated that the precipitation of copper oxide is dependent on both concentrations of  $\text{H}_2\text{O}_2$  and nitrate. It was shown that higher initial concentrations of  $\text{H}_2\text{O}_2$  lead to more copper oxide is growth and the oxide growth was hindered in the presence of nitrate likely due to slow rate of nitrate reduction reaction. The results from this study further confirmed that proton (i.e.  $\text{H}^+$ ) has a much greater effect on the initial copper dissolution than the oxidizing power of the solution containing  $\text{H}_2\text{O}_2$  and nitrate.

The results from these studies will be compiled and published in graduate theses and peer-reviewed journals.

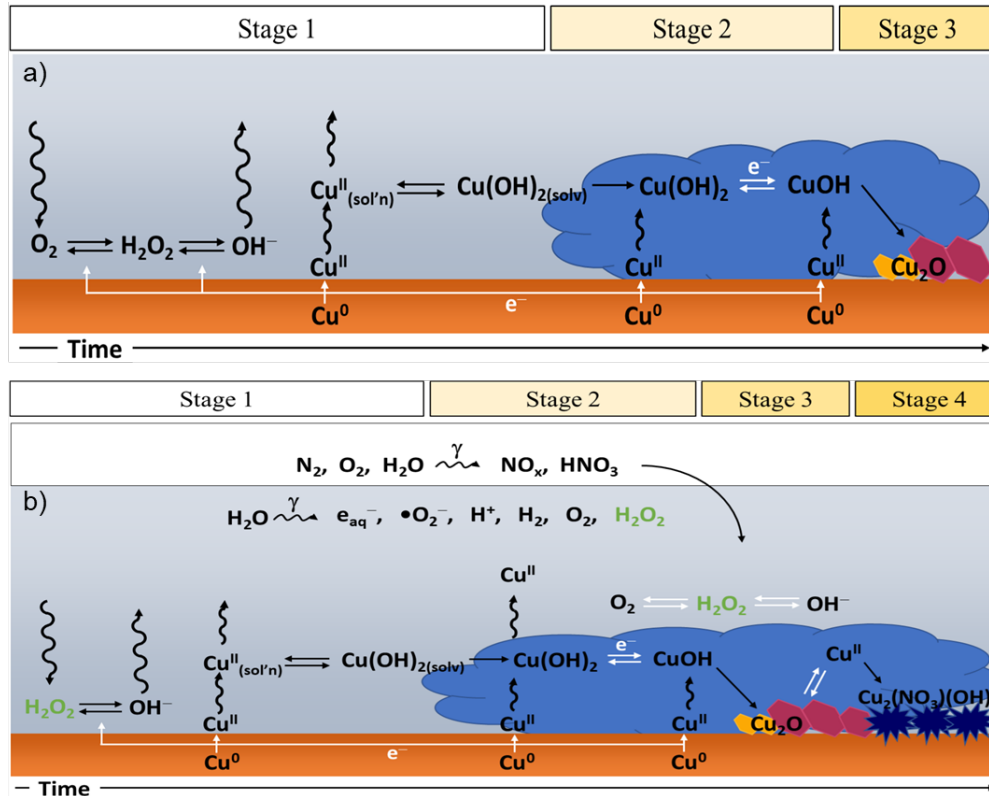


**Figure 4-24: Copper Corrosion Mechanism: a) In the Absence of Ionizing Radiation with Chemically Added H<sub>2</sub>O<sub>2</sub>, and b) In the Presence of Radiation (white arrows indicate electron transfer reactions)**

#### 4.2.1.4 Oxidic Corrosion of Copper

Following closure of a DGR, the conditions will evolve from an initial warm oxidic period to a long-term cool, anoxic period (Guo 2017). As a result, the maximum depth of copper corrosion during the early oxidic stage has been evaluated based on the quantity of O<sub>2</sub> trapped when the DGR is sealed (Hall et al. 2018).

The inventory of trapped oxygen was determined to be 13 mol per UFC (Hall et al. 2018), which corresponds to a maximum corrosion depth of 81 μm. Ongoing work on oxidic corrosion focusses on validating the corrosion mechanism, which is presumed to be via uniform, and not non-uniform, corrosion.

#### 4.2.2 Internal Corrosion of UFC

The nature of the environment inside the UFC has been described by Wu et al. (2019). Although the radiation fields are higher on the inside of the container, any effect on the corrosion of the C-steel vessel is limited by the availability of H<sub>2</sub>O. Wu et al. (2019) considered various scenarios based on whether or not the UFC internal void space was inerted with Ar during sealing and whether any fuel pencils were water-logged due to incomplete drying prior to encapsulation. Between zero and 2.2 mol O<sub>2</sub>(g) and between 0.34 and 4.5 mol H<sub>2</sub>O were considered in the various scenarios. The conclusion from the analysis was that due in part to the limited inventories of O<sub>2</sub> and H<sub>2</sub>O, there is negligible risk from general corrosion, pitting, crevice, corrosion, or stress corrosion cracking of the closure weld. In addition, the fast neutron fluence was insufficient to cause radiation embrittlement of the C-steel vessel. To complement the mass balance analysis and previous experimental studies (Wu et al. 2017, Guo et al.

2020a,b), development of a quantitative rate model for C-steel corrosion is underway as a function of solution parameters over the ranges anticipated inside the UFC. In parallel, further experimental studies are ongoing to build a database on C-steel corrosion as a function of solution conditions. The database will be used to extract the values of rate parameters for the rate and flux equations included in the model during model development, and to provide data for model validation and refinement

### **4.2.3 Microbial Studies**

The design of the repository emplacement room utilizes HCB to suppress microbiological activity near the UFC. However, as microbiological activity may occur within bentonite that is improperly placed, as well as elsewhere underground, considerable efforts are being made to study it. Recent work has focused specifically on extraction and characterization of the DNA held within the bentonite clay, as this material is present in extremely low quantities (Engel et al. 2019a). Much of this work is conducted in concert with corrosion and bentonite programs, as well as within work that is performed at the underground research laboratories (Mont Terri and Grimsel) in Switzerland (Engel et al. 2019b). To supplement the in-situ work being performed in underground labs, pressure vessels (Figure 4-25(a)) have also been designed, fabricated and commissioned to perform a large number of ex-situ experiments at Western University. Figure 4-25(b) shows the bentonite plug that is extracted from a pressure vessel following an experiment. A custom bentonite press is utilized to core the center of the bentonite plug to allow for comparison between the inner and outer bentonite behaviour. A schematic illustrating the locations of copper samples for corrosion analysis and bentonite samples for microbiological and water analysis are shown in Figure 4-25(c). In 2020, an initial set of scoping experiments investigating different bentonite dry densities and experiment durations were continued from 2019 with the goal of comparing the results of similar experiments conducted by Stroes-Gascoyne et al. (2010) thereby validating the experimental apparatus.

Tests of one and three months were completed in 2020 and corrosion and microbiological analyses are underway. Initial results indicate that the bentonite in one-month experiments does not reach full saturation and are therefore representative of an early stage DGR while water ingress from the surrounding rock is occurring. Bentonite extracted from three-month experiments appear much more uniform with respect to colour indicating a more even wetting of the bentonite, however, the interior of the bentonite plug does not yet appear to be saturated. It is expected that the longer-term experiments (6 and 12 months) will approach full saturation and be representative of the long-term behaviour of a DGR. Corrosion and microbiology results will become available in 2021 and will be used to compare to previous work by Stroes-Gascoyne et al. (2010). Should these results be comparable to the work by Stroes-Gascoyne et al. (2010) in aerobic conditions, follow up experiments will be conducted to investigate saline waters in an anoxic environment for up to two years duration. Such an experimental campaign which has simulated a range of possible DGR environments has not been conducted in a laboratory setting before.

#### **4.2.3.1 Mont Terri HT (Hydrogen Transfer) Project**

The Hydrogen Transfer experiment occurs at the Mont Terri underground rock laboratory in Switzerland. This is an in situ experimental study investigating the interactions and transport of hydrogen in a borehole in an Opalinus Clay environment. Hydrogen is injected near the borehole mouth and borehole water is analyzed to track the generation/consumption of the hydrogen. To date, it has been seen that hydrogen consumption does occur within the borehole and this has been attributed to microbiological activity. In order to more accurately track what consumption pathways exist, injection of deuterium has commenced which will allow for the

unambiguous assignment of the sources and sinks of hydrogen. Once complete, computer modelling of these processes will commence to better understand the mechanisms at play.

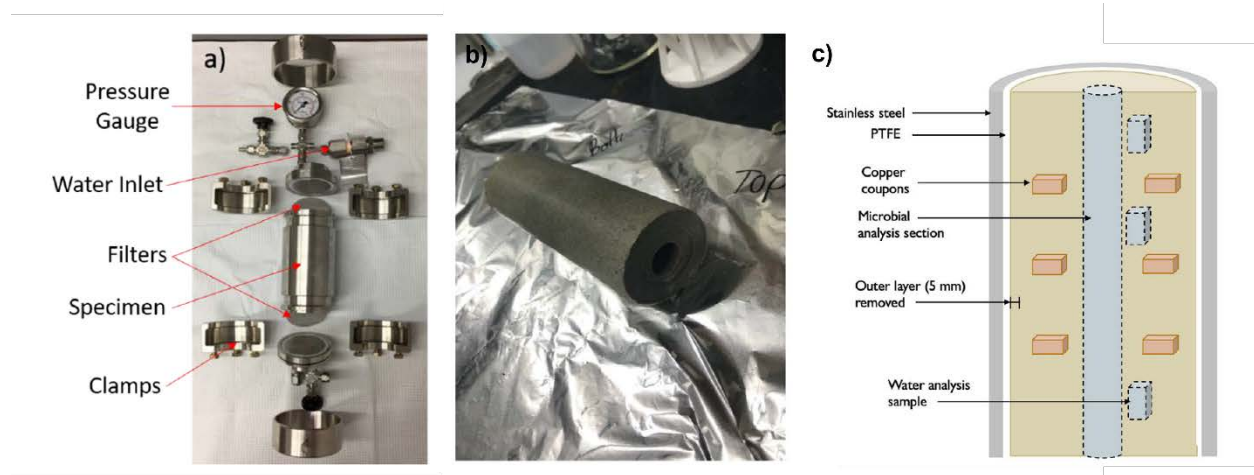


**Figure 4-25: (a) Components of a Pressure Vessel for Ex-situ Microbiological and Corrosion Analyses; (b) A Cored Bentonite Plug Following Water Exposure in a Pressure Vessel and Prior to Sample Extraction for Analysis; (c) Schematic of a Pressure Vessel Indicating the Location of Copper Samples and Bentonite Samples Extracted for Microbiological and Water Analysis**

#### 4.2.4 Field Deployments

While much work in the Engineered Barrier Science group has focused on laboratory-based experiments which focus on fundamental processes related to copper and bentonite integrity, more recent work is focused on the synergistic behaviour of copper embedded in bentonite deployed in DGR-like environments. This work is based off experience working with international collaborators in the Grimsel and Mont Terri Underground Research Laboratories (URLs) in Switzerland. However, in 2020, the NWMO has adapted these experimental methodologies (so-called “module experiments”) and applied them in environments which more closely resemble potential Canadian DGR sites.

##### 4.2.4.1 Ocean Deployments

Starting in 2019, in partnership with Ocean Networks Canada, the NWMO fabricated custom modules which contain copper coupons embedded in bentonite inside porous stainless-steel modules and deployed them in different locations in the Pacific Ocean. The modules contain holes to allow ingress of water but are lined with a sintered steel mesh which prevents the extrusion of bentonite out of the module, thus maintaining the density of the bentonite. An initial scoping experiment was conducted at Saanich Inlet for 6 months at ~90 m depth and followed by 1.5-year experiment deployed at Barkley Canyon at ~1000 m depth. These experiments are DGR-like in that they are highly saline, low oxygen, microbially active and high-pressure environments. Thus, while not identical to potential DGR conditions, these experiments will provide valuable information on engineered barrier behaviour, particularly under high pressures for long periods of time. Ultimately, the results of these experiments will contribute to defining important NWMO engineering specifications such as gapfill material dry density and copper purity. While results from this program are currently preliminary, they are consistent with the low corrosion rates and microbiological behaviour similar experiments conducted in international URLs.



**Figure 4-26: (a) Photos of the Test Modules Containing Copper Embedded in Bentonite Clay on the Immersion Platform; (b) Recovery of Modules Following a 6-month Test Immersion in the Pacific Ocean**

#### 4.2.4.2 NWMO Borehole Deployments

Over the course of 2020, the NWMO Site Investigations team has continued to conduct borehole drilling operations in NWMO borehole regions. This provides a unique opportunity to test NWMO engineered barrier components (copper embedded in bentonite) in-situ at a potential future NWMO DGR site. This year, a custom deployment system, modeled after the module experiments describe in section 4.2.3 was designed and fabricated for deployment in an NWMO borehole. Figure 4-27 shows the various components of this test system. Figure 4-27(a) and (b) show the module exterior and interior, respectively, which will contain the copper and bentonite samples. Figure 4-27(c) shows the custom packers which will be used to suspend the modules near the repository horizon (~500 m below ground) and isolate the interval in which the modules sit to create a closed system. This will mimic conditions that will be present in an actual NWMO DGR. Modules will be retrieved every 2-3 years for up to 10 years and sent to NWMO academic contractors for corrosion and microbiological analysis. This first of a kind experiment will serve to increase confidence in the proposed engineered barrier system and will be compared with other international and lab-based programs to confirm the NWMO copper corrosion allowance. The deployment of this experiment will occur in 2021 in an NWMO siting borehole.



**Figure 4-27: (a) External View of Borehole Test Module Measuring Approximately 50 cm in Length; (b) Internal View of Test Module Showing Sintered Steel Mesh Which Lines the Modules; (c) Custom Made Packers (black) and Supporting Equipment to Install the Borehole Experiments.**

#### 4.2.4.3 Mont Terri IC-A (Iron Corrosion A)

In collaboration with the Swiss nuclear waste management organization, Nagra, NWMO are contributors to the IC-A (iron corrosion A) project at the Mont Terri underground research lab. This project is focused on studying the long-term synergistic behaviour of copper and steel embedded in bentonite and stored in a borehole in the native groundwater of the Mont Terri lab. These experiments utilize the porous module apparatus similar to the experiments described in sections 4.2.4.1 and 4.2.4.2. Modules are retrieved every one to two years and are dissected to retrieve samples of bentonite for microbiological analysis and metallic coupons for corrosion rate measurements. To date, modules which were placed in the borehole for 34 months have been retrieved and analyzed. Via mass-loss measurements recorded on electrodeposited and cold spray copper samples, average corrosion rates of 0.02  $\mu\text{m}/\text{yr}$  to 0.17  $\mu\text{m}/\text{yr}$  have been calculated which are well in line with the expected behaviour.

#### 4.2.5 Corrosion Modelling

##### 4.2.5.1 Localised Corrosion Modelling

The development of a probabilistic model to predict the extent of localised (pitting) corrosion of copper canisters was on-going in 2020. The model accounts for not only the stochastic nature of pitting corrosion but also the variability and uncertainty in the repository environment and in how it evolves with time. Because of the availability of mechanistic information and of suitable input data, the model was developed on the assumption of aerobic, saturated conditions in the near field. This work was previously presented at 7<sup>th</sup> International Workshop on Long-term Prediction of Corrosion Damage in Nuclear Waste Systems (LTC 2019) and published in 2020 (Briggs et al. 2020).

##### 4.2.5.2 FE-G Oxygen Modelling

Gas monitoring in FE-G was on-going in 2020 and included gas composition studies, numerical modelling, and complementary table-top experiments. The gas composition in the FE-G, like a potential DGR, is controlled by different relevant bio-, geo, chemical and transport processes. Continued in 2020 was analysis of aerobic conditions after backfilling, gas advection through the tunnel EDZ and plug, gas exchange with the clay host rock and other biochemical processes. Composition of the bentonite pore-space has been monitored since construction in 2014 to capture long term behaviour of, for example, unsaturated transport of corrosive species (ex.  $\text{O}_2$  and  $\text{H}_2\text{S}$ ) and gas generation (eg.  $\text{H}_2$ ).

### 4.3 PLACEMENT ROOM SEALS AND OTHERS

#### 4.3.1 Reactive Transport Modelling of Concrete-Bentonite Interactions

The multi-component reactive transport code MIN3P-THCm (Mayer et al. 2002; Mayer and MacQuarrie 2010) has been developed at the University of British Columbia for simulation of geochemical processes during groundwater transport. Prior reactive transport modelling work related to engineered barriers (e.g., bentonite) included the Äspö EBS TF-C benchmark work program (Xie et al. 2014), and the geochemical evolution at the interface between clay and concrete (Marty et al. 2015).

Reactive transport simulations with MIN3P-THCm have been continued in 2020 to investigate long-term geochemical interactions driven by diffusion-dominated transport across interfaces between bentonite, concrete and host rock (limestone and granite) in the near field of a repository. The impact of altered interfaces on the migration of radionuclides (i.e. I-129) has also been numerically investigated. Simulation results indicate that porosity reduction and pore clogging at the interfaces can significantly inhibit radionuclide migration. A technical report and a

journal paper documenting the reactive transport simulation across interfaces are expected in 2021.

MIN3P-TMCm is also being used to simulate the CI (Cement - OPA Clay Interaction) and CI-D (Diffusion Across 10-year Old Concrete-Claystone Interface) long-term experiment at the Mont Terri underground research laboratory to predict the cement-clay interactions.

#### **4.3.2 Gas-Permeable Seal Test (GAST)**

Potential high gas pressure within the emplacement room due primarily to corrosion of metals and microbial degradation of organic materials is a significant safety concern for long term repository performance. To address this potential problem, Nagra initiated the GAST project at Grimsel Test Site, Switzerland in late 2010. The main objective of GAST is to demonstrate the feasibility of the Engineered Gas Transport System which enables a preferable flow path for gas at over-pressures below 20 bars where the transport capacity for water remains very limited. NWMO has been part of the GAST project since its inception.

Presently the experimental facility is still in the saturation phase. The delay is due to a major leak event occurring in 2014 and due to the slow rate of the saturation process in the sand bentonite mixture. The saturation process is expected to finish by the end of 2021.

In 2019, a smaller scale, well instrumented laboratory experiment – mini-GAST was initiated at UPC (Polytechnic University of Catalonia), Barcelona, Spain. The mini-GAST project aims to mimic the GAST experiment in a much better controlled fashion in the lab within a much shorter testing time frame. The mini-GAST experiment comprises of two semi-cylindrical shape mock-up tests, MU-A (50 cm in length and 30 cm in diameter) and MU-B (1/3 size of MU-A).

In 2020, preliminary experiment was carried out using MU-B to gain more understanding and experience for MU-A. 3-D modelling with Code Bright was carried trying to simulate the saturation process of the MU-B test. More experiments are planned for both MU-B and MU-A in 2021.

#### **4.3.3 DECOVALEX**

DECOVALEX (DEvelopment of COupled models and their VALidation against EXperiments) is an international research and model comparison collaboration program, initiated in 1992, for advancing the understanding and modeling of coupled thermo-hydro-mechanical-chemical (THMC) processes in geological systems. Prediction of these coupled effects is an essential part of the performance and safety assessment of geologic disposal systems for radioactive waste and spent nuclear fuel, and for a range of sub-surface engineering activities.

DECOVALEX is on a four-year cycle and the current iteration DECOVALEX-2023 runs from April 1, 2020, through March 31, 2024, while results from the previous DECOVALEX-2019 are still being published.

The NWMO is currently participating in the following DECOVALEX Tasks.

- DECOVALEX-2019 Task E – Coupled THM (Andra URL)
- DECOVALEX-2023 Task C – Coupled THM (FE Mont Terri)
- DECOVALEX-2023 Task F – Performance Assessment

#### 4.3.3.1 DECOVALEX-2019 Task E: Coupled Thermal-hydraulic-mechanical Modelling of the Multi-Scale Heating Experiments

The Thermo-Hydro-Mechanical (THM) behavior of the Callovo-Oxfordian claystone (COx) is of great importance for the design and safety assessment of a high-level and intermediate-level long-lived waste repository in such formation. This work was conducted in the context of the Task E within the DECOVALEX-2019 framework, an international program with a 4-year duration that began in 2016, which is a multidisciplinary, co-operative international research effort in modelling coupled Thermal-Hydraulic-Mechanical-Chemical (THMC) processes in geological systems and addressing their role in Performance Assessment for radioactive waste storage (Birkholzer et al. 2019).

The purpose of Task E of the DECOVALEX-2019 project is to investigate upscaling THM modelling from small-scale experiments (some cubic meters) to full-scale experiments (some ten cubic meters) and finally to the scale of the waste repository (cubic kilometers). To achieve this aim, the data of two in-situ heating experiments performed by Andra (the French National Radioactive Waste Management Agency) in the Meuse/Haute-Marne Underground Research Laboratory (MHM URL) have formed the basis for the understanding of the THM behavior of the COx at different scales (Figure 4-28 and Figure 4-29). The first experiment provided the reference values of the THM parameters by means of a calibration exercise and they were used for a blind prediction and an interpretative analysis of the second one.

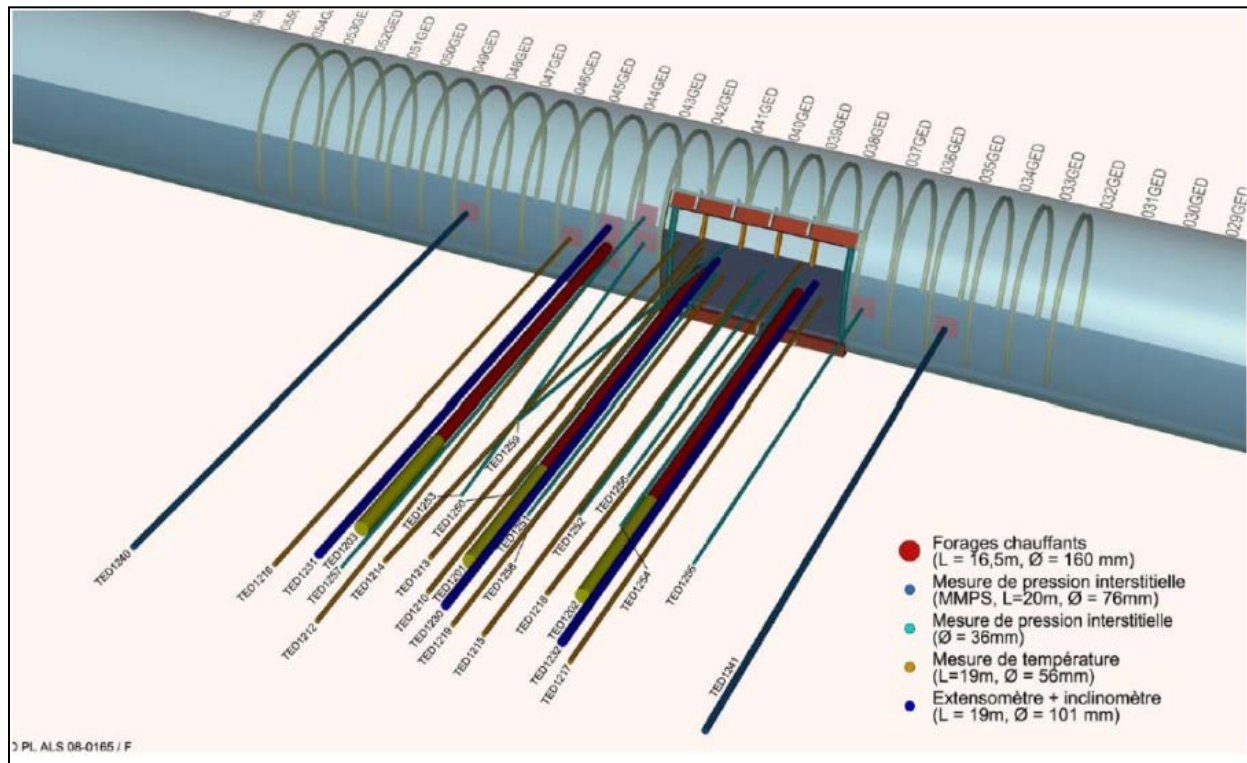
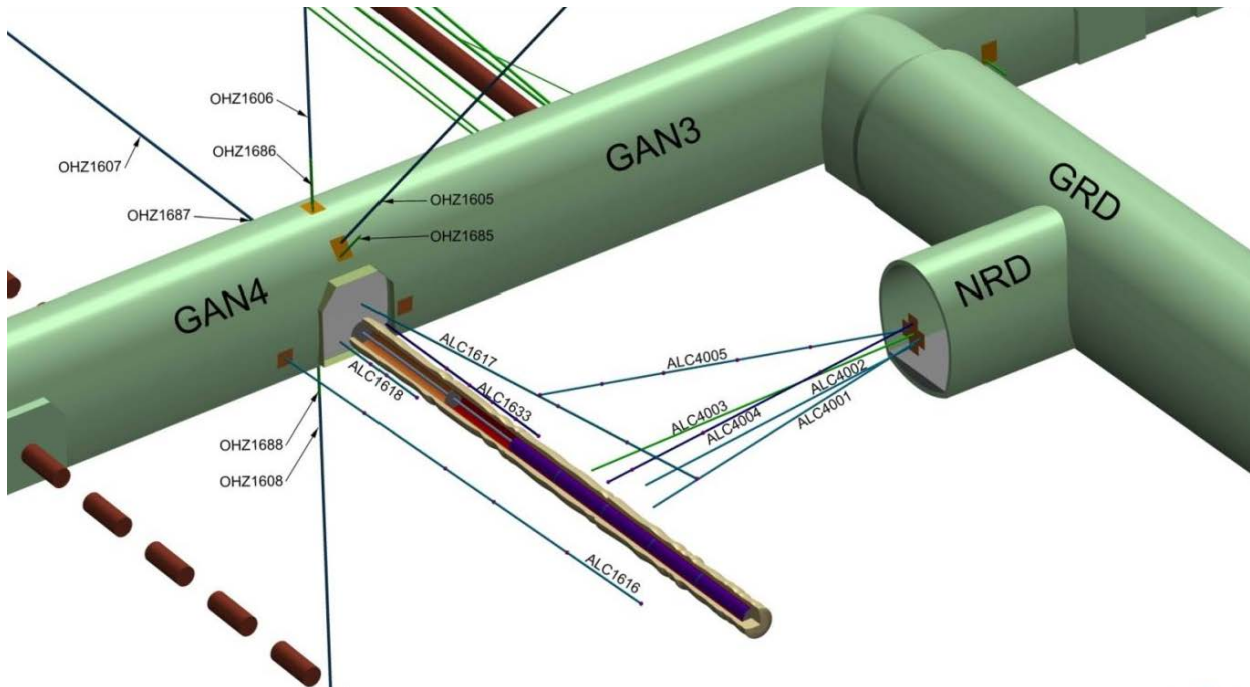


Figure 4-28: Three-dimensional Layout of the TED Experiment Indicating Heaters and Instrument Boreholes (Armand et al. 2017)



**Figure 4-29: Three-dimensional Layout of the ALC Experiment Indicating Heaters and Instrument Boreholes (Armand et al. 2017)**

The modelling teams showed that the use of a thermo-poro-elastic model yielded satisfactory predictions of the two in-situ heating experiments (Figure 4-30). A correct interpretation of the boundary conditions, as well as finding permeability values keeping an anisotropy ratio consistent with respect to what is observed in the field, were essential for plausible and well-calibrated models (Guo 2020, Guo et al. 2020c). Numerical modelling of the whole waste repository was also performed (Figure 4-31), in which the teams had more freedom to set their models lead to different and original approaches. The assumptions and hypothesis enacted in the different modelling approaches were verified by the inter-comparison of the numerical results to finally provide several best practice guidelines for modelling large-scale deep geological repositories (Figure 4-32 and Figure 4-33) (Guo et al., 2020d).

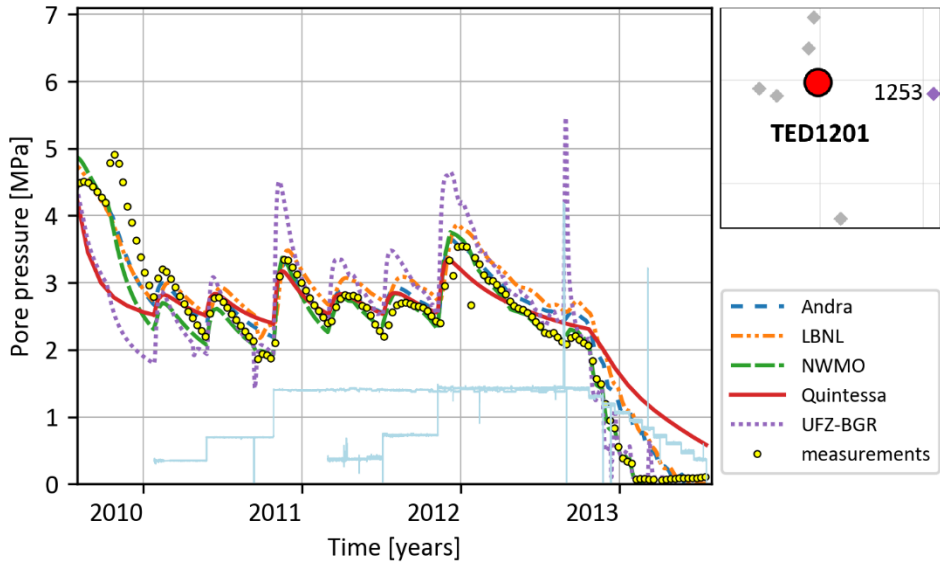


Figure 4-30: Pressure Evolution at the Sensor TED1253\_PRE\_01

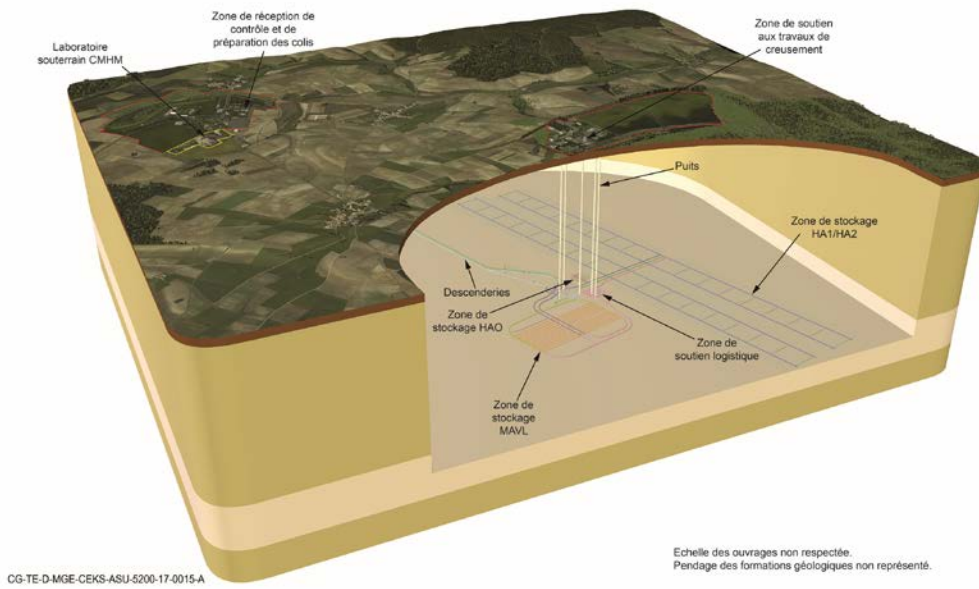


Figure 4-31: Diagram of the Facilities of the Cigéo Project

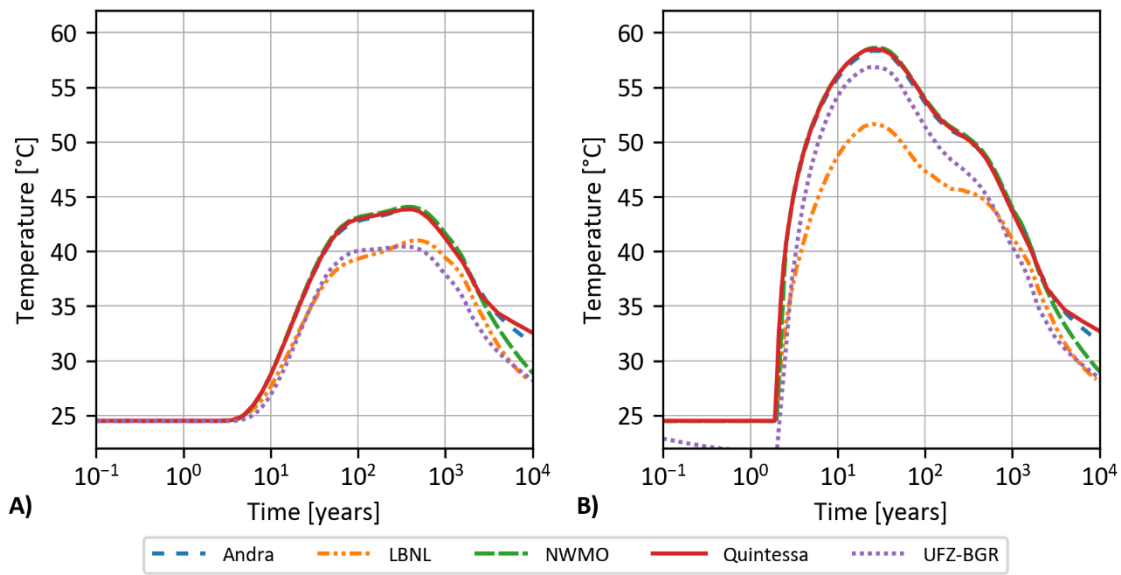


Figure 4-32: Temperature Evolution at Points A) P1 and B) P2

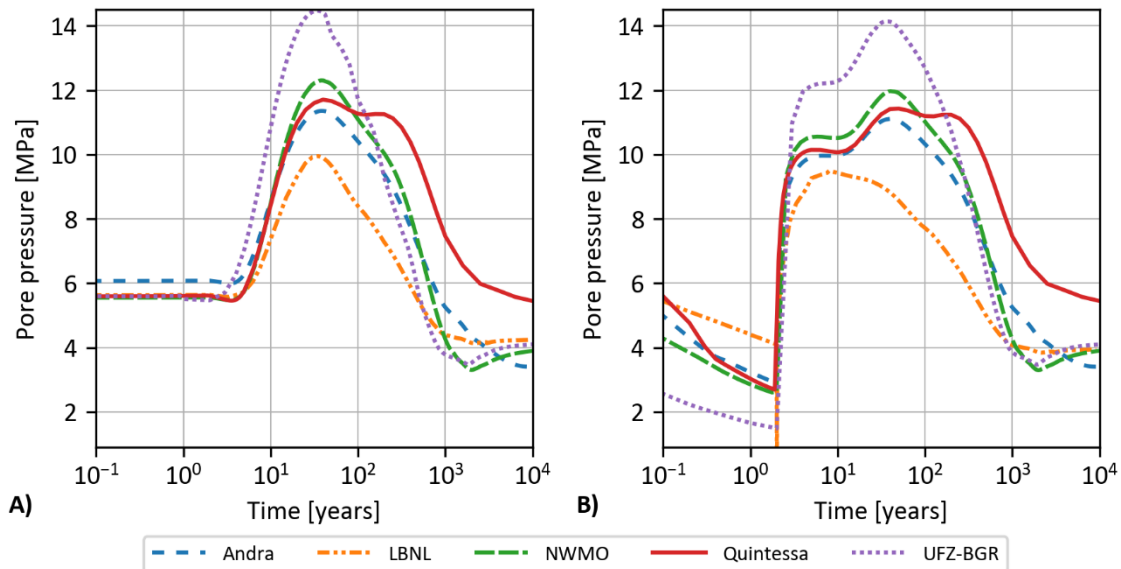


Figure 4-33: Pore Pressure Evolution at Points A) P1 and B) P2.

#### 4.3.3.2 DECOVALEX-2023 Task F: Performance Assessment

The DECOVALEX program is interested in coupled processes (e.g., thermal, hydrological, mechanical, and chemical) relevant to deep geologic disposal of nuclear waste. Task F of DECOVALEX-2023 involves comparison of the models and methods used in post-closure performance assessment of deep geologic repositories.

Task F considers the generic reference case describing a repository for commercial spent nuclear fuel in a fractured crystalline host rock is proposed as the primary system for comparison. The NWMO is participating in the crystalline comparison. A second generic reference case describing a repository for commercial spent nuclear fuel in a salt formation

(bedded or domal) is also a component of Task F however the NWMO is not participating in the component of task F.

The primary objectives of Task F are to build confidence in the models, methods, and software used for performance assessment of deep geologic repositories, and/or to bring to the fore additional research and development needed to improve performance assessment methodologies. The objectives will be accomplished through a staged comparison of the models and methods used by participating teams in their performance assessment frameworks, including: (1) coupled-process submodels (e.g., waste package corrosion, spent fuel dissolution, radionuclide transport) comprising the full performance assessment model; (2) deterministic simulation(s) of the entire performance assessment model for defined reference scenario(s); (3) probabilistic simulations of the entire performance assessment model; and (4) uncertainty quantification and sensitivity analysis methods/results for probabilistic simulations of defined reference scenario(s).

In 2020, Task F participants will focus on benchmarking of the various software programs and performance assessment tools used in Task F against hydrogeological flow and transport problem with known analytical solutions. The NWMO will be performing these benchmarks and will complete the Task F work with the Integrated System Model (See Section 6) and its constituent codes COMSOL and HydroGeoSphere. Benchmark Comparisons are expected to be published in early 2022.

#### **4.3.4 Shaft Seal Properties**

In 2020, the NWMO continued with its program to identify an optimized shaft seal mixture by evaluating the behavior of bentonite/sand blends having composition ratios other than 70:30. In this study, the use of a crushed limestone sand is being examined in addition to granitic sand. Composition ratios of bentonite/sand of 50:50, 60:40, 70:30, 80:20 and 90:10 (by weight) are being assessed.

The tests evaluate the following:

1. Compaction/fabrication properties of the materials (to Modified and Standard Proctor density).
2. Consistency limits (Atterberg Limits) and free swell tests.
3. Moisture content and density of fabricated material.
4. Mineralogical/chemical composition, including measurements of montmorillonite content.
5. Swelling pressure.
6. Saturated hydraulic conductivity.
7. Two-phase gas/water properties, specifically the capillary pressure function (or soil water characteristic curve, (SWCC)) and relative permeability function, measured over a range of saturations that include the fabricated and fully saturated condition.
8. Mineralogical/chemical composition of the materials exposed to brine for an extended period of time.

Based on the results to date, it is anticipated that for low salinity groundwater conditions, compaction to 98% of the Standard Compaction Maximum Dry Density of the bentonite/sand mixtures studied will be sufficient to achieve the swelling pressure and hydraulic conductivity targets ( $>100$  kPa and  $<10^{-10}$  m/s, respectively). Under high salinity conditions, it is expected that heavy compaction to ~95% of Modified Compaction Maximum Dry Density will be required to achieve swelling pressure and hydraulic conductivity targets for the blends studied. The swelling pressures observed for the materials examined in this study generally were also within the range of previously observed values for both low and high salinity conditions.

#### 4.3.5 Thermo-hydro-mechanical Modelling of NWMO Placement Room

In 2020, the NWMO continued to use fully coupled Thermo-Hydro-Mechanical (THM) CODE\_BRIGHT models to study the unique NWMO placement concept. Modelling programs to assess heterogeneous wetting fronts, and the influence of drying on the cracking of the HCB block were completed. A wetting front and associated bentonite swelling aligned parallel with the long axis of the placement room was shown to potentially push the Buffer Boxes should vertical gaps be present between the placed boxes. A wetting front aligned perpendicular to the long axis of the room, was shown to potentially move the UFC in a horizontal direction no more than 10 mm. The modelling of the drying highlighted areas of the HCB block that may be susceptible to cracking within the block, namely along the centerline of the block oriented perpendicular to the axis of the UFC.

#### 4.3.6 Coupled Thermo-hydro-mechanical Benchtop Experiments

In late 2018, the NWMO and its contractor (the National Research Council of Canada) launched a work program to design and construct test cells to perform experiments examining the thermal-hydro-mechanical response of bentonite. Results of the experiments will be compared against numerical THM models such as COMSOL and CodeBright.

Two cylindrical experimental cell designs have been developed. The first cell design is intended to be simpler and examine the effect of heating only. The heating only cells are approximately 80 cm in length and 34 cm in diameter and has a resistive heater along the central axis of the cylindrical cell. The heater is then surrounded by concentric rings or highly compacted bentonite and gapfill (See Figure 4-34). The heating only cell length was designed such that three identically instrumented sensing zones along the length of the apparatus were available. At each sensing zone measurements of temperature and moisture are taken at various radial depths. The heating only design was finalized in late 2019 and construction of the heating only cells was completed in 2020.



**Figure 4-34: Heating Only Apparatus**

The second cell design is similar to the heating only cell. It is cylindrical, contains a resistive heater along the centre axis and contains concentric rings of highly compacted bentonite and

gapfill. However, second cell includes both heating and wetting of the bentonite. Water can be delivered by a pressurized water delivery system and is distributed through a geotextile membrane along the interior of the cell wall. The wetting cell design is also smaller (48 cm in length and 30 cm in diameter) to help facilitate resaturation of the gapfill and highly compacted bentonite. Due to the reduced cell size, the wetting cell only contains a single instrumented sensing zone with temperature and moisture sensors (See Figure 4-35). The wetting cell will also contain strain gauges on the perimeter of the steel shell to determine swelling pressure. The wetting cell design is expected to be finalized and cell construction complete in 2021.

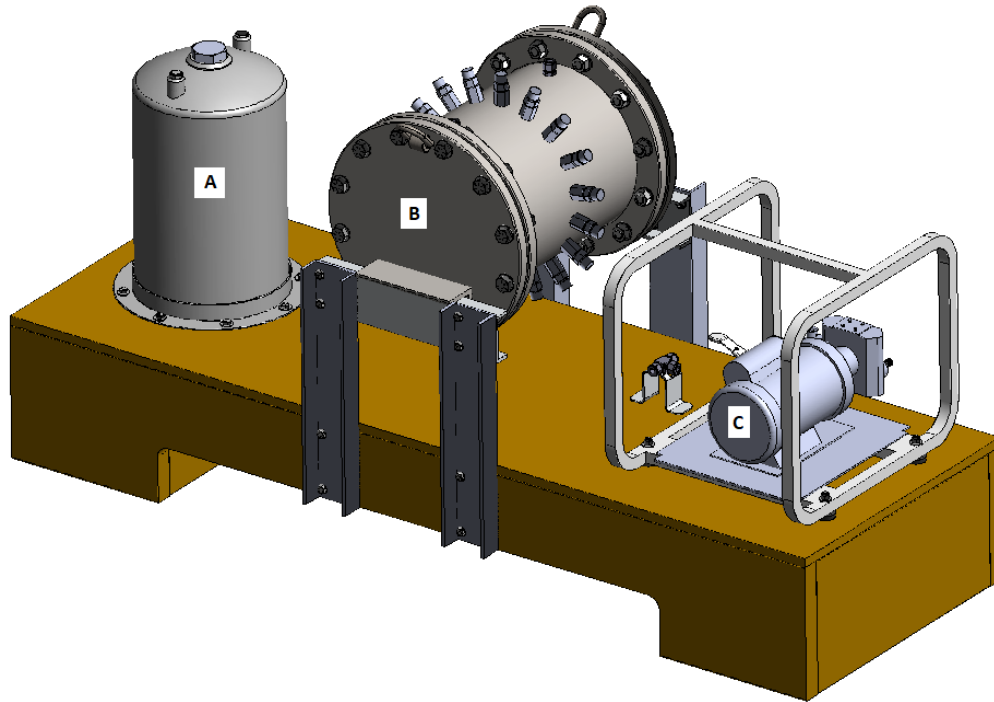


**Figure 4-35: Rendering of the Wetting Cell Design (A) Is the Water Reservoir, (B) Is the Test Cell, and (C) Is the Water Pump**

Both cells contain a variety of instrumentation to measure temperature, moisture content, relative humidity and swelling pressure. The most novel of which is the moisture sensors developed specifically for this project. The moisture sensor design is a capacitive based moisture pin sensor, to be calibrated with the dielectric constant of bentonite across differing moisture contents. The moisture sensor consists of two 2.38 mm diameter stainless steel pins, separated by a space of 1.59 mm. The sensing pins are held rigid and thermally decoupled in the bentonite via a rigid Teflon sleeve (See Figure 4-36).



**Figure 4-36: Capacitive Based Moisture Sensor**

The primary focus of 2021 work will include calibration of apparatus instrumentation, commissioning of an initial heating only test as well as finalization of the design and construction of the wetting cell.

## 5 GEOSCIENCE

### 5.1 GEOSPHERE PROPERTIES

#### 5.1.1 Geological Setting and Structure

##### 5.1.1.1 Lithostratigraphic Framework for the Paleozoic Bedrock of Southern Ontario

The Geological Survey of Canada, in collaboration with the Oil, Gas and Salt Resources Library (OGSRL) produced a regional three-dimensional (3-D) lithostratigraphic model of the Paleozoic bedrock of southern Ontario using Leapfrog® Works software. This model provides important updates to the regional lithostratigraphic model previously released by Carter et al., 2019. The model encompasses the entire Phanerozoic succession of southcentral and southwestern Ontario consisting of approximately 1500 meters of Paleozoic bedrock and an area of 110,000 km<sup>2</sup>. Fifty-three Paleozoic bedrock layers representing 70 formations, as well as the Precambrian basement and overlying unconsolidated sediment, are modelled at a spatial resolution of 400 m. The principal input data source was obtained from the Petroleum well records in the Ontario Petroleum Data System (OPDS), supplemented by Ontario Geological Survey (OGS) deep boreholes, measured sections, control points, Michigan boreholes, and select bedrock provincial water well records. Where strong evidence exists, previously interpreted faults by mapping of linear vertical displacements of formation top surfaces in the subsurface Paleozoic bedrock formations have been incorporated in the model with normal sense of movement. These faults are mostly located in the southwestern quadrant of the model. Faults identified elsewhere in the model extent were previously defined by sparse well control and recorded with small vertical displacements. These other faults are not incorporated in the model.

An important update to the model includes detailed review of formation tops picks in the Ontario Petroleum Data System (OPDS). Project geologists and data support staff of the Oil, Gas and Salt Resources Library (OGSRL) completed edits to 17,595 formation tops in a total of 3,419 wells, resulting in a revised data set and permanent improvements to the petroleum well database. As a result of the review, a total of 20,836 Ontario petroleum wells, 199 OGS stratigraphic tests, 15 measured sections, 3 Michigan petroleum wells, and 30 control points were utilized for formation top data, including seven new control wells added to improve layer extrapolation beneath Lake Huron. The new model improves the resolution of the subcrop surface and there is a more accurate and realistic rendering and correlation of the topography and bedrock geology of the Niagara Escarpment (Figure 5-1). Other model enhancements include the addition of a model layer for the Salina D Salt, as well a focus on improving the data quality and quantity for the formations of the Lockport Group. Other features such as 3-D volumes of salt beds leased for underground mining at Ontario's 2 salt mines, solution-mined caverns in salt beds including those constructed for storage of liquified hydrocarbons and petrochemicals, two-dimensional representations of oil and natural gas reservoirs, regional faults, and lithotectonic boundaries in the Precambrian metamorphic basement have also been incorporated as model objects.

NWMO will use the updated 3-D lithostratigraphic model as the basis for a site-specific model of South Bruce, which will be further refined with site specific data as it becomes available.

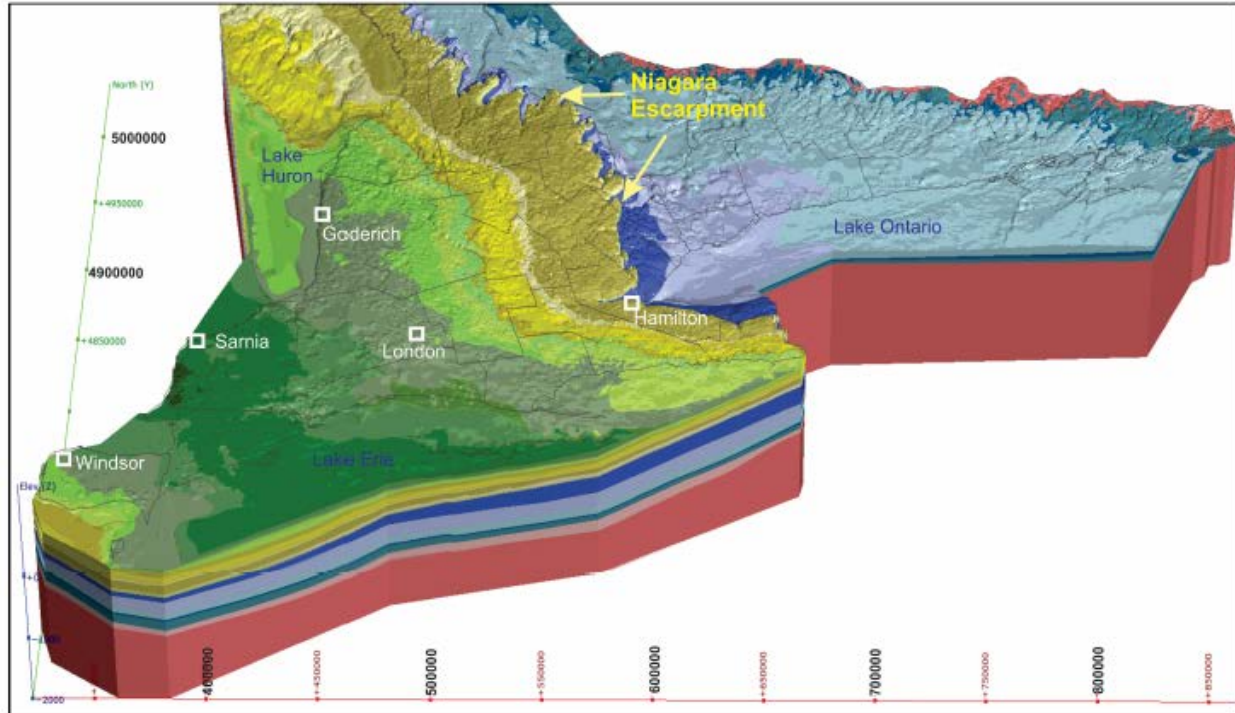


**Figure 5-1: Updated 3-D Lithostratigraphic Model of the Paleozoic Bedrock of Southwestern and Southcentral Ontario, Surficial Sediment Cover Removed (Carter et al. *in press*)**

### 5.1.1.2 Fractures and Fracture Zones, Faults, and Joints

#### 5.1.1.2.1 Numerical Methods – Discrete Fracture Networks

Fracture network modelling involves using 3-dimensional (3-D) geostatistical tools for creating realistic, structurally possible models of fracture zone networks within a geosphere that are based on field data. The ability to represent and manage the uncertainty in the geometry of fracture networks in numerical flow and transport models is a necessary element in the development of credible geosphere models. Fracture network modelling will also be used in 3-D integrated geosphere models. The creation of fracture network models in MoFrac (software that generates 3-D fracture network models for rock mass characterization) is a multistep process that involves integrating interpretations of lineament data and other available field data to define fracture orientations and size distributions.

MoFrac is capable of creating DFN models at the tunnel-, site- and regional scale (e.g., Bastola et al. 2015; Junkin et al. 2017, 2018, 2019a, 2019b, 2020). During 2020, version 3.6 of MoFrac was used within the site investigations program. In parallel to MoFrac use in site characterization activities, further development and refinements to MoFrac are conducted through the research program. This enables model development and validation to occur in an iterative manner to support site characterization activities.

In 2020, work continued on developing version 4.0 of the code. Two examples of key development tasks chosen to further advance the code for application to additional site-specific information as it becomes available are:

- Fracture branching and clustering: Fracture branching will permit MoFrac to simulate either branching or coalescing fractures. Fracture clustering will allow for control of the spatial distribution of fractures.
- Time slicing: Time slicing will be used to propagate multiple fractures simultaneously. Propagation will no longer be a whole-fracture process, but instead will operate on extending a partially-complete-fracture mesh.

#### **5.1.1.2.2 *Mont Terri Seismic Imaging (SI-A) experiment:***

During 2020, the NWMO joined as a partner in the SI-A Experiment (Seismic Imaging Ahead of and Around Underground Infrastructure) to investigate the applicability of high-frequency seismic impact or vibration sources, combined with three-component geophones integrated in rock bolts, for transmission and reflection imaging in an argillaceous environment to allow imaging of faults and fractures. The experiment is a high-resolution exploration test with resolution in the dm- to m-scale and within an observation range of several decameters to a few hundreds of meters. In 2020, seismic measurements were completed in Ga08, Ga04 and Niche CO2 within the Mont Terri Underground Laboratory. In 2021, the focus will be on acquisition of a seismic profile within the safety gallery.

#### **5.1.1.3 *Metamorphic, Hydrothermal, and Diagenetic Alteration***

##### **5.1.1.3.1 *Hydrothermal Alteration in Crystalline Rocks***

An understanding of brittle and ductile deformation observed in the granitoid plutons of the Wabigoon Subprovince is required to understanding how fluids have migrated throughout the plutons in the past. The research is unique in that it uses granitoid rocks of the Wabigoon Subprovince—instead of greenstone belts—as proxies of metamorphism in the region. This research combines structural studies with an examination of the mineralogy and petrology (petrographic analysis and mineral chemistry characterization) of the hydrothermal alteration assemblages. The research findings at a regional scale will later be integrated and interpreted together with site-specific observations from the Revell batholith. Figure 5-2 shows the localities for sample collection and structural mapping as part of the research.

Results of the structural mapping campaigns and the petrographic analyses indicate that the twelve plutons studied across the Wabigoon Subprovince display the following features:

- Hydrothermal chlorite and/or epidote along oblique strike-slip faults.
- Alteration of wall-rock that consists of the replacement of feldspars by epidote, chlorite, white mica, biotite, and sphene.
- Ductile deformation temperatures in the amphibolite facies of metamorphism.
- Faulting/hydrothermal alteration occurred during regional-scale Amphibolite facies Archean deformation (coeval brittle-ductile deformation) in at least 5 of the plutons.

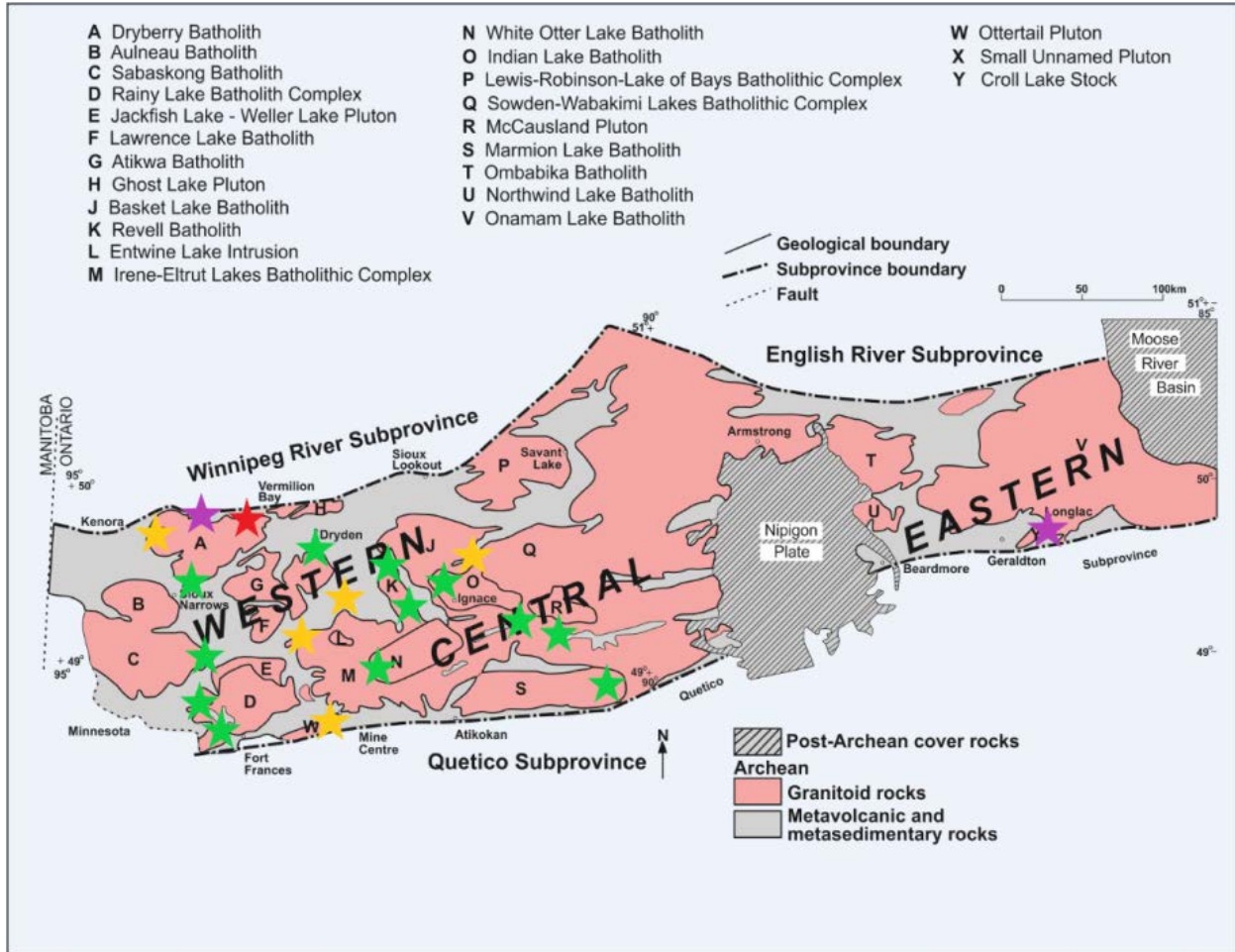


**Figure 5-2: Outcrop Locations Where the Hydrothermal Alteration and Deformation of Plutons Have Been Studied. Green Stars Represent 1 Outcrop, Red Stars Represent 2 Outcrops, Yellow Stars Represent 3 Outcrops and Purple Stars Represent 5 Outcrops**

The second phase of the study focuses on assessing the chemistry of the hydrothermal fracture infill and the wall rock alteration via SEM-EDX analysis. This phase will assess whether the chlorite-coated shear fractures are suitable for stable isotope analysis ( $\delta^{18}\text{O}/\delta^2\text{H}$ ). To date, the results have shown a consistency in the mineral chemistry of the wall-rock alteration minerals and the fracture infill minerals - at least on an outcrop scale. This phase will also assess the usefulness of cathodoluminescence imaging technique of quartz and feldspar currently being used to study alteration and deformation features at a mineral scale.

### 5.1.1.3.2 Diagenetic Alteration of Sedimentary Formations

#### 5.1.1.3.2.1 Dolomitization in Southern Ontario

Research has been underway since 2015 to investigate the nature and origin of strata-bound, near-horizontally layered dolomitized beds occurring within the bedrock formations of the Black River Group in the Huron Domain of southern Ontario. A summary of the research conducted between 2015 and 2017 is available in Al-Aasm and Crowe (2018).

During 2019, the research scope shifted to focus on the determination of Rare Earth Elements (REE) in both previously examined samples and new samples collected during 2018. The

purpose of this next phase of the research is to better understand the provenance of the source fluids involved in dolomitization the formations. This research further improves the fundamental understanding of fluid sources, movement, and interactions with the sedimentary rocks over geologic time. In 2020, the research findings were published for core samples from two deep boreholes analyzed for petrographic, stable and Sr isotopes, fluid inclusion microthermometry and major, minor, trace and rare-earth elements (REE) of different types of dolomite in the Silurian and Devonian carbonates of the eastern side of the Michigan Basin (Tortola et al. 2020). Due to laboratory closures in 2020 associated with the pandemic, the completion of some laboratory analyses required for this research were delayed. Consequently, a draft of the final publication summarizing all work conducted since 2014 is now expected in 2021.

#### *5.1.1.3.2.2 Clumped Isotope Paleothermometer for Dolomite*

During 2020, a new research project was developed with the Geological Survey of Canada, Quebec, to employ a different type of geothermometer to assess fluid longevity within carbonate sedimentary rock mass. The clumped-isotope thermometer is a relatively new geothermometer which functions on the principle that rare 'heavy' isotopologues in a molecule prefer to bond together, with a dependence on the temperature of the system. Specifically,  $^{13}\text{C}$  and  $^{18}\text{O}$  in a carbonate mineral are thermodynamically ordered or 'clumped' depending on the temperature of the depositional environment. Determining the abundance of clumped isotopes in carbonate ( $\Delta 47$ ) then allows constraints to be placed on the formation temperatures. This approach has the advantage of being able to directly infer the isotopic composition of the parent fluid, which is often difficult to reconstruct given 1) the prevalence of diagenesis in buried sedimentary successions and 2) the formation of secondary minerals over a wide range of temperatures. Using clumped isotopes analysis on carbonate as a tool, and with the objective of establishing a new paleothermometer for dolomite as well, key aims of the research program are to reappraise the evolution of the Ordovician limestone sedimentary units in Southern Ontario and provide additional insights on the origin of mineralising fluids and post-depositional modifications to the rock.

### **5.1.2 Hydrogeological Properties**

#### **5.1.2.1 Hydraulic properties of Fractured Crystalline Rock**

##### ***5.1.2.1.1 Advances in Defining Hydraulic Properties of Crystalline Rock***

Research at the University of Waterloo is being undertaken to develop improved approaches to characterize the hydraulic behaviour and evolution of groundwater systems in Canadian Shield settings. Snowdon et al. (2020) investigated how variations in horizontal spatial scales in numerical groundwater models impact net exchange fluxes between surface-water and groundwater systems. The study compared 10 m, 50 m, and 250 m horizontal grid discretizations, and found that although the 50 m grid resolution was able to provide similar predictions for exchange fluxes, the 250 m grid resolution showed significant deviations. For increasing horizontal spatial discretizations, the net exchange flux between the surface and groundwater was found to decrease compared to the point recharge estimate.

An extensive literature was undertaken in 2019 to define hydraulic and geochemical properties of crystalline rock. Data were drawn from technical documents developed by Atomic Energy of Canada Ltd between 1975 and 1996 and includes 620 permeability estimates from sites across the Canadian Shield. During 2020, the database was verified and used to define depth dependent variations in EPM rock mass and fracture zone permeability for Canadian Shield

settings. The depth dependent variations determined specifically for plutonic rocks within the Canadian Shield will be used as a platform to develop early site-specific groundwater models for the Revell site, which will be refined with site-specific data as it becomes available. A journal article documenting this work was prepared and submitted for publication (Snowdon et al, 2020 - *submitted*).

#### **5.1.2.1.2 HM Coupling of Rock Mass Stress and Permeability**

During 2020, NWMO joined with SKB to sponsor research which examines the impact of in-situ stress conditions on the fractured rock mass bulk permeability and develops a hydromechanical formalism to link them. This research is conducted by the Fractory group, which is a joint laboratory of Itasca Consultants s.a.s., the French institute for scientific research (CNRS) and the University of Rennes, France. Research activities in 2020 focused on 1) identifying a set of fracture aperture-stress models relevant to conditions expected for deep storage of nuclear fuel; 2) determining an approach to account for stress fluctuations due to fractures when significant; 3) designing a numerical tool to calculate an equivalent permeability tensor from multiple DFN flow simulations; and 4) designing a theoretical relationship linking the properties of the DFN and stress conditions to the effective permeability of the rock.

A literature review was first conducted to select an appropriate relationship between fracture aperture and in-situ stress. An exponential model based on studies by Hökmark et al. (2010), Barton (1982), Liu et al. (2004), and Fransson (2009) was chosen. This model has only few parameters that can be partially constrained by data and experiments:

[  $e_h = e_{hr} + (e_o - e_{hr}) \cdot \exp(-\sigma_n/\sigma_c)$ , where  $e_o$  the hydraulic aperture at zero pressure,  $e_{hr}$  the residual aperture and  $\sigma_c$  the characteristic stress range]. A mathematical framework derived from Kachanov (1987) was then designed to compute the effective normal stress  $\sigma_n$  on a fracture plane that considers the fluctuations (and interactions) due to surrounding fractures. When this framework was applied to Fractory's baseline DFN model, it was shown that the effect of fluctuations cannot be neglected in most cases, since it redistributes stress within the DFN and therefore can significantly modify  $\sigma_n$  on most fractures (Figure 5-3).

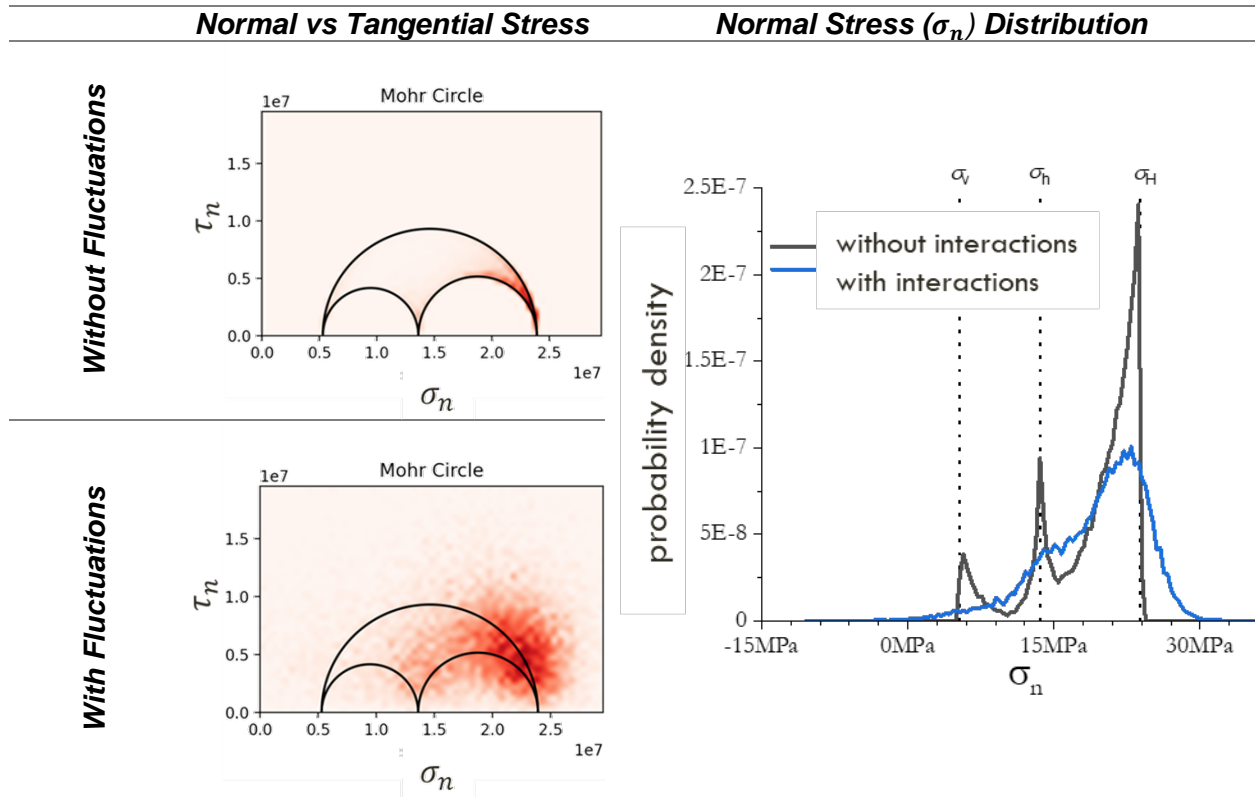


**Figure 5-3: (left) “Heat” Map Representation of Normal Versus Tangential Stress on the Fracture Planes of the Baseline DFN and (right)  $\sigma_n$  Probability Density without (top) and with (bottom) Stress Fluctuations**

A complete numerical setup to compute the effective permeability of a fractured rock in multiple directions and define, where applicable, the equivalent permeability tensor was implemented in the DFN.lab software developed by the Factory (Le Goc et al. 2019). The entire process is illustrated in Figure 5-4.

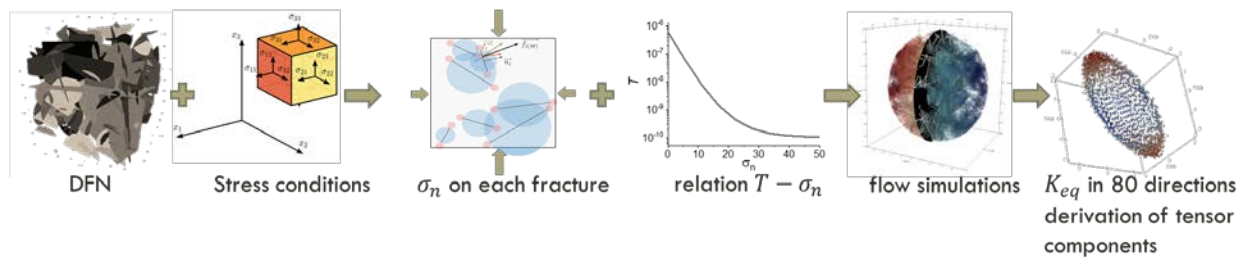


**Figure 5-4: Illustration of Numerical Methodology and Setup to Derive Directional Equivalent Permeabilities. From Left to Right: DFN and Stress Conditions Provided as Input, Normal Stresses Computed Accounting for Stress Fluctuations, Fracture Aperture Transmissivity Relationship, Flow Simulations in Specific Directions and Finally Equivalent Directional Permeabilities. The Last Process is Repeated 80 Times to get 80 “Directional Permeabilities” and, When Relevant, a Permeability Tensor is Defined**

### 5.1.2.1.3 *Äspö Task Force – Task 10*

SKB originally initiated the Äspö Task Force on Modelling of Groundwater Flow and Transport of Solutes (the Task Force) in 1992 to enhance the understanding and increase the ability to model problems of interest in the field of groundwater flow and solute transport. In 2020, NWMO re-joined the Äspö Task Force to participate in Task 10 which is dedicated to building confidence in and “validating” models of flow and transport in fractured rock. The objective of this task is to develop pragmatic approaches to model validation. The first step was the development of a “White Paper” to set out possible approaches for discussion and further refinement by the members. Task 10.2 which focusses on the single fracture scale and channelling will be undertaken first. Subsequent tasks will consider networks of fractures at larger scales.

Flow channelling in fractured rock is a phenomenon that occurs on different scales and can have a range of safety related implications. For example, channelling is relevant to:

- Characterization and interpretation of groundwater flow and transport in a fractured host rock,
- Assessing the potential for migration of meteoric water from the near surface to repository depths and subsequently radionuclide transport from the repository in the unlikely event of breached canisters,
- Inflows of groundwaters into deposition holes or emplacement rooms during buffer saturation and later flow within a deposition hole/emplacement room in the unlikely event of a breached canister.

Challenges when attempting to characterize flow channelling at a repository site include 1) most often, only a limited amount of data is available; and 2) the effects of channelling on mass transport on the scale of deposition holes/emplacement rooms needs to be “upscaled” to be used in larger scale groundwater flow and mass transport models.

### 5.1.2.2 **Investigation of Underpressures in Sedimentary Rocks**

A new research contract was initiated in 2020 with the United States Geological Survey (USGS) which continues to investigate of the anomalously low pressured shales observed within the rocks at the Bruce nuclear site. The proposed analysis is expected to strengthen arguments regarding the possible presence (or absence) of a methane gas phase in the rocks encompassing the proposed host rock (Cobourg Formation). There are two components which will be examined through this research:

1. Potential mechanisms by which the hydrogeologic system at the Bruce nuclear site could have reached its current (pre-drilling) state with gas-phase methane present will be examined through a series of TOUGH simulations. The results will be used to better understand how pressures measured in boreholes relate to liquid pressures in the rock when a separate phase gas is present.
2. The effects that a gas phase has on field-based pressure measurements will be examined. Specifically, the effects of gas-phase methane on glacio-mechanical loading and underpressure development at the Bruce nuclear site will be investigated through a new series of TOUGH simulations to clarify which, if any, are both plausible and lead to the pressure conditions observed in the field.

The project is scheduled to run into 2023 with a literature review due in 2021 and technical journal article paper to be submitted in 2023.

### **5.1.2.3 Numerical Methods – Groundwater**

HydroGeoSphere (HGS) is a 3-D integrated surface-subsurface flow and transport simulator developed by Aquanty Inc (Aquanty 2018). Currently, HGS is the reference NWMO computer code for groundwater flow and radionuclide transport simulations. In 2019, NWMO requested that Aquanty develop several new HGS features to better adapt the code to the unique modelling requirements of NWMO's projects. These new features will improve modelling capability and computational efficiency of future HGS simulations.

One of the main new features is the ability to identify fracture faces based on discrete fracture network data output from MoFrac in VTK format. MoFrac is a computer code that generates realistic, structurally possible models of fracture networks based on field data. In addition, this new feature will also allow users to assign unique property values (such as hydraulic conductivity, porosity, and thickness) to each individual fracture face. Other new features are the ability to directly import 3-D geology data (voxel) and 2-D elevation data (tsurf) from a GOCAD (a popular tool for creating 3-D geological models) model into HGS. In 2020, Aquanty completed most of the code development work and the entire project is expected to finish in early 2021.

### **5.1.3 Hydrogeochemical Conditions**

Chemical and isotopic compositions of groundwater and porewater within the rock matrix provide information on residence times and evolution of deep flow systems. Information on major ion compositions of the waters, pH and redox conditions, as well as characterization of microbial populations, support calculations of radionuclide solubility and transport, and are also relevant to assessments of the stability (i.e., performance) of engineered barrier materials such as shaft seals.

#### **5.1.3.1 Microbial Characterization – Waters & Rocks**

The microbiological organisms and their activity in water at the repository depth is an important parameter with respect to the long-term behavior of engineered barriers. If sulfate-reducing bacteria are present and active in either the water or rock, there is the potential for these microbes to produce the corrosive species sulfide via sulfate reduction. While the highly compacted bentonite in the emplacement rooms is expected to prevent any microbiological activity, if sulfide is produced at the bentonite-rock boundary or further out in the far-field, there is the potential for sulfide to diffuse towards the UFCs causing corrosion. Such corrosion is currently accounted for in the NWMO's copper corrosion allowance, but it is important to include site-specific data to ensure that the corrosion allowance is acceptable.

As part of NWMO's site characterization activities, samples of rock, groundwater and porewater are being collected at various depths from NWMO boreholes and analyzed using methods developed through applied research at multiple Canadian universities (Waterloo, Toronto and McMaster). These methods utilize DNA, RNA, PLFA and NMR techniques to determine the type of organisms present, the activity of these organisms, and the potential for the organisms to grow in the rock and in groundwater.

### 5.1.3.2 Measuring pH in Highly Saline Groundwaters

Hydrogeochemical research, whether it is lab- or field-based, commonly requires knowledge of the master variable, pH. pH measurements are commonly done potentiometrically, with electrodes, which is very challenging in high ionic strength ( $I$ ) systems, such as the brines that make up the porewater and deep groundwaters in the Michigan Basin (up to  $I = 8M$ ).

Spectroscopic methods offer an alternative approach for pH measurement in brines. This involves calibration of the spectroscopic properties of colorimetric indicators using specially-prepared buffer solutions, with the pH of the buffers determined by geochemical modelling. Initial work was completed using a single indicator (phenol red) in the measurement range of pH  $\approx 7 - 9$ . More recently, the technique has been extended over a wider range of pH ( $\sim 3 - 9$ ) using a multi-indicator solution. Results demonstrate that the technique is applicable up to  $I = 4M$ , but at higher ionic strength the sensitivity of the multi-indicator solution declines. Work is ongoing to formulate a multi-indicator that maintains sensitivity up to  $I = 8M$ .

### 5.1.3.3 Porewater Extraction Method Development

A significant area of research historically has been on development of techniques to extract porewater from the very low porosity crystalline and sedimentary rocks relevant to the Canadian program. There has been significant progress and several methods are now in use or have been recently applied as part of site characterization activities. However, techniques and approaches for the analysis and interpretation of results from porewater extraction experiments continues to be an active area of research - due to the indirect nature of these extraction procedures, as described in the following sections.

#### 5.1.3.3.1 Porewater Extraction – Crystalline Rocks

Vacuum distillation is a well-established method to extract porewater from low-permeability sedimentary rocks (Clark et al. 2013; Al et al. 2015). During vacuum distillation, water is evaporated from a substrate under vacuum and cryogenically trapped (using liquid nitrogen) in a sample vessel. Vacuum distillation can be coupled with aqueous leaching of solutes from post-dehydrated samples to reconstruct the geochemistry of the porewaters.

The objectives of research currently underway at the University of Ottawa are to 1) develop and optimize a vacuum distillation method to fully extract porewater from intact crystalline core samples; and 2) benchmark the approach (using crystalline rock saturated with water of known isotopic composition). The primary challenge of this work to-date was development of a method to fully re-saturate the cores with a water of known isotopic composition for use in benchmarking experiments, while avoiding fractionation of the porewater isotopes from the original re-saturating water. To resolve this, the testing criteria for achievement have been established as: (i) complete extraction of porewater (better than 95%) to avoid Rayleigh-type isotope fractionation and (ii) measured isotope contents of the extracted porewater that are within an acceptable margin of those of the saturating water reservoir.

Over the past two years, a resaturation method involving a combination of high vacuum (45 mTorr), followed by heating (120°C) at elevated pressure (15 PSI) for long durations has been developed and tested. Research findings demonstrate that for porewater extraction experiments using this protocol, close to 100% of the re-saturated water mass can be recovered by distillation at 150°C (with overnight extraction under vacuum for saturated cores). Furthermore, porewaters from fresh, fully saturated crystalline cores can be fully extracted without isotope

artifacts using the extended extraction method. The isotope results indicate that this extraction procedure is quantitative and without isotope exchange or fractionation, providing an accurate measurement of the in-situ porewater isotope content in crystalline core samples.

#### **5.1.3.3.2 Porewater Extraction – Sedimentary Rocks**

Benchmarking the extraction of porewaters from the low water content and low permeability sediments of the Ordovician sequences of the Michigan basin continues to be a focus of research. In 2020, experiments using both gravel-size (2-4 mm grains) and full-size cores from the Queenston, Georgian Bay and Blue Mountain formations were undertaken, and will continue into 2021.

The gravel-size fraction of core samples from the Bruce nuclear site (boreholes DGR-5/6) have been leaching in deionized water for ~10 years following their original analysis by 6-hour vacuum distillation at 150°C as part of work conducted for OPG's former L&ILW DGR program (these are defined here as 10-year gravels). In 2020, analyses began to extract water from the 10-year gravel samples; the majority of the samples were analyzed at 150°C for 6 hours, however, several were extracted at lower temperature (120°C for 6 hours). The purpose of the lower temperature extractions is to test whether high-fidelity measurements of water isotopes ( $^{18}\text{O}$  and  $^2\text{H}$ ) can be achieved at a lower temperature, in order to assess whether any exchange between the clay hydroxyl groups and porewater occurs. For results from both temperatures, no artifacts (enrichments or depletions in  $^{18}\text{O}$  and  $^2\text{H}$  with respect to the saturating water) were observed; waters extracted at both temperatures are within the range of the saturating fluid (0.5‰ for  $^{18}\text{O}$  and 5‰ for  $^2\text{H}$ ). Some evidence of evaporation in the signatures are noted for both the saturating water and the extracted water when compared to the original measurements, which is attributed to 10 years of storage of these fluids in plastic containers. Analyses, interpretation of results and reporting will continue during 2021.

Also, at the University of Ottawa, a novel method has been under development for several years to extract porewater from rock cores into cellulosic papers for subsequent analysis of the porewater composition. Research over the past several years has focused on verification of the major-ion data using core samples that have been equilibrated with a known synthetic porewater composition. The experiments designed for verification of the porewater chemistry are complete and results are encouraging. The porewater concentrations determined with the paper absorption method generally compare well with the known composition of the synthetic porewater. It is especially notable that this is true not only for Cl and Br which can be determined by crush and leach, but also for the major cations Ca, Mg, Sr, Na and K, which cannot be determined using crush and leach techniques, due to the occurrence of rock-water interactions (the concentrations of these cations in the porewater are not conserved during the experiment).

#### **5.1.3.4 Porewater Residence Times: Noble Gases and Sulfur Isotopes in Pyrite**

The isotopic analysis of heavy noble gases in porewaters within preserved cores was initiated to complement helium isotope studies performed as part of the sedimentary geosphere model development for the Bruce nuclear site. During 2019 and 2020, the functionality of the Helix multi-collector noble gas mass spectrometer was improved through upgrades to the noble gas purification and separation line. The noble gas laboratory at the Advanced Research Complex is the only one in Canada with instrumentation for analysis of the isotopes of helium together with the higher-mass noble gases, and the ingrowth of geogenic noble gases, including  $^4\text{He}$ ,  $^{21}\text{Ne}$ ,

$^{40}\text{Ar}$  and  $^{136}\text{Xe}$ , which can be used as measures of groundwater and porewater age. A refined method for heavier noble gas separation was advanced in 2019-2020 to improve the selective trapping of Kr and Xe, and to avoid the loss of Kr when sequentially trapped on the stainless steel in-line with a more aggressive activated charcoal trap. A polished stainless steel wool trap was found to improve the Kr signal 35-fold. The greater sensitivity on the instrument from improvements to gas separation on the sample preparation line have provided high quality data. Observations from archived core samples from the Bruce nuclear site, after 10 years of preservation, have suggested that many of the samples have degassed into the vacuum-sealed aluminum foil packaging over time. However, for many of these samples, this gas contains the same isotopic ratios of methane as those originally measured for adjacent core samples during site characterization activities. Gas samples have been taken from several of these long-preserved cores, and core crushing conducted for porewater content and water isotopic analysis. From these archived samples, a  $^{136}\text{Xe}$  excess has been discovered from select samples, with an average  $^{136}\text{Xe}/^{130}\text{Xe}$  value of 2.24. This degree of enrichment is expected if the porewaters are as old (>260 Ma) as suggested by previous helium isotope work. These results are being assessed together with uranium concentrations in these rocks to calculate the length of time for this  $^{136}\text{Xe}$  accumulation for comparison with He for these samples and will be summarized in a journal publication for submission in 2021.

It is anticipated that determination of the ingrowth of the higher-mass noble gas isotopes above their atmospheric ratios will provide robust chronologies of the porewaters in the sedimentary system. These techniques could be applied during future site characterization activities at South Bruce, and would be complementary to the He,  $\text{CH}_4$ , and  $^{87}\text{Sr}$  chronometers that have already been developed during earlier characterization activities at the Bruce nuclear site.

The sulphur system was the focus of a redox project at the University of Ottawa using  $^{34}\text{S}$  and  $^{18}\text{O}$  in sulphate, together with  $^{34}\text{S}$  in reduced sulphur phases (including organics, framboidal pyrite, and other iron-bearing phases). The sulphate project completed in 2018 focused on the source and timing of the emplacement of sulphate in the Ordovician aquiclude formations and the relationship of residual sulphate to co-existing framboidal pyrite in the shales. Analyses on the sulphide phases in the Ordovician and Cambrian sediments were undertaken subsequent to the sulphate project. This work included study of the  $\delta^{34}\text{S}$  and the morphology of framboidal pyrite. The results of the framboidal pyrite research were published in 2020. Key findings suggest that the pyrite in the units studied have retained  $^{34}\text{S}$ -isotope signatures consistent with a "closed system at the scale of pyrite formation" (Jautzy et al. 2020).

#### **5.1.3.5 Porewater Gases - Mont Terri PC-D Experiment**

The NWMO is currently leading the Porewater Gas Characterization Methods (Non-inert and Noble Gases): Field and Laboratory Methods Comparison (PC-D) Experiment at the Mont Terri URL. The objectives of the experiment are to: 1) compare results obtained for gas concentrations and isotopes using different techniques used by various nuclear waste management organizations and assess the comparability of the different methods as applied to homogeneous rock cores extracted from within the same shale unit (lower shale facies in the Opalinus Clay), and 2) assess the data from various approaches to determine if alternative (short-term or novel) methods can yield satisfactory results for site characterization needs in potentially less time than the current standard out-gassing approach employed by numerous researchers and laboratories around the globe for the purpose of gas characterization.

Over the course of 2020, due to delays associated with the global COVID-19 pandemic, emphasis was placed on experimental planning and establishing a drilling contract for an experiment-specific borehole. It is anticipated that drilling of the borehole and sampling will proceed in 2021.

#### **5.1.3.6 Profiles of Li, Mg and Ca Isotopic Compositions of Porewater**

Site characterization activities in low-permeability Ordovician sediments of the Michigan Basin at the Bruce nuclear site showed that the formations contain Na-Ca-Mg-Cl brines (>5 M) considered to originate as evaporated, post-dolomitic Silurian seawater, with residence times exceeding 400 Ma. To further constrain solute migration, research at the University of Ottawa has generated  $\delta^7\text{Li}$  and  $\delta^{26}\text{Mg}$  profiles of porewaters in these strata.

During 2019 and early 2020, research focused on preparing porewater leachates for isotopic analysis, based on extensive pre-treatment using ion-specific column chromatography to remove interfering geochemical matrices. Over the next two years, efforts will be focused on completing sample preparation and ICP-MS analysis, which were significantly delayed due to lab closures during 2020. Magnesium isotopic measurements will be carried out on a Neptune MC-ICP-MS at the Queen's Facility for Isotopic Research (QFIR). Lithium (Li) work to-date was done on a Nu Plasma II MC-ICP-MS at the Geological Survey of Canada (Ottawa) and on a Neptune MC-ICP-MS at QFIR.

Interpretation of the isotope profiles for  $\delta^{26}\text{Mg}$  focuses on shifts related to porewater-matrix exchange in association with dolomitization ( $\uparrow\delta^{26}\text{Mg}_{\text{pw}}$ ), possible secondary silicate formation ( $\downarrow\delta^{26}\text{Mg}_{\text{pw}}$ ) and possible shield-derived fluid mixing in the deep Ordovician. In addition to plans to expand the  $\delta^{26}\text{Mg}_{\text{pw}}$  porewater dataset in 2021 and beyond, measurement of  $\delta^{44}\text{Ca}$  in porewater will help to constrain the nature of fluid-rock interactions and potential mixing with a deep brine source in the Ordovician limestones.

Lithium is a highly soluble cation that is enriched in evaporative brines, but the isotope composition may be altered through secondary mineral formation, sorption onto clays and organics ( $\uparrow\delta^7\text{Li}_{\text{pw}}$ ), or mixing with crustal fluids in the deep Ordovician sediments. During 2020, a method for leaching the Ordovician shales to remove exchangeable Li, including interlayer Li in clays, was developed to isolate the structural Li in the silicates. Measurement of  $^7\text{Li}$  in the Ordovician shales will provide further insight into the fluid-rock interactions in these formations and will be the final step in this research.

#### **5.1.3.7 Stable Water Isotopes in Clay-bound Water**

Reliable measurement of the hydrogen (H) and oxygen (O) isotope compositions of porewater entrapped in Paleozoic shales in southern Ontario presents a challenge because of the very low water-contents of these rocks and possible porewater interaction with clay minerals. There is potential for modification of original porewater H and O isotope compositions arising from: (1) exchange between porewater and structural H and O in clay minerals, and (2) O and H isotope fractionation between mobile and bound water, depending on the porewater analysis method.

Research activities at Western University have focused on examination of the mineralogy, and O and H isotope geochemistry of clay minerals in Ordovician shales from the Bruce nuclear site and nearby locations. Key findings include: (1) abundances of illite > kaolinite > chlorite comprise the <2 $\mu\text{m}$  fraction of these shales; (2) the clay mineral O and H isotope compositions

plot to the left of terrestrial clay weathering lines in H and O isotope space; (3) calculated water O and H isotope compositions in equilibrium with these clay minerals at maximum geological burial temperature (~90°C) match porewater O and H isotope compositions measured by three different techniques; and (4) apparent H isotope clay mineral-water exchange was observed in 10-week experiments at 68°C. These preliminary data suggest that isotopic exchange with structural H in clay minerals can modify porewater H isotope compositions in low water-content shales.

The pandemic significantly affected research activities due to laboratory closures during March-July 2020, and a reopening schedule thereafter that permitted only limited laboratory occupancy. Nonetheless, progress was made to advance the project in 2020. Method development was completed for accurate and precise analysis of the H isotope composition of structural hydrogen in the swelling clay smectite. Atmospheric water vapour adsorbed onto smectite can contaminate H released from clay hydroxyl (OH) groups during isotopic analysis. It was determined that interlayer cation composition and cation hydration enthalpy affect the magnitude of this contamination and the apparent H isotope composition of smectite hydroxyl hydrogen ( $\delta^2\text{H}_{\text{OH}}$ ). The  $\delta^2\text{H}$  of different cation-saturated ( $\text{Ca}^{2+}$ ,  $\text{Na}^+$ ,  $\text{K}^+$ ) forms of six smectite standards from the Clay Minerals Society (CMS) Source Clays were measured using a modified sample drying and on-line High-Temperature-Conversion-Elemental-Analysis (TCEA) Continuous-Flow-Isotope-Ratio-Mass-Spectrometry (CF-IRMS) protocol. More negative interlayer cation hydration enthalpies ( $\text{Ca}^{2+} > \text{Na}^+ > \text{K}^+$ ) led to higher residual adsorbed water contents, which produced poorer reproducibility for  $\delta^2\text{H}_{\text{OH}}$ . The lowest adsorbed water contribution and the most reproducible and accurate values of  $\delta^2\text{H}_{\text{OH}}$  were obtained for K-saturated smectite dried for 4 hours or longer at 220°C, prior to isotopic analysis, and then rapidly transferred ( $\leq 2.5$  min) to a “zero-blank” autosampler. This research documented H isotope fractionation of adsorbed water during its gradual removal from smectite (Kanik, 2020). A journal publication based on this research is in preparation for submission in early 2021.

#### **5.1.3.8 Binding State of Porewaters – NEA CLAYWAT Project**

The CLAYWAT project, launched by the NEA Clay Club, is targeted at an improved understanding of the binding state of water in the nanometric pore space of argillaceous media. In addition to a literature review of methods of potential use in this context, the project included an experimental program on samples received from the Clay Club membership. A suite of measurements and experiments were performed by several laboratories, including differential thermogravimetry (TGA), differential scanning calorimetry (DSC), evolved gas analysis (EGA), mass loss upon heating to steady state at different temperatures, ad- and desorption isotherms for  $\text{H}_2\text{O}$ ,  $\text{N}_2$  and  $\text{CO}_2$ , and others. Further, nuclear magnetic resonance (NMR) relaxometry and imaging were applied to quantify porosity, pore-size distribution, to identify the relevant  $^1\text{H}$  reservoirs in the rock, to quantify diffusion coefficients for  $\text{H}_2\text{O}$  as well as to image the degree of heterogeneity of the  $^1\text{H}$  distribution in the samples.

Progress updates on CLAYWAT are shared among Clay Club members via the CLAYWAT Newsletter. In May 2020 a CLAYWAT workshop was held virtually at which eight participants delivered 12 technical presentations. A summary of this workshop was provided to the Clay Club members in the 4<sup>th</sup> CLAYWAT newsletter. Preparation of a final report for the project is underway and will continue during 2021.

### **5.1.3.9 Mont Terri Geochemical Data (GD) Experiment**

The NWMO is a partner in the Geochemical Data (GD) Experiment at the Mont Terri Underground Research Laboratory (URL) in Switzerland. The GD Experiment aims to collect and evaluate data from various activities in the URL, in terms of assessing coherence / agreement with the established porewater conceptual model for system evolution. Open questions that are identified in the model(s) or in the understanding of behaviour often become targeted research projects within GD (e.g., lab investigations, in-situ measurements and/or modelling activities). In 2020, research as a part of GD focused on advancing two of the projects: 1) carbonates in clay rocks, and 2) redox and the role of Fe-containing minerals in controlling system Eh.

### **5.1.4 Transport Properties of the Rock Matrix**

Near-field performance, safety assessment and groundwater transport/evolution models require knowledge of groundwater and porewater geochemical compositions, as well as petrophysical and solute transport properties, to provide representative estimations of long-term system behaviour. The following research programs contribute to the NWMO's technical capabilities in the context of assessing long-term solute mobility and retention.

#### **5.1.4.1 Permeability**

Research over the past year at McGill University focused on the estimation of the permeability of cuboidal blocks of granite obtained from Lac du Bonnet (western flank of the Canadian Shield) and from Stanstead (eastern flank of the Canadian Shield). The surface patch permeability test developed by Selvadurai (2010) and documented by Selvadurai and Selvadurai (2010) for the testing of Indiana Limestone was adopted and modified to test the cuboidal granite samples. The surface permeability was extrapolated to the interior regions using a kriging technique and a computational approach was used to estimate the permeabilities of the granites in three orthogonal directions. The experimental procedures are documented by Blain-Coallier (2020) and findings from this research are reported by Selvadurai et al (2020).

#### **5.1.4.2 Diffusion Properties**

##### **5.1.4.2.1 Method Development – X-ray CT Imaging**

The University of Ottawa acquired an X-ray CT system in 2016, and it has been tested extensively to assess its capabilities to improve imaging capabilities in low-porosity rock and to optimize measurement parameters for tracer experiments. One recent application was the monitoring of iodide and cesium diffusion in crystalline rocks which was presented at the 2020 Goldschmidt Conference (Cadieux et al. 2020). The instrument has since been modified to minimize the effects of beam hardening and increase signal-to-noise ratios for improved tracer detection. The spectrometry system is operated in two modes, X-ray absorption in transmission mode and X-ray fluorescence. The X-ray absorption approach has been used successfully to monitor iodide and cesium diffusion in the Queenston Formation shale and the data demonstrate that beam hardening effects are virtually eliminated. The X-ray fluorescence technique is currently being developed and preliminary results indicate that it has potential for experimental monitoring of diffusion and reaction processes with a diverse range of tracers that are of interest for evaluation of transport and attenuation properties in the near field of a DGR.

#### 5.1.4.2.2 *Mont Terri Diffusion Experiments – DR-B, CI-D*

The NWMO is a partner in both the Long-term Diffusion Experiment (DR-B) and the Diffusion across 10-year-old Concrete/Claystone Interface Experiment (CI-D) at the Mont Terri URL.

The objectives of the DR-B experiment are i) to develop a means for the long-term monitoring (>10 years) of in-situ iodide diffusion process at a large scale in a clay formation; and ii) to validate the diffusion process understanding developed and transport parameters determined through previous experiments. The experimental setup consists of a central borehole and 3 surrounding observation boreholes. Sodium iodide (NaI) solution was injected in the central borehole in April 2017 and is expected to diffuse over time toward the observation boreholes. Starting in November 2018, a breakthrough of iodide was detected in the observation borehole located closest to the injection borehole. The iodide concentration in the observation boreholes has been measured regularly (Jaquenoud et al. 2021).

The objectives of the CI-D experiment are i) to assess the impact of the long-term (10 years) cement-Opalinus clay interface reactions (CI experiment) on diffusion of solutes ( $^3\text{H}$  and  $^{36}\text{Cl}$ ); and ii) to provide in-situ data for reactive transport modelling. The CI-D experiment setup consists of a borehole which in 2007 was filled with three different types of concrete (OPC, LAC and ESDRED) and compacted bentonite (MX-80) (borehole for the CI experiment), an injection borehole, and monitoring boreholes. High pH fluid circulation started in July 2018, and tracer ( $^3\text{H}$ ,  $^{36}\text{Cl}$ ) injection began in May 2019. The CI-D experiment is expected to last for 3 – 4 years. An international joint CI/CI-D modelling team is modelling the alteration due to cement-clay interaction and the tracer transport across such interfaces with different reactive transport codes including MIN3P-THCm (section 6.4.1).

#### 5.1.4.3 Sorption

Sorption is a mechanism for retarding sub-surface radionuclide transport from a DGR to the environment. The NWMO initiated the development of a sorption distribution coefficient ( $K_d$ ) database for elements of importance to the safety assessment of a DGR (Vilks 2011). This initial database was further developed to include sorption measurements for Canadian sedimentary rocks and bentonite in saline solutions (with ionic strength  $I = 0.23\text{--}7.2\text{ M}$ ) including a reference porewater SR-270-PW brine solution (Na-Ca-Cl type with  $I = 6.0\text{ M}$ ) (Vilks and Yang 2018).

Researchers at McMaster University have continued to systematically study the sorption properties of Se and Tc on limestone, shale, illite and bentonite (MX-80) in SR-270-PW brine solution, as well as on crystalline rocks and bentonite in a reference groundwater CR-10 (Ca-Na-Cl type with  $I = 0.24\text{ M}$ ) under reducing conditions. The effects of ionic strength and pH on Se and Tc sorption on shale, illite, limestone, bentonite and crystalline rocks have been investigated (e.g., Racette et al. 2019, Walker et al. 2018). It was found that sorption of Se(-II) on illite and MX-80 showed little ionic strength dependency across the ionic strength range of 0.1-6 M. Sorption of Se(-II) on shale at low ionic strength (0.1 M and 0.5 M) were higher than those at higher ionic strength of 1-6 M. Sorption  $K_d$  values were fairly constant from ionic strength 1 M to 6 M, with a slight decrease for 6 M (Figure 5-5). Two journal articles documenting Se(-II) sorption on illite, bentonite, shale, and limestone in SR-270-PW, and Se(-II) sorption on granite and bentonite in CR-10 are expected to be submitted for publication in 2021.

Work was also done on the sorption of Pd on illite, MX-80 and shale in Na-Ca-Cl saline solutions (Goguen et al. 2020).

A new three-year, collaborative research program with McMaster University was initiated in 2020 to study the sorption properties of (1) U on limestone, shale, illite and bentonite in SR-270-PW reference water, as well as on crystalline rocks and bentonite in CR-10 reference water under both oxidizing and reducing conditions; and (2) Eu on limestone, shale, illite and bentonite in SR-270-PW, as well as onto crystalline rocks and bentonite in CR-10 under reducing conditions. The measured sorption  $K_d$  values will be used to update the NWMO sorption database.

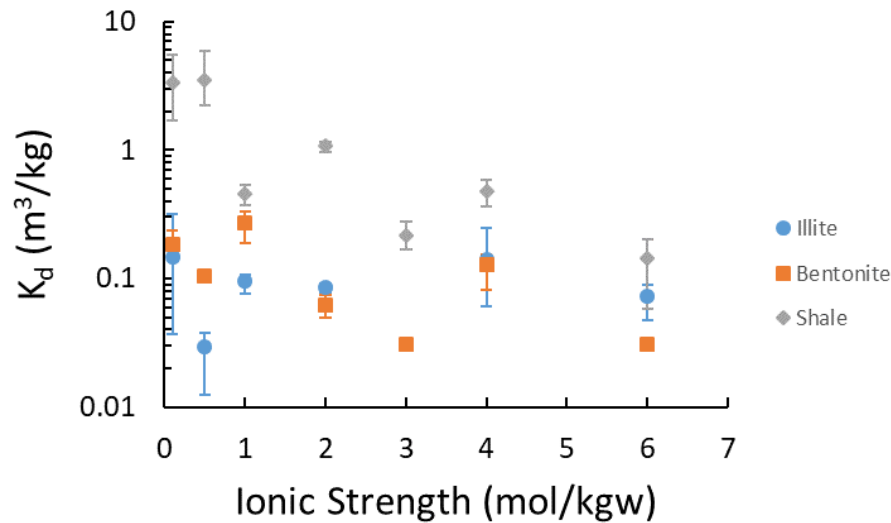


**Figure 5-5: Ionic Strength Dependency of Sorption of Se(-II) on Shale, Bentonite, and Illite**

#### 5.1.4.4 Surface Area & Cation Exchange Capacity

In 2018, the University of Bern completed research to characterize external surface area (BET) and cation exchange capacity (CEC) in sedimentary rock cores from the Bruce nuclear site. Samples from the Queenston, Georgian Bay, Blue Mountain and Collingwood Member formations were evaluated (rock types included claystone, marl and limestone). The research focused on addressing the question of mineralogical fractionation induced by sieving to different grain sizes (i.e., can a specific fraction for geochemical experiments be used and the results considered representative of the whole rock?), as well as the effect of crushing on determined CEC values (e.g., does crushing create new mineral surfaces, and is it permissible to extrapolate geochemical data obtained on disintegrated or crushed material to the intact rock?). The main findings are summarized below.

- 1) Chemical and mineralogical compositions do not vary systematically between grain-size fractions, indicating that size reduction and sieving do not lead to a resolvable fractionation (except for the limestone sample).

- 2) BET surface area increases with decreasing grain-size fraction by 50 – 100% (claystone and marl) and 300% (limestone). Crushing to smaller particle sizes, thus, provides access to surfaces that are either inaccessible or not present in the intact rock.
- 3) CEC of claystone and marl samples increase by 7–31% between fractions 1–4 mm and <0.063 mm. While crushing to smaller grain size creates new surfaces, these are predominantly related to minerals with a small or negligible CEC, such as carbonates or quartz. It is concluded that the effect of grain size plays a relatively limited role for CEC.
- 4) CEC of the limestone sample between fractions 1–4 mm and <0.063 mm increases by 110%. Care needs to be taken when extrapolating data produced on crushed limestone samples to the intact rock.
- 5) Good linear correlations are observed between clay content, BET surface area and CEC. BET surface measurement can be used as a proxy of the cation-exchange capacity of the sample, which is a feature known for other sedimentary rocks.

The results of this research were compiled into a technical report for the NWMO in 2019, and it is expected that a final report will be published by the NWMO.

## **5.1.5 Geomechanical and Thermal Properties**

### **5.1.5.1 In-Situ Stress**

The in-situ stress state is a fundamental parameter for the engineering design and safety assessment of a DGR. Obtaining reliable estimates of in-situ stress is important, however, this is often hindered by small numbers of field stress measurements as well as by variability arising from the geological environment. Bayesian data analysis applied to a multivariate model of in-situ stress can potentially overcome these problems and generate a multivariate stress tensor for a site. In 2020 together with SKB (Sweden), NWMO initiated a new research program at the University of Toronto to investigate the use of Bayesian data analysis in the statistical quantification of in-situ stress variability. Recently developed, novel techniques will be applied to the analysis of site-specific data provided by SKB, with the objectives of (i) generating design stress tensors for the site and (ii) developing protocols suitable for application at other sites.

### **5.1.5.2 Rock Properties from Laboratory Experiments**

#### **5.1.5.2.1 Thermal Properties**

The thermal conductivity characteristics of the Cobourg limestone was estimated using a multiphasic approach for the estimation of the lighter species containing predominantly calcite and dolomite and the darker regions containing, calcite, dolomite and a clay fraction. The spatial distribution of the nodular fractions was determined by previous research that investigated the effective permeability of the Cobourg limestone by dissecting a cuboidal sample (Selvadurai, 2019a). The research that investigated the estimation of the effective thermal conductivity of the Cobourg limestone was documented by Selvadurai and Niya (2020). A research program was initiated to determine the thermal conductivity characteristics of the Lac du Bonnet Granite. During 2020, the research activities were temporarily suspended, in part because of Covid-related laboratory closure, but also because the Master's student working on the project transferred to a Master's program based on coursework. The experiments will be resumed by a new doctoral student beginning in 2021.

#### **5.1.5.2.2 Poroelastic Properties**

A key poroelastic parameter relevant to the constitutive modelling of fluid saturated rocks with an elastic skeletal behaviour is the Biot coefficient that defines the partitioning of externally applied stresses between the porous skeleton and the pore fluid. A critical experiment used in these investigations relates to the estimation of the compressibility of the solid phase composing the porous fabric, during applications of an isotropic stress. To perform the experiments required for the estimation of the Biot coefficient, the pore space must be completely saturated with no influence of any trapped air. When the permeability of the rock is extremely low, as in the case of the Cobourg limestone, the estimation of the solid phase compressibility by saturation is less reliable and time consuming. In the research conducted in connection with the Cobourg limestone, the compressibility was estimated by appeal to the mineralogical composition of the rock and a widely accepted multiphase theory (Selvadurai, 2019b; Selvadurai and Suvorov, 2020; Selvadurai et al, 2020). The same procedures were applied to estimate the effective compressibility of the solid phase of the Lac du Bonnet granite. Estimates for the Biot coefficient for the Lac du Bonnet granite are documented in a journal article submitted for publication during 2020 (Selvadurai, *in press*).

#### **5.1.5.2.3 Effect of Temperature on Mechanical Properties**

The alteration of the thermal, hydraulic and mechanical (THM) properties of the Lac du Bonnet granite subjected to extreme heating up to 90 degrees Celsius and possibly higher (150 degrees Celsius) will be examined at McGill University. This research was originally planned to begin in 2020 but was delayed, in part due to the pandemic. It is anticipated that a new Ph.D. project will be initiated during 2021 on this topic and will also include the thermal conductivity measurements of the Lac du Bonnet granite as described in section 5.1.5.2.1.

#### **5.1.5.3 Rock Properties from In-situ and/or Large-Scale Experiments**

##### **5.1.5.3.1 POST Project**

The goal of the POST project is to develop an understanding of the mechanics of rock joints during shearing under loads that are representative for depths of approximately 300-500 m. This is an area of research which is important for assessing the long-term safety of a DGR.

The second phase of the project (POST2) began in 2017. In parallel, there are two on-going PhD-projects in Sweden in collaboration with KTH (Royal Institute of Technology) which use data from the project. One project investigates rock and replica joints in direct shear loading including an examination of scale effects. The second project is focused on the improvement of tools - laboratory, analytical and numerical - for estimation of rock fracture peak shear strength, including scale effects.

POST2 initially contained four major components:

1. Design and manufacture of new shear test equipment for large specimens.
2. Develop methods for conducting well-controlled direct shear tests experiments with thorough documentation of specimen before, during and after experiments.
3. Develop methods for manufacturing replicas of real rock joints.
4. Conduct direct shear tests on medium-scale rock joints and rock joint replica specimens at both constant normal stiffness (CNS) and constant normal load (CNL) loading conditions.

Three of these components (2-4 above) were completed in 2018. Back-analysis of preliminary direct shear test results of rock and replica materials in 3DEC continued during 2020.

Research in 2020 on testing small (35 x 60 mm) and intermediate scale (70 x 100 mm) specimens continued, with the preparation of additional specimens with tensile induced joints needed to complete the testing program. An example of the blocks prior to the final cutting stage of specimens are shown in Figure 5-6. The joint is kept closed undisturbed by clamps during handling and cutting.

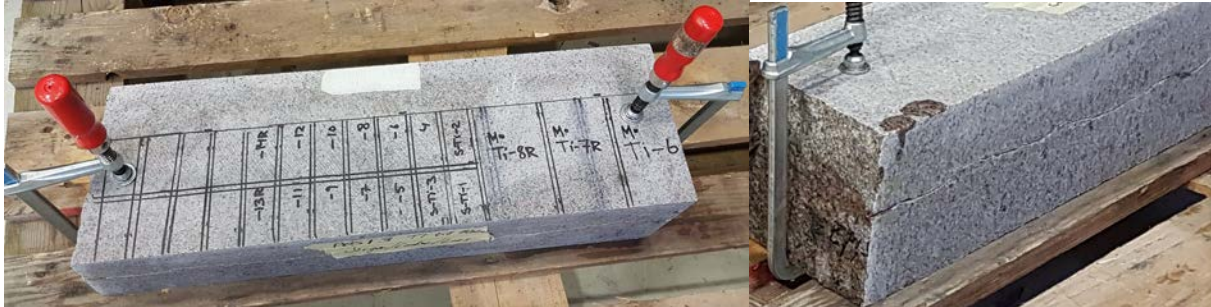


**Figure 5-6: Blocks Before of Final Cutting Stage of the 35 x 60 mm and 70 x 100 mm with Tensile Induced Joints**

The results from the manufacturing of replicas were further analysed by comparing the geometries of the joint surfaces of the replicas and the original rock joint, in this case natural joint (Figure 5-7). The replica development technique was refined in stages, yielding successively less deviation of the average aperture, which was selected as a metric. The RPM-N1-CNL-4, RPM-N1-CNL-5 and RPM-N1-CNL-6 were the final stages of method development. A clear relation is observed between the geometry deviation and the mechanical response, where the specimens with the least deviation display behaviour closer to that of the natural rock joint. The various stages of evolution in method development are described in Larsson et al. (2020).

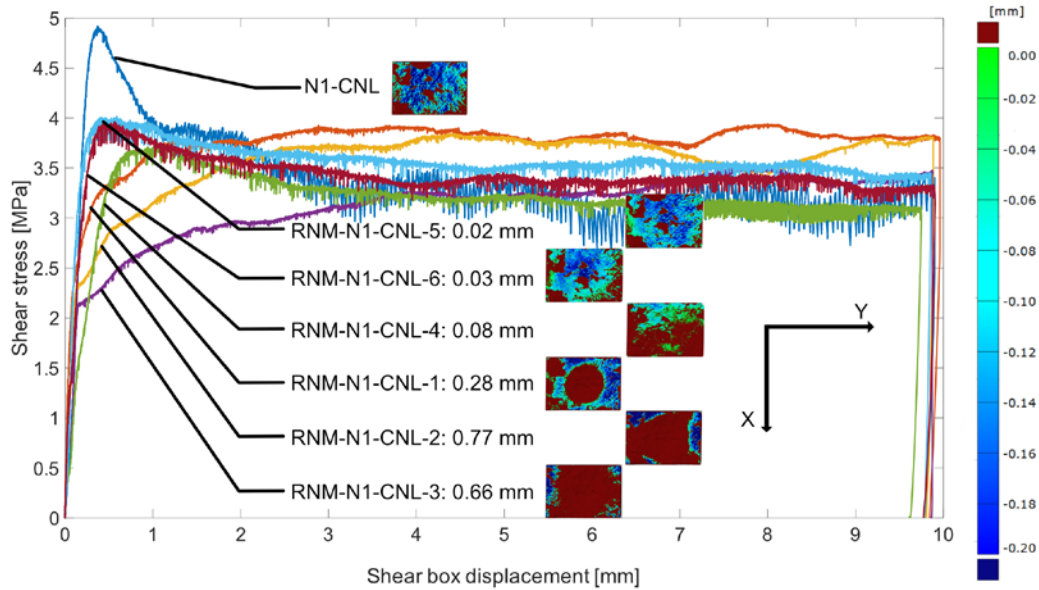


**Figure 5-7: Results from Direct Shear Tests on Rock Joint (N1-CNL) and Replicas of the Surface (RNM-N1-CNL). The Average Geometrical Aperture Deviation of the Replicated Surfaces Versus the Parent Rock Joint is Shown by the Images and the Scale to the Right (From Larsson et al. 2020)**

In 2020, the large shear testing equipment was prepared and verified for tests on rock specimens. The results of the normal loading experiments of the steel specimen conducted in December 2019 and January 2020 showed that the normal deformation measured by the LVDTs was about 0.6 mm at a load of 4.5 MN load, equal to 30 MPa normal stress for the 300 x 500 mm specimen. This shows that the system stiffness in the normal direction is in line with the expectations, the effect of which is particularly important for calibrating direct shear test results under CNS normal loading condition as recently studied by Larsson and Flansbjerg (2020). Complementary experiments using the same steel specimens were conducted during August and September to study the shear response. The optical measurement system for direct measurements of the relative displacement of the rock joints was tested and showed good results.

The first experiments on rock joints in the large shear testing equipment were conducted on specimens with natural joints. The tests can be considered as pre-tests and was an opportunity to check the whole procedure starting from casting the specimens in the large holders, scanning the joint surfaces, reassembling the joints in the initial position with mated joints, installing the specimens in the testing equipment, conducting the mechanical testing, and post-test scanning of the joint surfaces. Overall, the testing sequence and measurements progressed smoothly, however, one problem was revealed with the control of actuator providing the shear displacement. The shear displacement was supposed to be applied as a ramp with a constant shear displacement rate, but an oscillation on top of the ramp was noticed yielding a variation of the shear stress. This issue will be resolved before the tests of the POST specimens begin.

#### **5.1.5.3.2 Mont Terri FE-M Project**

The FE-M experiment, long-term monitoring of the full-scale heater test, continues with the heating phase which commenced in December 2014. This experiment was designed to

demonstrate the feasibility of: (1) constructing a full-scale 50 m long and 3 m in diameter deposition tunnel using standard construction equipment; (2) heater emplacement and backfilling procedures; (3) early post-closure monitoring to investigate repository-induced coupled thermo-hydro-mechanical (THM) effects on the backfill material and the host rock (i.e., Opalinus Clay); and (4) validation of THM models.

Field measurements are on-going include temperature, pore-water pressure, humidity/water content and suction, thermal conductivity, deformations, and stresses. The program is currently focused on the long-term monitoring of the THM processes confirming the technical readiness of the conceptual modelling framework pertinent to assessment of the long-term performance in the near field scale. Nagra has established a THM modelling task force consisting of Technical University of Catalonia (UPC), the École Polytechnique Fédérale de Lausanne (EPFL), and BGR/TUBAF/UFZ. In 2020, modelling activities continued as part of subtask 1.1, which comprises code and calculation verification of TH and THM model results amongst the three teams which used Code\_Bright, Code\_Aster and OpenGeoSys, respectively. This task was nearly complete by the end of 2020, with only final refinement calculations to be undertaken in early 2021 by one modelling team. Notably, a versatile calculation and verification approach has been developed by the Task Force (TF), which includes questionnaires, comprehensive yet flexible code-to-code or code-to-measurement assessment strategy, and rigorous evaluation metrics. Subtask 1.2, which involves back-analyses of FE monitoring data was also initiated during 2020.

#### **5.1.5.3.3 Mont Terri GC-A Experiment**

The main objective of this experiment is to understand the geomechanical in-situ response of the Opalinus clay during excavation at the transition from shaly to sandy facies.

This experiment consisted of multiple components including:

- Monitoring of the excavation convergence and pore pressure response,
- Laboratory and field geophysical measurement of static and dynamic elastic properties of the Opalinus clay, and
- In-situ stress measurements.

In 2020, activities in GC-A focused on continued 1) monitoring of pore pressures and convergence measurements in Niche 2; and 2) detailed interpretation of pressure meter tests conducted to measure in-situ stress by the University of Alberta. During 2020, an abstract was submitted and accepted for presentation at the 6<sup>th</sup> International Conference on Geotechnical and Geophysical Site Characterization to be held in Budapest in 2021 (Liu et al. accepted).

#### **5.1.5.4 Shear-Induced Pore Pressure Around Underground Excavations**

In 2020, a new Ph.D. research project, co-funded by NWMO and Nagra, was initiated at the University of Alberta. The overarching objective of this research is to advance the understanding of the coupled hydro-mechanical processes that occur during underground excavations in heavily overconsolidated clays and weak rock-like shale deposits. Previous field tests completed at Mont Terri Underground Rock Laboratory (Mont Terri) established that deformations around underground openings in Opalinus Clay are highly dependent on the direction of the excavation relative to the materials bedding. Excavations completed in a direction parallel to the materials bedding have shown higher pore pressures, yielding at

relatively small strains compared to laboratory results, and larger than predicted deformations. This research program will examine these findings through two mine-by experiments completed at Mont Terri, one parallel and one perpendicular to the materials bedding, where instruments were strategically placed in front of and around the tunnel's excavation zone. The findings from these experiments will then be compared to the results of a laboratory testing program. The laboratory program will utilize a novel direct shear apparatus that is being developed at the University of Alberta. This apparatus will be the first to incorporate micro fibre optic pressure sensors (MFOPs) into a direct shear test to measure the pore pressure response along the shear zone of the sample while applying a strain-controlled boundary condition.

Fundamental behavioral models for saturated, overconsolidated soils such as shales have historically been derived using stress-controlled boundary condition tests. In nature, this experimental boundary condition is comparable to a rock sliding on a slope where dilation can occur at the shear boundary. Around underground excavations, dilation cannot occur as the surrounding ground restricts movement like a spring that is controlled by the rock mass and stiffness (strain-controlled). Restricting dilation creates the potential for pore pressures to increase during shearing. The presence of shear-induced pore pressures contradicts the current fundamental model for overconsolidated saturated shales. If shear-induced pore pressures are confirmed, this may change how engineers assess application challenges in shale where strain-controlled boundary conditions exist.

The research hypothesis is that the current fundamental model is overestimating the strength of this class of material to short term undrained shearing events when a strain-controlled boundary condition exists. The potential for these shear-induced pore pressures appears to be created in low permeability heavily overconsolidated soils during underground excavations completed parallel to the materials bedding. The extremely low permeability of the Opalinus Clay coupled with the existing strain-controlled boundary condition around the underground openings at Mont Terri makes it so that these higher than anticipated pore pressures are generated through their inability to dissipate and an accumulation effect as the tunnel is further excavated and additional undrained shear events occur. These higher than predicted pore pressures lead to the on-set of yielding at lower than anticipated strengths and increased deformations.

A three phased approach is planned for this program:

1. A field stage consisting of analysing the pore pressure response observed during two mine-by tunneling experiments at Mont Terri as described above. This will include modelling of the experiments in the commercially available software FLAC3D developed by Itasca Consulting Inc.
2. A laboratory stage consisting of the design, construction and operation of a novel triaxial test setup that incorporates MFOPs placed near the center of the samples to gather internal pore pressure measurements. The triaxial tests will be used to confirm the validity of the MFOPs readings, which will then be applied in the direct shear test. The second laboratory task will involve the design, construction and operation of the novel direct shear apparatus with MFOPs placed near the shear zone and a strain-controlled boundary condition, as described above. Similarly, FLAC3D will be used to model the findings of the laboratory testing program.
3. The third stage involves comparing the results from the field and laboratory programs to validate or disprove the research hypothesis.

The program officially kicked off in July of 2020. The work completed in 2020 included: grant applications to the Natural Science and Engineering Research Council of Canada (NSERC); literature review; data acquisition from Mont Terri, and the design, procurement and construction of the triaxial cell and MFOPs (Figure 5-8).

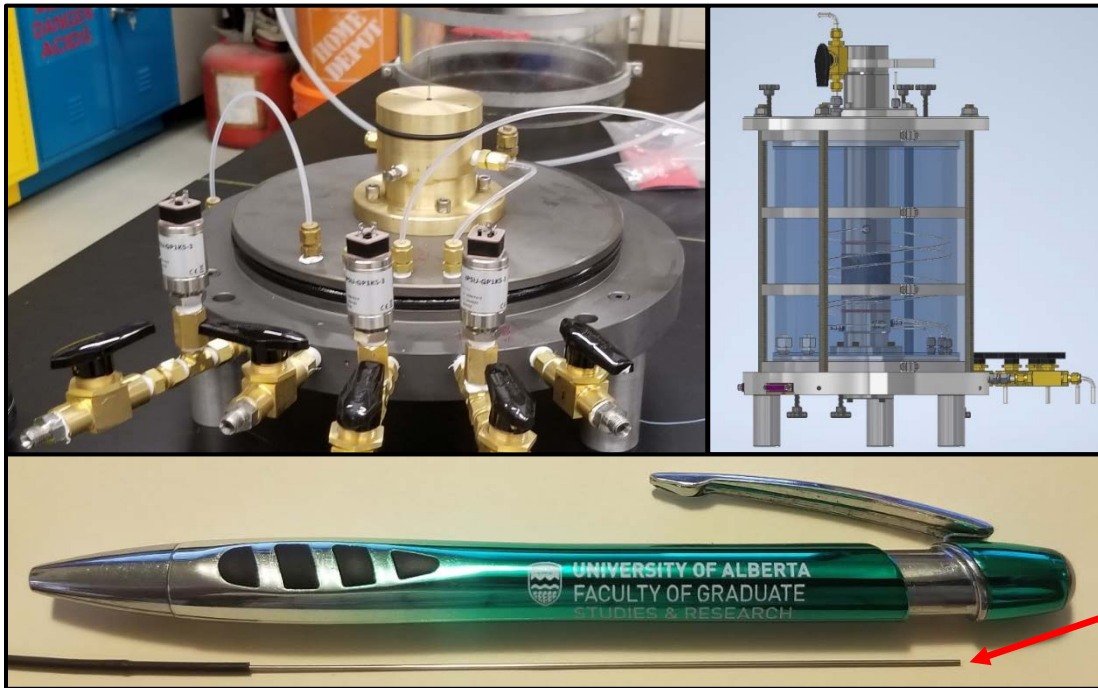


**Figure 5-8: (top left) Image Showing Base of Triaxial Cell with the Micro Fibre Optic Pressure Sensor; (top right) Image of Triaxial Cell Design Created in AutoCAD Inventor; and (bottom) Image Showing the Size of the Micro Fibre Optic Sensors Compared to a Standard Pen**

### 5.1.5.5 Numerical Modelling of Geomechanics

#### 5.1.5.5.1 Rock Mass Effective Properties

In 2016, POSIVA, SKB, and NWMO jointly sponsored a research program with ITASCA Consultants s.a.s. (ICSAS) and the Fractory (Joint Laboratory between ICSAS, CNRS and the University of Rennes, France) to improve our understanding of the role played by the fractures on rock mass mechanical behavior. In order to overcome the limitations of the available rock mass classification systems, numerical modelling using a Discrete Element Method is done with the final goal of developing guidelines and a numerical tool (PyRockMass) for upscaling the mechanical properties of a rock mass containing Discrete Fracture Network (DFN). During this first phase of the project (Phase 1), numerical modelling and mechanical testing of Synthetic Rock Mass (SRM) specimens (Min and Jing 2003, Esmaili et al. 2010, Mas Ivars et al. 2010; Harthong et al. 2012; Le Goc et al. 2014; Le Goc et al. 2015; Poulsen et al. 2015) were largely

used to support the project fundamentals and applied developments, as it is not possible to perform laboratory tests of rock mass samples with dimensions compatible with DFN scales. Theoretical developments achieved during Phase 1 created the foundation used to define a DFN-based rock mass effective properties methodology. These major achievements were relative to elastic properties, specifically specimen scale effective elastic properties and stress distribution below the specimen scale. The derived method predicts the change in elastic properties of a rock mass (Young's modulus and Poisson's ratio in simple cases and more generally all the terms of the compliance tensor), relatively to intact rock conditions, the embedded DFN model (geometry and fracture mechanical properties), scale of interest and remote stress conditions. The method is analytical and thus eliminates computational burden and numerical limitations inherent to rock mass numerical modelling. It also provides a means to understand which characteristics of the fractured system (i.e., DFN model) are critical for the mechanical behavior, and to relate these DFN model metrics to rock mass properties with simple relationships (Davy et al. 2018). An application to the Forsmark site FFM01 Fracture Domain was published in Darcel et al. (2018). To reproduce the project results and apply it to new cases, core functionalities were implemented in a Python program referred to as PyRockMassTool. PyRockMassTool computes the equivalent compliance tensor of a rock mass specimen defined from a DFN description of the fracture system embedded in the rock.

The same scientific approach described above - i.e., fundamental developments, use of numerical modelling, testing and methodology development - will be applied to Phase 2 of this research, which was initiated as a joint project between SKB and NWMO in 2020. The main objectives of Phase 2 are to further test the methodology application for elastic conditions, and to develop a fundamental understanding of the relationship between DFN model properties, stress fluctuations and rock mass effective strength. The basis of the approach (i.e., relationships between remote stress, local stress and fracture normal and shear displacement) will be also used to provide individual fracture apertures, as a prerequisite for hydromechanical coupling and flow modelling.

#### **5.1.5.6 NSERC Energi Simulation Industrial Research Chair Program in Reservoir Geomechanics**

In 2019 NWMO joined the renewal of a multi-sponsor NSERC/Energi Simulation Industrial Research Chair (IRC) in Reservoir Geomechanics at the University of Alberta. This IRC chair aims at advancing experimental and numerical methods as well as field studies to help mitigate operation risks and to optimize reservoir management as they pertain to the coupled processes in oil and gas reservoirs. Some of the findings are expected to be also applicable to crystalline settings.

Overall, participation in this multi-faceted IRC program is expected to advance our understanding of how intact rock and fractures at various scales respond to thermal-hydro-mechanical processes associated with a DGR. During 2020, planning was underway for the first annual research symposium to be held in February 2021. This symposium will provide sponsors with progress updates on all key research areas underway as part of the program.

## **5.2 LONG-TERM GEOSPHERE STABILITY**

### **5.2.1 Long Term Climate Change – Glaciation**

#### **5.2.1.1 Surface Boundary Conditions**

Glaciation associated with long-term climate change is considered the strongest external perturbation to the geosphere at potential repository depths. Potential impacts of glacial cycles on a deep geological repository include: 1) increased stress at repository depth, caused by glacial loading; 2) penetration of permafrost to repository depth; 3) recharge of oxygenated glacial meltwater to repository depth; and 4) the generation of seismic events and reactivation of faults induced by glacial rebound following ice-sheet retreat. The ability to adequately predict surface boundary conditions during glaciation is an essential element in determining the full impact of glaciation on the safety and stability of a DGR site and will be a necessary component supporting site characterization activities. For the NWMO's studies into the impact of glaciation, such boundary conditions have been defined based on the University of Toronto's Glacial Systems Model (GSM) predictions. The GSM is a state-of-the-art model used to describe the advance and retreat of the Laurentide ice-sheet over the North American continent during the Late Quaternary Period of Earth history.

Following the update to the GSM methodology and subsequent validation, a new phase of research was undertaken with the goal of refining the representation of the evolution of paleolakes and surface drainage basins within the model, as well as further analyses of fits to relative sea-level data in Southeastern Hudson's Bay region. Additional modelling capabilities to University of Toronto GSM are currently being developed to deliver improvements to simulations of Laurentide ice sheet evolution. During 2020, research to understand the impact of glaciation on the Great lakes continued to advance by further characterizing glacial meltwater in the University of Toronto GSM, and by investigating the impact of glacial meltwater on the formation of proglacial lakes, as well as the evolution of the Great Lakes.

#### **5.2.1.2 Glacial Erosion of crystalline rocks**

Since late 2019, research has been underway at Dalhousie University to study the effects of glacial erosion within crystalline bedrock settings. A key outcome of this research will be a state-of-the-science review of published information relating to glacial erosion in crystalline bedrock settings (planned for submission in 2021). This review includes consideration of i) recent advances in theoretical work on glacial erosion; ii) erosion studies involving numerical modelling of ice sheets; iii) any prior erosion rates from studies in the Canadian shield and other areas with similar lithology and glacial histories; iv) synthesis of factors that control glacial erosion and a ranking of their relative importance for crystalline bedrock settings in Ontario; v) descriptions and applications of cosmogenic radionuclides or other emerging approaches or measurement techniques to provide estimates of erosional processes and erosional rates and; vi) detailed sampling strategies for cosmogenic nuclide methods, as well as any special considerations for associated field and laboratory work.

In mid-2020, a postdoctoral fellow was on-boarded to Dalhousie University and work on the state-of-science review began. A draft journal publication is planned for NWMO review by end of 2021.

### 5.2.1.3 Glacial and Proglacial Environment – Numerical Modelling

#### 5.2.1.3.1 *CatchNet Project*

CatchNet (Catchment Transport and Cryo-hydrology Network) is a joint international program formed by international nuclear waste organizations and cold region hydrology researchers (URL: <https://www.skb.se/catchnet/>). It was established in 2019 to advance our understanding of hydrological and biogeochemical transport processes for a range of cold-climate conditions in the context of long-term, deep geological disposal of used nuclear fuel. CatchNet has identified three research packages (RP) to address important knowledge gaps:

- RP1: connecting the glacial and sub-glacial hydrology with the periglacial hydrological system on landscape scale,
- RP2: permafrost transition periods, and
- RP3: biogeochemical cycling.

Currently CatchNet has three full members (SKB, NWMO and RWM) and one supporting member (COVRA). Each full member funds a PhD student or postdoctoral fellow to work on a research topic related to cold-climate conditions.

NWMO is supporting a Ph.D. student based at McGill University. This Ph.D. research program started in September 2020 and the research topic is to examine the impacts of permafrost transition on surface and subsurface hydrologic processes (RP2).

#### 5.2.1.3.2 *University of Montana – Joint Work with SKB*

In 2019, NWMO and SKB initiated a new project to support researchers at the University of Montana (USA) to study coupled ice sheet, groundwater, and surface water hydrological processes through new data analysis and numerical modeling. This modelling study uses the field data previously collected from two international projects (GAP and GRASP) in the Kangerlussuaq area of western Greenland. This joint project focuses on the following two main areas:

- Evolution of the thermal state of the ice sheet bed, and
- Ice-sheet processes influencing the ice sheet - bedrock boundary and underlying groundwater pressures near the ice sheet margin.

The researchers work closely with the CatchNet program, participating in the CatchNet annual meeting and other activities regularly. In particular, the results of this study will be used as boundary conditions by CatchNet RP1.

In 2020, most of the analyses of observed data were completed. In addition, a journal article was submitted for review (Harper et al., 2020 – *submitted*), expected to be published in 2021.

## 5.2.2 Groundwater System Stability and Evolution

### 5.2.2.1 Numerical Modelling Approaches

Reactive transport modelling is a useful approach for assessing long-term geochemical stability in geological formations. Reactive transport modelling is used to assess: 1) the degree to which dissolved oxygen in recharging waters may be attenuated within the proposed host rock; 2) how geochemical reactions (e.g., dissolution-precipitation, oxidation-reduction, and ion exchange

reactions) may affect groundwater salinity (density) and composition along flow paths; and 3) how diffusive transport of reactive solutes may evolve in low-permeability geological formations.

Unstructured grid capabilities were implemented into the multi-component reactive transport code MIN3P-THCm for 3-dimensional (3-D) systems, including the parallelization of the unstructured grid functions (Su et al. 2020a, Su et al. 2020b). A NWMO technical report providing additional details on the implementation of unstructured grids in MIN3P-THCm is expected in 2021. A 3-D demonstration simulation based on the Michigan Basin is underway for the evaluation of MIN3P-THCm code capabilities for large-scale 3-D flow and reactive transport simulations using unstructured meshes.

MIN3P-THCm was applied to investigate the formation mechanisms for sulfur water observed in the Michigan Basin (Xie et al. 2018). The simulations have been further improved using a more realistic geochemical network including ferrous and ferric iron and associated redox and mineral dissolution/precipitation reactions. Simulated results show improved agreement with the available field data. The impact of paleo-glaciation on the formation and distribution of elevated sulphide is also being investigated through reactive transport simulations. A journal paper documenting the improved reactive transport simulation of sulfur water is expected to be submitted in 2021.

#### **5.2.2.2 MICA – Michigan International Copper Analogue project**

A new collaborative research project, The Michigan International Copper Analogue (MICA) project, involving NWMO, RWM, SKB, Nagra and the Geological Survey of Finland (GTK), will be initiated early in 2021. The purpose of the MICA project is to provide evidence of the behaviour of metallic copper on geological timescales. The internationally renowned copper deposits of the Keweenaw peninsula, USA, will be studied to ascertain both genesis and evolution - and by extension stability - in response to changing conditions such as Eh, pH, groundwater chemistry, temperature, presence/absence of oxygen, etc. The knowledge gained could be considered subsequently by waste management organizations in relation to the stability of copper on long timescales. The project may also enhance the robustness of a safety case that considers a disposal concept that uses metallic copper as part of the engineered barrier system, concerning, for example, the persistence of metallic copper under certain geochemical conditions that could be experienced by an evolving deep geological repository in certain environments. Such knowledge could be used in subsequent work to evolve the disposal concept, or to initiate further research activities. This project will be undertaken by the Geological Survey of Finland (GTK) and various technical experts.

The MICA project is anticipated to comprise at least 2 phases. Phase I will provide a comprehensive, state-of-the-science review, including a catalogue of available relevant samples, a description of the geologic history of each sample, information on environment(s) of exposure (including timing and length(s)), identification and planning of analytical research and some preliminary analyses as proof of concept. This phase will take approximately 18 months and will assess the feasibility of completing research in Phase II and potential relevance to the safety case. Phase II will be the main research phase on selected Keweenaw-based natural analogues from Phase I; specific testing will be decided after Phase I is complete.

### **5.2.3 Seismicity**

#### **5.2.3.1 Regional Seismic Monitoring**

The Canadian Hazards Information Service (CHIS), a part of the Geological Survey of Canada (GSC), continues to conduct a seismic monitoring program in the northern Ontario and eastern Manitoba portions of the Canadian Shield. This program has been ongoing since 1982 and is

currently supported by a number of organizations, including the NWMO. CHIS maintains a network of sixteen seismograph stations to monitor low levels of background seismicity in the northern Ontario and eastern Manitoba portions of the Canadian Shield. All the stations are operated by CHIS and transmit digital data in real-time via satellite to a central acquisition hub in Ottawa. CHIS-staff in Ottawa integrate the data from these stations with those of the Canadian National Seismograph Network and provide monthly reports of the seismic activity in northern Ontario.

A technical report submitted to NWMO in late 2020 summarizes operational statistics and additions to the earthquake catalogue for the year 2019. It is anticipated that NWMO will publish this report in 2021. During 2019, 35 earthquakes were located in the northern Ontario study area (**Figure 5-9**), ranging in magnitude from 1.2 to 3.3  $m_N$ . The pattern of seismicity generally conformed to that of previous years. The largest earthquake was an event at 15 km depth, north of Kapuskasing. There were no felt earthquakes in the study area in 2019.

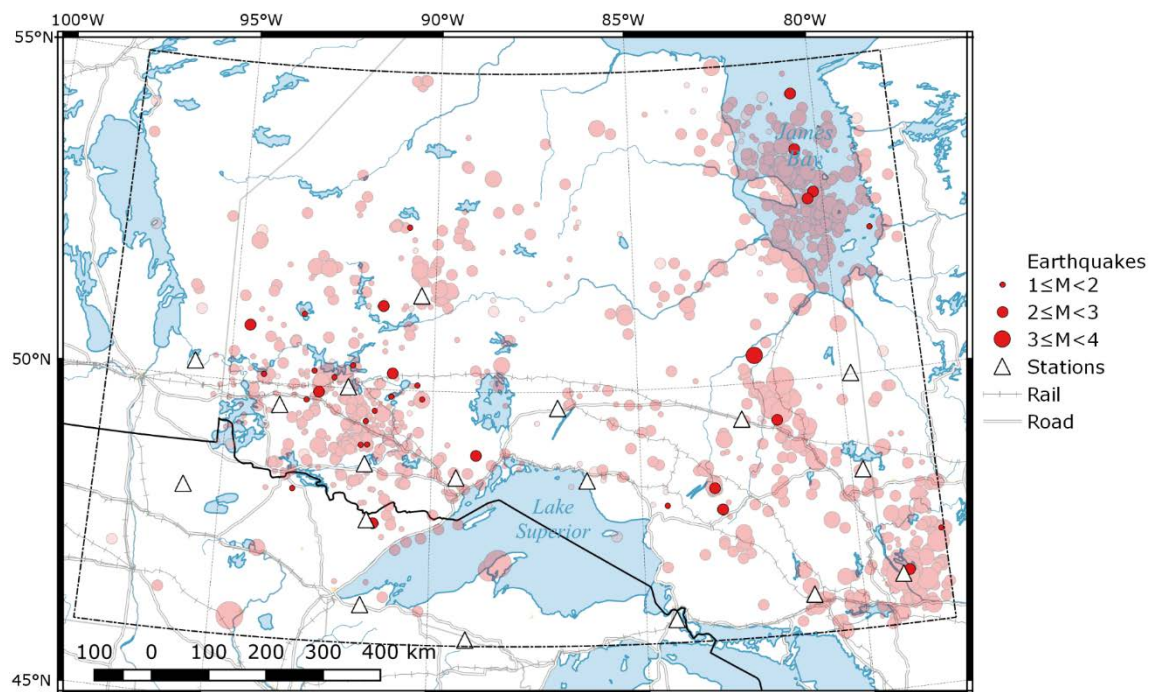


**Figure 5-9: Earthquakes in Northern Ontario, 2019. Events in 2019 Have Black Outlines, while Events from 1900–2018 are Plotted Semi-transparently and Have Grey Outlines. Events and Stations are Plotted in the Study Area Only. The Study Area is Outlined with a Dash-dotted Line. Only Stations with Data Available in 2019 are Shown**

### 5.2.3.2 Paleoseismicity

Due to the long life cycle of a repository, potential perturbations from rare strong earthquakes ground motions requires consideration. No such earthquakes have occurred in Ontario in human-recorded history. However, the NWMO is carrying out research to look for evidence, or absence of evidence, of such events in the past as described below.

During 2020, new research project with the Geological Survey of Canada in Ottawa was initiated focusing on i) developing criteria to objectively distinguish between neotectonic and glaciotectonic faulted sediments; and ii) assessing the inferred neotectonic origin of the Timiskaming East Shore fault. Similar reconnaissance profiling was also carried out in Tee and

Kipawa lakes, Quebec. This research continues to build on work that began in 2012 and is aimed at providing an understanding of seismicity over time frames dating over the Holocene.

Over the duration of this research project from 2020 to 2023, the scope of the research includes:

1. Investigating the distribution and character of the mass transport deposits generated by the 1935  $M_w$ 6.1 Timiskaming earthquake, Témiscaming area, Quebec; and
2. Distinguishing neotectonic versus non-neotectonic faulting within the glaciolacustrine deposits in the Lake Timiskaming basin, Ontario-Quebec

Restrictions associated with the pandemic during 2020 prevented initiation of the sub-bottom acoustic profiling and overwater hammer seismic surveys planned in the Temiscaming area and on Lake Timiskaming, respectively. This caused a critical delay in the data collection needed to address the two project components during the first year of this project. This field work has been rescheduled to 2021 and it is anticipated the duration of this research program will also be extended by at least one year.

### **5.2.3.3 Mont Terri Nanoseismic Monitoring (SM-C) Experiment**

The NWMO is involved in the Mont Terri Nanoseismic Monitoring (SM-C) Experiment, which serves as a comparative tool for the NWMO site-specific microseismic monitoring program. SM-C objectives for 2020 included:

- Continual micro-seismic monitoring of the Mt Terri facility and its surrounding region.
- Identify the source mechanism and structure associated with the recorded seismicity.
- Produce an earthquake catalogue for all events down to 0.0ML.

A period of recalibration and processing is scheduled for 2021.

## **5.2.4 Geomechanical Stability of the Repository**

### **5.2.4.1 Excavation Damaged Zones**

The Queen's Geomechanics Group has been investigating the mechanics of, and developing predictive and characterization tools for, Excavation Damage Zone (EDZ) evolution around deep geological repositories in sedimentary and crystalline rock. Past research focussed on fundamental mechanics of EDZ, damage threshold definition, detection in laboratory testing, prediction and assessment of EDZ using continuum models, and secondary effects such as time dependency and saturation. More recently, new geomechanics simulation approaches have been developed and adapted by Queen's to allow for deeper mechanistic investigation of EDZ evolution. In parallel, Queen's research has updated conventional testing and investigation tools and developed new protocols for characterization.

During 2020, on-going EDZ modelling focused on discontinuum simulation of EDZ evolution and behaviour, including hydromechanical coupling, pre-existing discontinuities and internal defects and structure (intra-block structure). This advanced modelling puts increased demands on the research teams' ability to define relevant materials and structural properties in the laboratory and to log appropriate geomechanical details in the field. In addition, discontinuum models pose special challenges in verification, calibration and upscaling. In response, this research is based on the appreciation that conventional geotechnical characterization and analysis tools are not optimized for the demands of EDZ study. Physical laboratory testing was curtailed by COVID-19 pandemic, but advances were nevertheless made in probing direct shear testing and the

relevant inputs into discontinuum modelling, as well as full strain mapping with fibre optic loops around lab specimens, a first of a kind testing approach.

The primary role of the Queen's Geomechanics Group is to improve the routine use of these advanced tools for the specific purpose of EDZ analysis in the DGR context and to develop protocols and guidelines for optimized model construction, calibration, verification and interpretation. These advanced tools, however, also require advancements in the way that lab-scale testing and field sampling and logging is carried out. Past work has focussed on the mechanical properties of homogenous intact rock, relevant to EDZ development from damage initiation through accumulation to unstable propagation and macro-fracture development. Current work is aimed at improving and upgrading techniques for physical investigation of discontinuum components and property definition using the previously standardized compression, tensile, confined strength and direct shear testing methods (including boundary condition implications).

The research team at Queen's presented and published three journal articles detailing past and current EDZ work including Farahmand and Diederichs 2020, Forbes et al 2020a,b. In addition, the group published two conference papers as part of the 2020 EUROCK conference (Hegger et al. 2020a; Innocente et al. 2020). These included 1) a numerical investigation of the applicability of time-dependent models (Innocente et al. 2020), which critically examined the behaviour of a visco-elastic creep model known as the Burgers model, the two-component power law, and a modified strain-hardening law, when modelled at the lab scale and tunnel scale at various times and induced stresses using rock salt as an analogue, calibrated at 10 MPa. A sensitivity analysis using different applied stresses for the models was also examined; and 2) A laboratory investigation of distributed fibre optic strain sensing to measure strain distribution of rock samples during uniaxial compression testing (Hegger et al. 2020). In this study, fibre optic strain sensing was applied to laboratory scale rock samples during conventional uniaxial compression testing to produce continuous strain profiles along their length and circumference. The results of this study illustrate the potential of this technology to provide a full-field view of surface strains and detection of failure locations during testing. Papers were submitted to ARMA 2020 although this conference was cancelled due to the COVID-19 pandemic. Papers are still available, however, including 1) Packulak et al 2020, detailing data processing for removing system stiffness artifacts from direct shear testing; 2) Diederichs and Day 2020, on sensitivities of EDZ to fabric elements in limestone; and 3) Hegger et al 2020a,b further developing the fibre optic strain measurement technique for uniaxial testing of rock.

## **5.2.4.2 Repository Design Considerations**

### **5.2.4.2.1 THM Analysis of Shaft and Cavern Stability**

The excavation of the underground openings (i.e., including placement rooms, shafts) for a repository, and the subsequent backfilling with heat-emitting UFCs as well as the buffer material, will induce coupled THM processes in-situ. NWMO has been conducting numerical analyses at near- and far-field scales to enhance our understanding of the response of the rock mass to hypothetical Canadian DGR configurations in both sedimentary and crystalline settings (ITASCA 2015). These studies considered perturbations induced by the repository as well as the natural processes expected during a 1 Ma period. In the study by ITASCA (2015), the THM processes were one-way coupled, whereas a recent THM modelling study (also by ITASCA) employed fully coupled THM analyses using refined input parameters. The sensitivity of the model predictions to some uncertain model input parameters (e.g. block-to-contact stiffness ratio for discontinuum modelling, poroelastic properties, and rock mass permeability) were also

investigated. NWMO's review of the final technical report on this research was on-going during 2020.

Once site-specific DFN information is available, similar analyses will be conducted to support repository engineering and design, as part of a complementary study during detailed site characterization.

#### **5.2.4.2.2 Fault Rupturing**

ITASCA has completed a research project with NWMO to numerically simulate a sizable seismic event resulting in the mobilization of surrounding fracture networks. Rupture of a seismogenic fault and its effect on the deformation of the off-fault fractures were examined. The purpose of the analysis was to determine the off-fault fracture displacements to inform the selection of respect distance within the repository horizon in crystalline rock.

Three different models were constructed to accommodate the fault size for moment magnitudes ( $M_w$ ) of 6.1, 6.6 and 6.9 seismic events occurring at the end of the glacial cycle when the vertical stress due to ice sheet is zero but glacially-induced horizontal stresses still remain. This base case analysis was conducted for five DFN realizations developed from the structural geology of Forsmark, Sweden. The modelling results revealed that for an earthquake with a moment magnitude,  $M_w$  of 6.1 and a dip angle of  $40^\circ$  (base case), the fault average shear displacement during the slip is about 1.6 m and the maximum shear displacement along the fault is 3.4 m. No DFN fractures slip more than 5 cm were observed in all DFN realizations except for a fault dip angle of  $30^\circ$ . Increasing the event magnitude while maintaining a dip angle of  $40^\circ$  (base case) resulted in a greater number of off-fault fractures with slippage over the 5 cm criterion and an increase in the distance to the fractures with such large displacements. NWMO's review of the final technical report on this research was on-going during 2020.

Once site-specific DFN information is available, similar analyses will be conducted to support repository engineering and design, as part of a complementary study during detailed site characterization.

## 6 REPOSITORY SAFETY

The objective of the repository safety program is to evaluate and improve the operational and long-term safety of any candidate deep geological repository. In the near-term, before a candidate site has been identified, this objective is addressed through case studies and through improving the understanding of important features and processes. Activities conducted in 2020 are described in the following sections.

The NWMO has completed studies that provide a technical summary of information on the safety of repositories located in a hypothetical crystalline Canadian Shield setting (NWMO 2017) and the sedimentary rock of the Michigan Basin in southern Ontario (NWMO 2018). The reports summarize key aspects of the repository concept and explain why the repository concept is expected to be safe in these locations (see Table 6-1).

**Table 6-1: Typical Physical Attributes Relevant to Long-term Safety**

Repository depth provides isolation from human activities  
 Site low in natural resources  
 Durable wastefrom  
 Robust container  
 Clay seals  
 Low-permeability host rock  
 Spatial extent and durability of host rock formation  
 Stable chemical and hydrological environment

### 6.1 WASTE INVENTORY

#### 6.1.1 Physical Inventory

Currently there are about 3 million used CANDU fuel bundles. Based on the known plans for refurbishment and life extension, there could be about 5.5 million used CANDU fuel bundles (about 106,000 Mg heavy metal) from the current generation of nuclear power (Gobien and Ion 2020).

The CANDU fuel bundles are a mature product, with small design variations over the years primarily in the dimensions and the mass of each bundle, as well as variations in the number of elements per bundle by reactor type. The 37M bundle recently introduced in some stations has slightly different dimensions compared to the previous standard bundle.

In addition to the CANDU used fuel, AECL also has ~500 Mg of prototype and research reactor fuel fuels in storage at the Chalk River Laboratories and Whiteshell Research Laboratories. Most of this is UO<sub>2</sub> based fuel from the Nuclear Power Demonstration (NPD), Douglas Point and Gentilly-1 prototype reactors. AECL also holds a small amount (i.e., less than ~100 Mg) of various research fuel wastes with a variety of compositions and enrichments. There is also a very small amount of fuel still in service in low-power research reactors at McMaster University, Royal Military College of Canada and Polytechnique Montréal.

The Canadian used fuel inventory and forecast are updated annually by NWMO (Gobien and Ion 2020). A database with key information on fuel bundles produced to date is maintained by NWMO.

### **6.1.2 Radionuclide Inventory**

An update of the reference CANDU radionuclide inventory was completed in 2020. Calculations were carried out using the most recent Industry Standard Tool version of the ORIGEN-S code and the latest CANDU specific nuclear data (e.g., cross-sections, decay data, and fission product yields) for a range of used fuel burnups of interest to the safety assessment or design. A report documenting the updated inventory and thermal power as a function of decay time for a reference CANDU fuel bundle was published (Heckman and Edward 2020).

### **6.1.3 Chemical Composition**

Measured data on main and trace elemental composition from 21 unirradiated CANDU fuel bundles (UO<sub>2</sub> pellets, Zircaloy end caps, Zircaloy tubing, Zircaloy tubing with a braze and spacer, and Zircaloy tubing with CANLUB coating), which encompassed a range of manufacturers, bundle types and manufacture dates, was previously completed to support the development of a recommended elemental composition value for UO<sub>2</sub> pellets and Zircaloy cladding (which includes the tubing as well as end caps, braze region and CANLUB).

Additional analysis was completed in 2020, which expanded the material composition database and improved the method detection limits of select elements. In particular, the additional analysis focused on nitrogen and halogens in the fuel and Zircaloy cladding, and protactinium in the fuel, which are potential precursors of activation products.

### **6.1.4 Irradiation History**

The NWMO maintains a statistical summary of the key parameters for the large majority of used CANDU fuel bundles: bundle type, source reactor, date of discharge, burnup and peak linear power. Burnup is important for determining the radionuclide content of a fuel bundle. Peak linear power is a secondary parameter that has small effect on radionuclide inventory, however it provides an indicator of the peak temperatures reached in the fuel. This in turn is relevant for the nature of the fuel microstructure and assessing the radionuclide distribution within a fuel pellet.

The Canadian stations all operate within a fairly consistent set of operating conditions, so have similar irradiation history. The burnup and peak linear power distributions for CANDU fuel discharged from the Bruce, Pickering and Darlington nuclear stations were determined for 1970 to 2006 (Wilk and Cantello 2006) and up to 2012 (Wilk 2013). The typical burnup of CANDU fuel ranges from about 130 to 220 MWh/kgU, with a mean burnup value from about 170 to 200 MWh/kgU between the stations, on a per station per decade basis. The 95<sup>th</sup> percentile values vary between about 220 MWh/kgU and 290 MWh/kgU (Wilk 2013).

This information is being updated for used fuel generated in the years since the last update, and also to evaluate older fuel records that are not available electronically, as fuel irradiation data from the first decade or so of the CANDU reactor program is not fully available on an individual bundle basis. These represent less than 10% of the current fuel bundle inventory. The report detailing the updated fuel irradiation data is expected to be available in 2021.

## **6.2 WASTEFORM DURABILITY**

### **6.2.1 Used Fuel Dissolution**

The first barrier to the release of radionuclides is the used fuel matrix. Most radionuclides are trapped within the UO<sub>2</sub> grains and are only released as the fuel itself dissolves (which in turn

only occurs if the container fails). The rate of fuel dissolution is therefore an important parameter for assessing long-term safety.

UO<sub>2</sub> dissolves extremely slowly under reducing conditions similar to those that would be expected in a Canadian deep geological repository. However, in a failed container that has filled with groundwater, used fuel dissolution may be driven by oxidants, particularly hydrogen peroxide (H<sub>2</sub>O<sub>2</sub>) generated by the radiolysis of water.

Research on UO<sub>2</sub> dissolution continued at Western University to further understand the mechanisms of a number of key reactions remaining unresolved, in particular the influence of H<sub>2</sub>O<sub>2</sub> decomposition and the reactions of the fuel with H<sub>2</sub> produced either radiolytically or by corrosion of the steel vessel. The mechanistic understanding of the corrosion of UO<sub>2</sub> under used fuel container conditions is important for long-term predictions of used fuel stability (Liu et al. 2017a, 2017b, 2017c, 2018, 2019). A study on the kinetics of H<sub>2</sub>O<sub>2</sub> decomposition on SIMFUELS (simulated spent nuclear fuels; doped UO<sub>2</sub> specimens containing noble metal particles) has been conducted to determine the influence of noble metal particles on the reactions of H<sub>2</sub>O<sub>2</sub> with UO<sub>2</sub> (i.e. UO<sub>2</sub> corrosion and H<sub>2</sub>O<sub>2</sub> decomposition) by a combination of electrochemical, surface analytical and solution analytical methods (Zhu et al. 2019). It was observed that > 98% of the H<sub>2</sub>O<sub>2</sub> was consumed by H<sub>2</sub>O<sub>2</sub> decomposition.

The study of the kinetics of H<sub>2</sub>O<sub>2</sub> decomposition has been extended to standard CANDU fuel pellets to investigate variations in fuel reactivity due to differences in the manufacturing process. The characteristics of a series of standard UO<sub>2</sub> pellets (1965-2017) has been investigated using electrical resistance measurements and Raman spectroscopy. Experiments on H<sub>2</sub>O<sub>2</sub> decomposition on the standard UO<sub>2</sub> pellets are underway.

The kinetics of H<sub>2</sub>O<sub>2</sub> reduction on SIMFUEL, RE<sup>III</sup>-doped UO<sub>2</sub> and non-stoichiometric UO<sub>2</sub> have been conducted using standard electrochemical methods at rotating disk electrodes. It was found the rate of H<sub>2</sub>O<sub>2</sub> reduction decreased in the order of SIMFUEL > Gd-doped UO<sub>2</sub> > Dy-doped UO<sub>2</sub> with the rate suppressed on the RE<sup>III</sup>-doped UO<sub>2</sub>. The slightly faster rate on the SIMFUEL may be attributable to the catalysis of reduction on the noble metal particles. The H<sub>2</sub>O<sub>2</sub> reduction on all three specimens was found to be suppressed by the presence of the ground water anion HCO<sub>3</sub><sup>-</sup>/CO<sub>3</sub><sup>2-</sup> (Zhu et al. 2020). The results of the research on the kinetics of H<sub>2</sub>O<sub>2</sub> reduction on SIMFUEL and RE<sup>III</sup>-doped UO<sub>2</sub> will be presented in a journal publication.

The H<sub>2</sub> effect in suppressing the corrosion behavior of UO<sub>2</sub> (un-doped and RE<sup>III</sup>-doped UO<sub>2</sub>) without catalysis of noble metal particles has been studied by producing H radicals electrochemically and radiolytically to simulate radiation effects on UO<sub>2</sub> corrosion when H<sub>2</sub> is present. It was observed that the combination of gamma radiation and H<sub>2</sub> was required to reduce the UO<sub>2</sub> matrix, and the reduction of U<sup>V</sup> was reversible for specimens close to stoichiometric (UO<sub>2+x</sub> with x < 0.005) but only partially reversible for RE<sup>III</sup>-doped UO<sub>2</sub> with a much higher U<sup>V</sup> content. At high gamma dose rates and dissolved H<sub>2</sub> concentrations the matrix reduction appeared to be irreversible. The results of the research on the H<sub>2</sub> effect in suppressing the corrosion behavior of UO<sub>2</sub> without catalysis of noble metal particles will be published in Corrosion Science.

### 6.2.2 Solubility

The maximum concentration of a radionuclide within or near a failed container will be limited by the radionuclide solubility. Radionuclide solubilities are calculated by geochemical modelling using thermodynamic data under relevant geochemical conditions. These data are compiled in quality-controlled thermodynamic datasets.

NWMO continues to support the joint international Nuclear Energy Agency (NEA) effort on developing thermodynamic databases for elements of importance in safety assessment (Mompeán and Wanner 2003). Phase VI of the project from February 2019 to January 2023 will provide (1) an update of the chemical thermodynamics of complexes and compounds of U, Np, Pu, Am, Tc, Zr, Ni and Se with selected organic ligands, (2) a review of the chemical thermodynamics of lanthanides, and (3) a state-of-the-art review on thermodynamics at high temperatures.

The review of the thermodynamic data for iron Part 2 (Lemire et al. 2020) and the second update of the actinides and technetium thermodynamic data (Grenthe et al. 2020) were completed. The reviews of molybdenum thermodynamic data, ancillary data, the state-of-the-art reports on the thermodynamics of cement materials and high-ionic strength systems (Pitzer model) are underway.

The NEA TDB project provides high-quality datasets. This information is important, but is not sufficient on its own, as it does not address the full range of conditions of interest. For example, the NEA TDB project has focused on low and moderate salinity systems in which activity corrections are described using Specific Ion Interaction Theory (SIT) parameters. The SIT model is most useful in ionic strength up to 3.5 molal (M) (Grenthe et al. 1992). Due to the high salinity of porewaters observed in some deep-seated sedimentary rock formations in Canada, a thermodynamic database including Pitzer ion interaction parameters is needed for radionuclide solubility calculations for sedimentary rock environment.

The state-of-the-art report on high-ionic strength systems (Pitzer model) will be useful to identify the data gap for Pitzer ion interaction parameters. The THEREDA (THERmodynamic REference DAtabase) Pitzer thermodynamic database (Altmaier et al. 2011) is a relevant public database for high-salinity systems. It has been assessed by the NWMO and found to provide a good representation of experimental data for many subsystems.

The NWMO is also co-sponsoring the NSERC/UNENE Senior Industrial Research Chair in High Temperature Aqueous Chemistry at the University of Guelph, where there is capability to carry out various thermodynamic measurements at high temperatures and high salinities. This Chair program initiated in 2016. Progress has been made in several areas: (1) the equilibrium constants and transport properties for uranyl with sulfate at high salinities from 25 to 350 °C determined by Raman spectroscopy approach (Alcorn 2019); (2) the equilibrium constants and transport properties for uranyl with chloride at high salinities from 25 to 300 °C determined by Raman spectroscopy approach; and (3) the equilibrium constants and transport properties of lanthanum with chloride at high salinities from 25 to 250 °C determined by Raman spectroscopy and conductivity approach. Two journal papers documenting the thermodynamic properties of uranyl with chloride and lanthanum with chloride are expected to be submitted in 2021.

In 2020, the NWMO updated the database of radionuclide solubility for Canadian crystalline rock environment. The radionuclide solubility limits were calculated in a reference groundwater CR-10 (Ca-Na-Cl type with  $I = 0.24$  M) under three scenarios: 1) groundwater directly enters the canister without interacting with the bentonite buffer or the canister materials; 2) groundwater interacts with the carbon-steel container prior to contacting the used nuclear fuel waste inside the container; and 3) groundwater interacts with both bentonite buffer and carbon-steel container prior to contacting the used nuclear fuel waste inside the container. The effect of temperature on the solubility was evaluated at four different temperatures (15°C, 25°C, 50°C and 80°C) in each scenario. A technical report documenting the radionuclide solubility

calculation under crystalline rock conditions is expected to be published in 2021. Work on updating NWMO's database of radionuclide solubility will continue in 2021, with calculations of the radionuclide solubility at Canadian sedimentary rock conditions.

## **6.3 BIOSPHERE**

### **6.3.1 General Approach – Post-closure Biosphere Modelling and Data**

The biosphere is a complex system, that will evolve over the one-million-year timescales considered in a safety assessment. In the context of deep geologic repositories, biosphere models are developed to derive potential dose and non-radiological consequence by calculating constituent of potential concern concentrations in the biosphere and considering dominant or representative pathways.

In 2020, the NWMO continued the development of a new system modelling tool known as the Integrated System Model or ISM (Gobien and Medri 2019). One of the components of the ISM tool is a dynamic biosphere model, ISM-BIO which was implemented using the AMBER software. The model simplifies the biosphere as a series of compartments which can each receive, accumulate, and transfer contaminants. Transfer between some compartments is dynamically modelled, while others are modelled by ratios that assume the compartments are in quasi-equilibrium over the time scales of interest. In the model, the calculated constituent of potential concern environmental concentrations are then used to calculate the dose to stylized human receptors by applying dose coefficients and lifestyle-specific exposure rates. The ISM-BIO will continue to evolve in an iterative approach as the sites are characterized and the assessment objectives evolve.

### **6.3.2 Participation in BIOPROTA**

BIOPROTA is an international collaborative forum created to address key uncertainties in long-term assessments of contaminant releases into the environment arising from radioactive waste disposal. Participation is aimed at national authorities and agencies with responsibility for achieving safe radioactive waste management practices. Overall, the intent of BIOPROTA is to make available the best sources of information to justify modelling assumptions made within radiological assessments constructed to support radioactive waste management. In 2020, the NWMO continued to participate in the C-14 and BIOMASS 2020 update projects. The BIOMASS 2020 update project was finalized in 2020.

#### BIOMASS 2020 Update

The International Atomic Energy Agency (IAEA) BIOMASS report on reference biospheres for solid radioactive waste disposal was published in 2003 (IAEA 2003). BIOPROTA has undertaken to review and enhance the BIOMASS methodology. The work programme was coordinated with IAEA MODARIA II working group 6 (WG6). BIOPROTA held workshops during 2016-2017, and published workshop reports identifying key areas of review and update of the BIOMASS methodology (Smith 2016, 2017a, 2017b). In 2018, an interim report on the BIOPROTA / BIOMASS project was published (SKB 2018), along with three workshop reports and a journal publication on climate change and landscape development with respect to the BIOMASS update (Lindborg et al. 2018). In 2020, the report proposing a common framework for addressing climate and environmental change in post-closure radiological assessment was published (IAEA 2020), and the draft report detailing the revised BIOMASS methodology was submitted to the IAEA.

## **6.4 SAFETY ASSESSMENT**

### **6.4.1 Pre-closure Safety**

The pre-closure period includes site preparation, construction, operation, decommissioning, monitoring and closure. Topics include normal operations safety (public and worker dose), and malfunctions and accidents. In the context of a geological repository and related facilities for used fuel, these topics were addressed as part of AECL's Environmental Impact Statement (AECL 1994, OHN 1994), and reviewed as part of the NWMO options study (NWMO 2005). The pre-closure safety assessment will be updated in parallel with the ongoing work to develop more detailed plans for operations and surface facilities.

#### **6.4.1.1 Normal Operations**

A preliminary dose assessment of the facility was carried out in 2014 to guide ALARA (As Low As Reasonable Achievable) development of the repository concepts (Reijonen et al. 2014).

A study was initiated in 2019 to estimate the potential radiological impact to the public and the non-nuclear energy workers (non-NEW) from normal operation of the DGR. A conceptual design of the DGR was considered, and a generic site was assumed for this study. The potential radiological doses to the public are estimated assuming potential airborne and waterborne emissions during normal operations of a DGR and its related surface processing facilities. The direct and skyshine external radiation doses from used fuel to public or non-nuclear energy worker (non-NEW) receptors are also estimated. The study assumes exposure to receptors at a potential fence line location. During normal operations, airborne radioactivity could be released during handling of the used fuel from surface contamination that is generally present on used fuel bundles and from cladding failures in the fuel element. Waterborne emissions could result from cell washdowns and decontamination of used fuel modules, used fuel transportation packages, and containers. Simple conservative models are used to estimate the dispersion of airborne and waterborne emissions. Radiological doses to the public are calculated using the methodology described in the Canadian Standards Association (CSA) N288.1-14 (CSA 2014) for a reference case, as well as sensitivity cases used to bound uncertainties associated with input parameters. The initial results from this study will inform the further development of the conceptual DGR design. This study continues to 2021.

A preliminary assessment of the radon hazard was completed in 2020, to determine whether there is health hazard to workers during construction and operation of the DGR, and a need for radon monitoring or development of any action levels in order to be in compliance with the applicable regulatory requirements. The study was conducted for a generic crystalline or sedimentary rock site. The results of the study, published in Liberda (2020), indicate that there is no significant radon hazard to the workers or the general public during construction and operation of the DGR. For workers, the highest radon concentration in an area where workers may be present is in the ventilation exhaust shaft. The concentration of radon in all worker locations is less than the Derived Working Limit of 200 Bq/m<sup>3</sup>, based on the Canadian Guidelines for Management of Naturally Occurring Radioactive Materials (unrestricted classification). For members of the public, even those very close to the facility, the dose contribution from radon during construction and operation of the facility is much less than from natural sources indicate that there is no significant radon hazard to the workers or the general public during construction and operation of the DGR.

#### **6.4.1.2 Abnormal Events and Accidents**

A preliminary study was carried out to identify potential internal accident scenarios that may arise during the operations phase for the repository, based on a conceptual design of the UFPP

and repository (Reijonen et al. 2016). In this preliminary study, a failure modes and effects analysis (FMEA) was used to identify potential internal hazards resulting from, for example, failure of equipment, failure of vehicles, failure of the shaft hoist system, loss of electric power, ventilation and filtration system failure, and human error. The estimates of the internal initiating event frequencies were obtained based on data from the nuclear industry and from earlier used fuel management studies (AECL 1994). The potential external events were also identified for a generic site based on literature review.

A preliminary analysis was completed in 2020, assessing the potential public dose consequences for the accident scenarios identified in the previous hazard identification study (Reijonen et al. 2016) for a generic site. The recent study considered exposure to a person standing at various distances from the fence line under conservative atmospheric conditions. Atmospheric dispersion factors were derived based on the Gaussian dispersion model described in CSA N288.2-M91 (CSA 2003). Radiological doses to the public were calculated for accidents classified as Possible Events (occurring at least once every 100 years of operation) or Unlikely Events (occurring less frequent than Possible Events). The presence or absence of ventilation system High Efficiency Particulate Air filters was also considered in combination with specific accident scenarios. The preliminary results indicate that the calculated public doses for inhalation, air immersion and ground exposure pathways remain below the interim dose criterion of 0.5 mSv for Possible Events and 20 mSv for Unlikely Events for all accidents considered. This study also looked at the minimum site boundary distance by calculating public doses at various distances from the UFPP, Ventilation Shaft, and Main Shaft. Sensitivity cases were carried out to determine the effect of stack release height, the effluent exit velocity, and the release orientation on the calculated minimum site boundary distance.

The potential external hazard events are dependent on the site. As part of the site characterization phase, the external hazard events will be evaluated. Two specific important external events are seismicity and flooding. The work related to the seismic hazard potential is being assessed under site characterization. The potential impact of climate change on flood risk also needs to be considered given the operating timeframe for the repository and is described below.

#### **6.4.1.3 Climate Change Impacts Studies**

A study was initiated in 2018 to review anticipated climate change impacts on climate conditions (e.g., temperature and precipitation) and develop a methodology to incorporate these climate changes into probable maximum precipitation (PMP) estimation appropriate for the DGR study areas in Ontario. A report documenting the study was issued in 2019 (Wood 2019).

In 2019, the preferred method by Wood (2019) has been applied to assess the climate change impacts on the PMP and Intensity-Duration-Frequency (IDF) amounts for the Ignace study area. The approach follows the key steps in Figure 6-1. Of these steps, the approach to evaluating future climate impacts on precipitation uses the state of science and publicly available climate projections to complete the climate change impact assessment on the PMP and the IDF values. The multi-model ensemble approach is used to describe the probable range of results and potential climate changes to PMP and IDF amounts expressed as percentiles, so that the level of acceptable risk can be selected by using the desired percentile. The study considered projected changes in climate over three separate time periods – mid-century (2041 to 2070); end-of-century (2071-2100); and beyond 2100. These periods coincide with the different phases for a possible deep geological repository, including site preparation and construction; the operational period; extended post-closure monitoring; and decommissioning. There is a level of inherent uncertainty when projecting future climate; however, the approach taken in this study

aims to address this uncertainty by relying on a multi-model ensemble and providing percentiles. The work for both Ignace (Schardong et al. 2020) and South Bruce (Breach et al. 2020) study areas were completed in 2020.

In the end of 2020, a new study was initiated to estimate the flood potentials and associated climate change impacts for the Ignace and South Bruce study areas. It is expected that the climate change impacts would be periodically updated in the future as part of the safety assessment / licensing review.

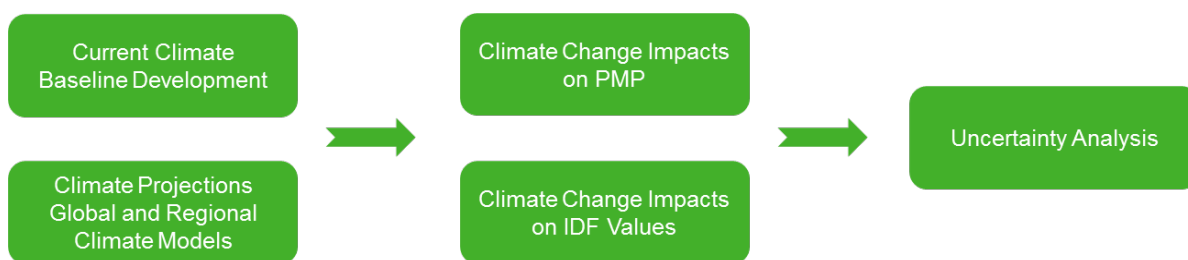


**Figure 6-1: High Level Stepwise Approach in Climate Change Impacts Study**

#### 6.4.1.4 Site-Specific Properties for Safety Assessment

Pre-closure safety assessment in Sections 6.4.1.1 and 6.4.1.2 employs an environmental transfer model to calculate potential dose to the public from the airborne and aqueous releases from a nuclear facility under normal and accident conditions. CSA provides guidelines for the model calculations (CSA 2003, 2008 and 2014). CSA (2014) also provides regional default values for some parameters for southern Ontario, western Ontario, eastern Ontario, Quebec and Maritimes. However, there are no default values provided for aqueous dilution factors (AqDF). Site specific data will be needed to determine the AqDF.

Depending on the site location, additional site-specific data may be needed and integrated with regional or other relevant generic data. These site-specific data will be acquired as parts of baseline monitoring program, e.g., installation of a meteorology tower at the Ignace study area.

#### 6.4.1.5 Behaviour of Used Fuel / Packages under Normal and Accident Conditions

A key aspect of the pre-closure safety assessment is the behaviour of the used fuel and packages under normal and accident conditions. CANDU fuel is a solid waste form, non-volatile and contained within Zircaloy sheathing. All used fuels have small amount of surface contamination. However, some used fuels may be damaged during transport to the DGR, or during handling within the UFPP. These could result in some release of particulate, gases, or volatile elements from the used fuel. These releases would be handled within the surface facilities as part of the design basis (e.g., particulates captured on a High Efficiency Particulate Air (HEPA) filter system).

From a pre-closure safety assessment perspective, uncertainties in fuel integrity will be handled by conservative assumptions. Normal operations and accident assessments are discussed in Section 6.4.1.1 and 6.4.1.2 respectively. Of interest from a pre-closure safety assessment perspective are cases where the fuel is not yet sealed in a container, or the container itself is not fully closed. The NWMO are looking for opportunities to learn from others' used fuel handling experience such as participation in the NEA Expert Group on Operational Safety and data available in literature (for example, from U.S. Idaho National Laboratory (INL) 2005). Used fuel handling experiences at Canadian Nuclear Laboratories and at Ontario Power Generation's Dry Storage facilities will also be sought for.

In order to estimate the radiological release source terms during a potential accident, the preliminary assessment as discussed in Section 6.4.1.2 follows the U.S. Department of Energy (DOE)'s five factor formula - material at risk, damage ratio, airborne release fraction, respirable fraction, and leakpath factor. The assigned values for the five factors in this study are based mostly on the U.S. DOE Handbook (U.S. DOE 1994) and the subsequent U.S. DOE standard (U.S. DOE 2007), as well as values used in the Yucca Mountain assessment (U.S. DOE 2009).

For preliminary normal operation assessment, as discussed in Section 6.4.1.1, radionuclide release from intact fuel bundles and fuel bundles with an intentionally defected fuel element are based on experimental data (Chen et al. 1986, 1989). A range of radionuclide release rates are reported in literature, and the highest measured release rates are conservatively used for the reference case. The fuel bundle failure rates during transportation and handling are considered to be low, as the fuel processing facilities in the UFPP will be designed to minimize the impact on the used fuel. Conservative assumptions are made to bound the uncertainty in the fuel bundle failure rates. These source term values are considered overall conservative, taking into account in part differences in used fuel characteristics, container and handling requirements (e.g., the lower burnup of CANDU bundles).

The NWMO will continue to monitor the literature and international practices, and experience in Canadian fuel handling to support these values.

## **6.4.2 Post-closure Safety**

### **6.4.2.1 Post-closure Safety Assessment Methods**

The purpose of a post-closure safety assessment is to determine the potential effects of the repository on the health and safety of persons and the environment during the post-closure timeframe.

The ability of the repository to safely contain and isolate used nuclear fuel is achieved by multiple barriers, these being the ceramic used fuel pellet, the fuel sheath, the robust long-lived container, a series of clay-based seals and backfill material, and the site-specific geology.

Preliminary work towards site-specific assessments of post-closure safety included:

- Using early results from literature surveys of measured rock permeabilities at varying depths for several sites across the Canadian Shield to estimate general relationships between depth and rock permeability for the Revell site.
- Developing complementary methods for calculating hypothetical transport of imagined contaminant transport within the rock neighbouring the repository vault.
- Construction of groundwater flow and transport models, building on the approaches developed in previous case studies (e.g., Kremer et al. 2019); and
- Developing preliminary approaches to assess repository performance as a function of depth within the Revell site.

Further effort was given to exploring additional metrics for assessing site suitability, including multiple types of water-supply wells, a broad set of lifestyles, and an expanded series of imagined repository failures.

Post-closure assessment methodology was based on guidance from the Canadian Nuclear Safety Commission (CNSC 2018).

#### 6.4.2.1.1 Integrated System Model

In late 2018, the NWMO initiated development of a new system modelling tool known as the Integrated System Model (ISM). The ISM consists of a connected series of models developed in commercially available codes each representing a specific portion of the repository system. The ISM-NF model was developed using COMSOL and contains the waste form, containers, engineered barrier system, and excavation damaged zone surrounding the placement room. It assumes the failure of some containers, degradation of the used fuel by water, and transport of species from the fuel, through the engineered barrier system and into the geosphere. The ISM-GEO model developed using HGS describes the movement of species from the repository via the groundwater through the rock mass and fractures, to the surface environment. The ISM-BIO model developed using AMBER determines the concentration of species in environmental media (e.g., surface water, groundwater, sediments, soils, air) and estimates the consequent radiological dose to a critical group living near the repository.

The initial versions (v1.0 and v1.0.1) of ISM were released in 2020. The theory of the component models is described in Gobien and Medri (2019). Work was initiated in 2020 for the development of a data processing and linking tool known as paLINK. This tool will manage data preprocessing, stochastic data sampling, model linking, and postprocessing of ISM data and models. It is anticipated that the initial release of the paLINK tool will be available in 2021. Figure 6-2 shows the structure of the combined paLINK-ISM configuration.

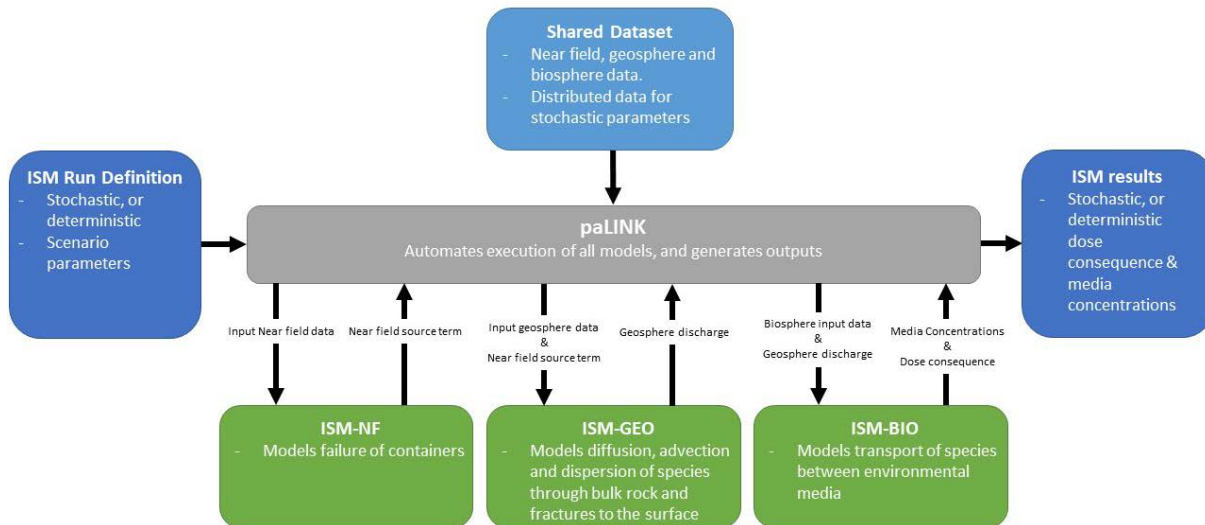


**Figure 6-2: paLINK-ISM Configuration**

The NWMO continues to develop and test the ISM in a manner consistent with NWMO technical computing software procedures, and with the CSA Standard N286.7-16 (CSA 2016). The next iteration of the ISM model, ISM v1.1, is planned to be released in 2021 and will include versions of geosphere and biosphere models representative of the Revell and South Bruce sites. Other planned model improvements include addition of an improved solubility-limited release model in ISM-NF and consideration of number of additional lifestyles in the ISM-BIO model.

Validation of the ISM is an ongoing task, with further validation of specific process models or overall system-level comparisons performed when suitable opportunities arise (for example Decovalex Task F – see Section 4.3.3.2).

#### **6.4.2.2 Acceptance Criteria**

Acceptance criteria for radiological and non-radiological contaminants applicable to post-closure safety assessments are used to judge the acceptability of analysis results for the protection of humans and the environment. Currently, criteria are referred to as “interim” because they have not been formally approved for use in a used fuel repository licence application.

Interim acceptance criteria for the radiological protection of persons, expressed as an annual dose rate target, are based on the recommendations of the ICRP (2007) and IAEA (2006) and aligned with the reference risk value of ICRP (2013), Health Canada (2010), and IAEA (2006).

Protection policies for non-human biota are not as mature as those for humans. As such, there are not internationally agreed upon environmental benchmarks of dose rate criteria against which to assess radiological effects to non-human biota. In the most recent post-closure safety assessment (NWMO 2018), the NWMO used a two-tiered criteria system, which includes proposed criteria from ERICA (Garnier-Laplace et al. 2006), PROTECT (Andersson et al. 2008) and the ICRP’s Derived Consideration Reference Levels (ICRP 2008). This approach is consistent with the approach proposed by BIOPROTA, an international forum which seeks to address key uncertainties in long-term assessments of contaminant releases into the environment arising from radioactive waste disposal (see Section 6.3).

With respect to the protection of persons and the environment from non-radiological contaminants, a set of criteria which span all environmental media (i.e., surface water, groundwater, soil sediment and air) and relevant elements in a used fuel repository are documented in Medri 2015. Work was initiated in 2016 to develop non-radiological acceptance criteria for relevant elements missing from Medri (2015): gold, bismuth, bromine, iodine, indium, osmium, palladium, platinum, rhodium, ruthenium, tellurium and tungsten. Criteria for these elements were developed using a comprehensive literature search, as well as aquatic and terrestrial toxicity tests for rhodium and ruthenium. These additional acceptance criteria were published in 2019 (Fernandes et al. 2019).

## **6.5 MONITORING**

### **6.5.1 Knowledge Management**

The NEA established in 2019 the Working Party on Information, Data and Knowledge Management (WP-IDKM) to further explore potential standardized approaches to manage information, as well to preserve the information in the long term for radioactive waste disposal and decommissioning. The work under this international collaboration builds on outcomes and learnings from recently completed NEA projects such as the Repository Metadata (RepMet) Management, and the Preservation of Records, Knowledge and Memory (RK&M) across Generations projects.

The NEA Repository Metadata (RepMet) Management project was a four-year initiative aimed to create sets of metadata that can be used by national programmes to manage their repository data, information and records in a way that is harmonized internationally and suitable for long-term management. RepMet focused on the period before repository closure. The NWMO

participated in this program since its start. An overview of the project, including deliverables produced since 2014, was presented in NEA (2018).

The NEA initiative on the Preservation of Records, Knowledge and Memory (RK&M) across Generations was a multi-year initiative looking to minimise the risk of losing records, knowledge and memory, with a focus on the period of time after repository closure. The NWMO participated in this program since its start. Three reports of the RK&M initiative were published in 2019, including the report describing the Key Information File concept for a repository (NEA 2019a), the report describing the Set of Essential Records concept for a repository (NEA 2019b), and the RK&M final report (NEA 2019c).

In 2020, NWMO continued monitoring the international collaborations and research on knowledge management and long-term preservation of knowledge and records.

## 7 SITE ASSESSMENT

In 2020, the NWMO continued to assess the potential suitability of siting areas within two regions in Ontario: the Ignace area in northwestern Ontario, and South Bruce area in southern Ontario. The status of the geological and environmental studies underway in these regions is described below.

### 7.1 IGNACE

#### 7.1.1 Geological Investigation

By the end of 2020, the Geoscience Site Assessment team and their contractors completed the drilling of 4, kilometre-long boreholes in the crystalline rock of the Revell Batholith west of Ignace, Ontario. Fieldwork paused temporarily in 2020, due to the COVID-19 pandemic.



**Figure 7-1: 2-D Seismic Source Vehicle, November 2020**

Planning is underway for completing the downhole testing of borehole 4, and drilling and testing of the next boreholes (boreholes 5 and 6), as well as additional geological work in the area, including geological mapping and installation of shallow groundwater monitoring wells

#### 7.1.2 Environmental Assessment

While respecting COVID-19 restrictions and NWMO's commitment to keeping siting communities safe, the NWMO achieved some environmental work in the Ignace area in northwestern Ontario in 2020. Some of this work included: hosting virtual community engagement sessions, conducting baseline surface water, soil and sediment sampling, and performing environmental monitoring and compliance checks for various work programs.

Prior to COVID-19 restrictions put into place early 2020, the NWMO had committed to completing the Environmental Community Engagement workshops with stakeholders and rightsholders. This workshop was the third and final group of workshops of this kind geared towards gaining valuable community input to help in the design of the environmental baseline sampling program. The first two workshops were completed in person but due to restrictions at the time, this event had to be completed using virtual platforms. Four virtual workshops were completed: two open to Ignace and Dymont community members, one targeting youth from the Ignace High School and one with regional MNO representatives. During the workshop the draft biodiversity design and project study areas were presented to the group. Participants had the opportunity to ask questions and provide input towards the design and proposed study areas. Valuable community input obtained through these sessions was used to inform the final design of the Northwest Environmental Baseline Sampling Program.

Another key piece of environmental work completed in 2020 was the baseline surface water, soil and sediment monitoring program. This program was completed by Tulloch Environmental in conjunction with the WLON environmental team. In recent years (2018 and 2019) this work consisted of 3 seasonal monitoring events, one in the spring, summer and fall. Due to COVID-19 limitations only the fall sampling campaign was completed for the 2020 field season. This work took place mid October 2020 and consisted of sampling at 11 out of 12 sediment and surface water sampling sites. The only site not completed could not be accessed while maintaining COVID-19 physical distancing safety protocols. Soil sampling was also completed during this campaign and consisted of post demobilization sampling of the fill on constructed drill pads adjacent to Boreholes 2 and 3. A total of 9 composite soil samples were collected at each site along with 2 reference samples adjacent to each drill pad.

The NWMO environmental team also provided environmental monitoring and compliance oversight to contractors completing work on the Revell site throughout the year. Most of this work was overseen by the geoscience and project management groups and consisted of borehole 4 drilling activities, trail clearing, 2-D seismic work and micro seismic station installation as well as additional site reconnaissance. Environmental oversight for these work packages included ensuring adherence to the contractors HSE plans, completing spot checks and ensuring minor environmental impacts were mitigated appropriately.

Going forward into 2021 the environmental team aims to continue monitoring, executing compliance initiatives for work completed in the Ignace area in northwestern Ontario, work with community members as part of the baseline monitoring program and begin executing the Environmental Baseline Sampling Program as designed

## **7.2 SOUTH BRUCE**

### **7.2.1 Geological Investigation**

In 2020, NWMO's land access program was announced, and the potential repository site in this area identified. Site assessment activities in South Bruce area in 2020 mainly related to initiating construction of access routes and pads for boreholes 1 and 2, in readiness for planned drilling of the boreholes, scheduled to begin in 2021.



**Figure 7-2: South Bruce Borehole Access and Pad Construction Underway, December 2020**

## **7.2.2 Environmental Assessment**

### **7.2.2.1 Field Work**

Field work in South Bruce completed in 2020 included acoustic bat monitor installation and maintenance throughout Bruce and Grey counties, and natural heritage surveys, soil and surface water sampling at Borehole 1 and 2 sites, for pre site preparation. A summary of the field work and associated findings is below.

#### **7.2.2.1.1 Acoustic Bat Monitoring Field Work – Collaboration with Toronto Zoo**

As part of the collaboration between the Toronto Zoo and the NWMO, assistance was provided for the logistics coordination, property access permission, and field work to install and maintain 7 acoustic bat monitors throughout Bruce and Grey Counties. Two monitors were installed on NWMO optioned properties, two were installed on Maitland Valley Conservation Authority (MVCA) properties (Saratoga Swamp and Stapleton Tract), and three were installed on Saugeen Valley Conservation Authority (SVCA) properties (Schmidt Lake, Kinghurst Nature Preserve Tract 42-320 and Taylor Drive Tract 42-360 45).

Additional field visits occurred monthly from August to November to replace battery and memory cards and to decommission the bat monitors for the winter.

#### **7.2.2.1.2 Natural Heritage Assessment and Soil Sampling at Borehole 1 Site**

A Natural Heritage Assessment of the Borehole 1 site in July 2020 was completed. The study area was assessed for suitable habitat for terrestrial crayfish, bobolink and meadowlark, migratory birds, snakes and reptiles, bats and barn swallows.

Soil sampling of the Borehole 1 site was completed in October 2020. Soil sampling consisted of collecting 19 soil samples, nine (9) on the proposed pad, two (2) adjacent the proposed pad, six (6) along the proposed access road, and two (2) in the ditch at the proposed pad drainage location. Soils mostly composed of moist dark brown sandy loam soils, with dispersed vegetation and gravel throughout. Samples were analyzed for PHCs, VOCs, PAHs, general chemistry and metals. No exceedances to O. Reg. 153/04 Table 1 benchmark values were detected in any parameters at Borehole 1.

#### **7.2.2.1.3 Natural Heritage Assessment, Soil and Surface Water Sampling at Borehole 2 Site**

A Natural Heritage Assessment, and surface water and soil sampling of the Borehole 2 site were completed in October 2020. The study area was assessed for suitable habitat for terrestrial crayfish, bobolink and meadowlark, migratory birds, snakes and reptiles, bats and barn swallows.

Borehole 2 site soil sampling consisted of collecting 11 soil samples: nine (9) on the proposed pad, two (2) adjacent the proposed pad, six (6) along the proposed access road. Soils are mostly composed of brown loam and dispersed cobbles, with patches of sand and silt. Samples were analyzed for PHCs, VOCs, PAHs, general chemistry and metals. No exceedances to O. Reg. 153/04 Table 1 benchmark values were detected in any parameters at Borehole 2.

Surface water samples were taken from two (2) upstream reference areas, two (2) near-field receptor sites and one (1) far-field receptor site, from discharge areas adjacent to the Borehole 2 site. In-situ water quality parameters were measured prior to surface water sample collection. Three (3) water samples exceeded the Canadian Council of Ministers of the Environment (CCME) guidelines for fluoride, and two (2) water samples exceeded CCME guidelines for chloride.

#### **7.2.2.2 South Bruce Environmental Engagement**

The NWMO held several workshops, both in person and virtually in the summer and fall of 2020 in South Bruce to engage local community members about the Environmental Baseline Program. The NWMO also engaged with the Maitland Valley Conservation Authority and the Saugeen Valley Conservation Authority to obtain further knowledge about both watersheds. Overall attendance was low due to COVID-19, however the participants that attended provided an abundance of input to inform the study designs.

The NWMO held a total of nine “Workshop 1” environmental workshops, both in person and virtually, that discussed three main questions with community members: 1) What are the key elements of a trustworthy environmental monitoring program; 2) What are the current pressures and stressors on your local environment; 3) What questions and concerns do you have about your environment?

The NWMO held a total of six “Workshop 2” environmental workshops, a combination of virtual and in-person, to follow up on what we heard from Workshop 1, and to present the draft Environmental Baseline Program Designs for environmental media and biodiversity to the public.

## REFERENCES

- AECL. 1994. Environmental Impact Statement on the concept for disposal of Canada's nuclear fuel waste. Atomic Energy of Canada Limited Report AECL-10711, COG-93-1. Chalk River, Canada.
- Al, T., I. Clark, L. Kennell, M. Jensen and K. Raven. 2015. Geochemical evolution and residence time of porewater in low-permeability rock of the Michigan Basin, Southwest Ontario. *Chemical Geology*, 404, 1-17.
- Al-Aasm, I.S. and R. Crowe. 2018. Fluid compartmentalization and dolomitization in the Cambrian and Ordovician successions of the Huron Domain, Michigan Basin. *Marine and Petroleum Geology*, 92, 160-178.
- Alcorn, C.D., J.S. Cox, L. Applegarth and P. Tremaine. 2019. Investigation of uranyl sulfate complexation under hydrothermal conditions by quantitative Raman spectroscopy and density functional theory, *J. Physical Chemistry B* 123, 7385-7409.
- Altmaier, M., V. Brendler, C. Bube, V. Neck, C. Marquardt, H.C. Moog, A. Richter, T. Schrage, W. Voigt, S. Wilhelm, T. Willms and G. Wollmann. 2011. THEREDA Thermodynamische Referenz-Datenbasis. Abschlussbericht (dt. Vollversion).
- Andersson, P., K. Beaugelin-Seiller, N.A. Beresford, D. Copplestone, C. Della Vedova, J. Garnier-Laplace, B. J. Howard, P. Howe, D.H. Oughton, C. Wells, P. Whitehouse. 2008. Deliverable 5: Numerical benchmarks for protecting biota from radiation in the environment: proposed levels, underlying reasoning and recommendations. PROTECT. Stockholm, Sweden.
- Armand, G., F. Bumbieler, N. Conil, R. de la Vaissière, J.-M. Bosgiraud and M.-N. Vu. 2017. Main outcomes from in-situ thermo-hydro-mechanical experiments programme to demonstrate feasibility of radioactive high-level waste disposal in the Callovo-Oxfordian claystone. *J. Rock Mech. Geotech. Eng.* 9, 415-427.
- Aquanty Inc. 2018. HydroGeoSphere User Manual, Aquanty Inc., Waterloo, Canada.
- Barton N, 1982. Modelling rock joint behavior from in-situ block tests: implications for nuclear waste repository design. Vol. 308 Office of Nuclear Waste Isolation, Battelle Project Management Division.
- Bastola, S., L. Fava and M. Cai. 2015. Validation of MoFrac 2.0 using the Äspö dataset. Nuclear Waste Management Organization Report NWMO TR-2015-25. Toronto, Canada.
- Birkholzer, J.T., C.F. Tsang, A.E. Bond, J.A. Hudson, L. Jing and O. Stephansson. 25 years of DECOVALEX - scientific advances and lessons learned from an international research collaboration in coupled subsurface processes. *Int J Rock Mech Min Sci.* 2019; 122: 103995.

- Blain-Coallier A (2020) Surface permeability mapping of Stanstead and Lac du Bonnet granite, MEng Thesis, McGill University.
- Breach, P., J. Kelly and S. Capstick. 2020. Climate Change Impacts on Climate Variables for a Deep Geological Repository (South Bruce Study Area). Nuclear Waste Management Organization Report NWMO-TR-2020-09. Toronto, Canada.
- Briggs, S., C. Lilja and F. King. 2020. Probabilistic model for pitting of copper canisters. *Materials and Corrosion*, 72(1-2). doi.org/10.1002/maco.202011784
- Cadieux C., S. Morfin, G. Maldonado Sanchez and T. Al. 2020. Diffusion and Ion-Exchange Properties for Conservative and Non-Conservative Ions in Granite: An X-Ray Radiography Method. Presented at the 2020 Goldschmidt Conference, <https://doi.org/10.46427/gold2020.301>
- Carter, T.R., F.R. Brunton, J.K. Clark, L. Fortner, C. Freckelton, C.E. Logan, H.A.J. Russell, M. Somers, L. Sutherland, and K.H. Yeung. 2019. A three-dimensional geological model of the Paleozoic bedrock of southern Ontario; Geological Survey of Canada, Open File 8618, <https://doi.org/10.4095/315045>, Ontario Geological Survey, Groundwater Resources Study 19.
- Carter, T.R., C.E. Logan, J.K. Clark, H.A.J. Russell, F.R. Brunton, A. Cachunjua, M. D'Arienzo, C. Freckelton, H. Ryzyszczak, S. Sun, and K.H. Yeung. (in press). A three-dimensional geological model of the Paleozoic bedrock of southern Ontario—version 2, Geological Survey of Canada, Open File 8795.
- Chen, J., M. Behazin, J. Binns, K. Birch, A. Blyth, A. Boyer, S. Briggs, J. Freire-Canosa, G. Cheema, R. Crowe, D. Doyle, J. Giallonardo, M. Gobien, R. Guo, M. Hobbs, M. Ion, J. Jacyk, H. Kasani, P. Keech, E. Kremer, C. Lawrence, A. Lee, H. Leung, K. Liberda, T. Liyanage, C. Medri, M. Mielcarek, L. Kennell-Morrison, A. Murchison, N. Naserifard, A. Parmenter, M. Sanchez-Rico Castejon, U. Stahmer, Y. Sui, E. Sykes, M. Sykes, T. Yang, X. Zhang. 2019. Technical Program for Long-Term Management of Canada's Used Nuclear Fuel - Annual Report 2019. Nuclear Waste Management Organization Report NWMO-TR-2020-01. Toronto, Canada.
- Chen, J.D., A.H. Kerr, E.A. Hildebrandt, E.L. Bialas, H.G. Delany, K.M. Wasywich, and C.R. Frost. 1989. Radiochemical Analysis of CANDU Used Fuel Stored in Concrete Canisters in Moist Air at 150°C. Proceedings Second International Conference on CANDU Fuel. pp. 337 – 351. Pembroke, Canada, October 1-5, 1989 (Also available at <https://inis.iaea.org>).
- Chen, J.D., P.A. Seeley, R. Taylor, D.C. Hartrick, N.L. Pshhyshlak, K.H. Wasywich, A. Rochon and K.I. Burns. 1986. Characterization of Corrosion Deposits and the Assessment of Fission Products Released from Used CANDU Fuel. Proceedings 2<sup>nd</sup> International Conference on Radioactive Waste Management. Winnipeg, Canada, 7-11 September 1986. Canadian Nuclear Society, Canada.

- Clark, I.D., T. Al, M. Jensen, L. Kennell, M. Mazurek, R. Mohapatra and K. Raven. 2013. Paleozoic-aged brine and authigenic helium preserved in an Ordovician shale aquiclude. *Geology*, 41, 9, 951-954.
- CNSC. 2018. Assessing the Long-Term Safety of Radioactive Waste Management. Canadian Nuclear Safety Commission Regulatory Document CNSC REGDOC-2.11.1 Volume III, Ottawa, Canada.
- CSA. 2003. Guidelines for Calculating Radiation Doses to the Public from a Release of Airborne Radioactive Material under Hypothetical Accident Conditions in Nuclear Reactors. Canadian Standards Association CSA N288.2-M91. Toronto, Canada.
- CSA. 2008. Guidelines for Calculating Derived Release Limits for Radioactive Material in Airborne and Liquid Effluents for Normal Operation of Nuclear Facilities. Canadian Standards Association CSA Guideline N288.1-08. Toronto, Canada.
- CSA. 2014. Guidelines for Calculating the Radiological Consequences to the Public of a Release of Airborne Radioactive Material for Nuclear Reactor Accidents. Canadian Standards Association CSA N288.1-14. Toronto, Canada.
- CSA. 2016. Quality assurance of analytical, scientific and design computer programs. Canadian Standards Association CSA N286.7-16, Toronto, Canada.
- Darcel C., P. Davy, R. Le Goc and D. Mas Ivars. 2018. Rock mass effective properties from a DFN approach. Proceedings of 2<sup>nd</sup> International Discrete Fracture Network Engineering Conference, Seattle, USA, June 20-22, 2018. American Rock Mechanics Association.
- Davy P, C. Darcel, R. Le Goc, and D. Mas Ivars. 2018. Elastic properties of fractured rock masses with frictional properties and power - law fracture size distributions. *Journal of Geophysical Research: Solid Earth*. Volume 123, p. 6521 – 6539. doi:10.1029/2017JB015329
- Diederichs, M., and Day, J. 2020. Sensitivity of long term EDZ development, around deep geological repositories, to internal structure of argillaceous limestones. Proceedings of ARMA, 2020. Golden.
- Engel K., S. Coyotzi, M.A. Vachon, J.R. McKelvie and J.D. Neufeld. 2019a. Validating DNA Extraction Protocols for Bentonite Clay. *mSphere* 4(5). doi: 10.1128/mSphere.00334-19.
- Engel K., S. Ford, S. Coyotzi, J. McKelvie, N. Diomidis, G. Slater and J. Neufeld. 2019b. Stability of Microbial Community Profiles Associated with Compacted Bentonite from the Grimsel Underground Research Laboratory. *mSphere*, 4(6). doi: 10.1128/msphere.00601-19.

- Esmaili K., J. Hadjigeorgiou and M. Grenon. 2010. Estimating geometrical and mechanical REV based on synthetic rock mass models at Brunswick Mine. *International Journal of Rock Mechanics and Mining Sciences*. Volume 47, issue 6, p. 915-926
- Farahmand, K. and Diederichs, M.S. 2020. Calibration of the Coupled Hydro-Mechanical Properties of the Grain-Based Model for Simulating Fracture Process and Associated Pore Pressure Evolution in the Excavation Damage Zone (EDZ) Around Deep Tunnels. *Journal of Rock Mechanics and Geotechnical Engineering* 13(1). P60-83 DOI: 10.1016/j.jrmge.2020.06.006
- Forbes, B., N. Vlachopoulos, M.S. Diederichs and J. Aubertin. 2020a. Augmenting the in-situ rock bolt pull test with distributed optical fiber strain sensing. *Inter J Rock Mechanics and Mining Sciences*, 126. doi:10.1016/j.ijrmms.2019.104202
- Forbes, B., Vlachopoulos, N., Diederichs, M.S., Hyett, A.J., Punkkinen, A.P. 2020b. An in-situ monitoring campaign of a hard rock pillar at great depth within a Canadian mine. *Journal of Rock Mechanics and Geotechnical Engineering*. V12(3) p427-448. DOI:10.1016/j.jrmge.2019.07.018
- Fernandes, S., K. Woolhouse and N. Thackeray. 2019. Supplementary Non-Radiological Interim Acceptance Criteria for the Protection of Persons and the Environment. Nuclear Waste Management Organization Report NWMO-TR-2017-05. Toronto, Canada.
- Fransson Å, 2009. Literature survey: Relations between stress change, deformation and transmissivity for fractures and deformation zones based on in-situ investigations. SKB R-09-13, Svensk Kärnbränslehantering AB.
- Garnier-Laplace, J., R. Gilbin, A. Agüero, F. Alonzo, M. Björk, Ph. Ciffroy, D. Copplestone, M. Gilek, T. Hertel-Aas, A. Jaworska, C-M. Larsson, D. Oughton and I. Zinger. 2006. Deliverable 5: Derivation of Predicted-No-Effect-Dose-Rate values for ecosystems (and their sub-organisational levels) exposure to radioactive substances. ERICA.
- Gobien, M. and M. Ion. 2020. Nuclear Fuel Waste Projections in Canada – 2020 Update. Nuclear Waste Management Organization Report NWMO-TR-2020-06. Toronto, Canada
- Gobien, M. and C. Medri. ISM v1.0 Theory Manual. Nuclear Waste Management Organization Report NWMO-TR-2019-06. Toronto, Canada.
- Goguen, F., A. Walker, J. Racette, J. Riddoch, S. Nagasaki. 2020. Sorption of Pd on illite, MX-80 bentonite and shale in Na–Ca–Cl solutions. *Nuclear Engineering and Technology*. doi: 10.1016/j.net.2020.09.001.
- Grenthe, I., X. Gaona, A.V. Plyasunov, L. Rao, W.H. Runde, B. Grambow, R.J.M. Konings, A.L. Smith and E.E. Moore. 2020. Second Update on the Chemical Thermodynamics of Uranium, Neptunium, Plutonium, Americium and Technetium. Vol 14. OECD Nuclear Energy Agency Data Bank, Eds., OECD Publications, Paris, France.

- Grenthe, I., J. Fuger, R.J.M. Konings, R.J. Lemire, A.B. Muller, C. Nguyen-Trung and H. Wanner. 1992. *Chemical Thermodynamics of Uranium*. New York: Elsevier Science Publishers.
- Guerreiro, B., P Vo, D Poirier, J-G Legoux, X Zhang and J Giallonardo. 2020. Factors affecting the ductility of cold-sprayed copper coatings. *J Therm Spray Tech* 29, 630-641.
- Guo M., J Chen, C Lilja, V Dehnavi, M Behazin, JJ Noel, DW Shoesmith. 2020a. The anodic formation of sulfide and oxide films on copper in borate-buffered aqueous chloride solutions containing sulfide. *Electrochimica Acta*, 362, #137087. doi.org/10.1016/j.electacta.2020.137087
- Guo, M., Chen J., Martino T., Lilja C, Johansson A. J., Behazin M., Binns W. J, Keech P. G., Noël J. J., Shoesmith D.W. 2020b. The nature of the copper sulphide film grown on copper in aqueous sulphide and chloride solutions. *Mater. Corr.* 72(1-2), 300-307.
- Guo, R. 2017. Thermal response of a Canadian conceptual deep geological repository in crystalline rock and a method to correct the influence of the near-field adiabatic boundary condition. *Engineering Geology* 218 (2017) 50-62.
- Guo, R. 2020. Influence of the interval length of hydraulic packer systems on the thermally-induced pore pressure measurement in rock. *International Journal of Rock Mechanics and Mining Sciences* 135 (2020) 104500.
- Guo R., Thatcher KE., Seyedi DM., Plúa C. 2020c. Calibration of the thermo-hydro-mechanical parameters of the Callovo-Oxfordian claystone and the modelling of the ALC experiment. *International Journal of Rock Mechanics and Mining Sciences* 132 (2020) 104351.
- Guo R., Xu H., Plúa C., Armand G. 2020d. Prediction of the thermal-hydraulic-mechanical response of a geological repository at large scale and sensitivity analyses. *International Journal of Rock Mechanics and Mining Sciences* 136 (2020) 104484.
- Hall, D. S., Standish, T. E., Behazin, M., & Keech, P. G. 2018. Corrosion of copper-coated used nuclear fuel containers due to oxygen trapped in a Canadian deep geological repository. *Corrosion Engineering, Science and Technology*, 53(4), 309–315. <https://doi.org/10.1080/1478422X.2018.1463009>
- Hall, D.S., Behazin, M., Binns, W.J., Keech, P.G. 2021. An evaluation of corrosion processes affecting copper-coated nuclear waste containers in a deep geological repository. *Prog. Mater. Sci.* 118, 100766.
- Harper, J., T. Meierbachtol, N. Humphrey, J. Saito and A. Stansberry. 2020 - *submitted*. Generation and Fate of Basal Meltwater During Winter, Western Greenland Ice Sheet. Submitted to *The Cryosphere*.
- Harthong B, Scholtès L, Donzé F-V, 2012. Strength characterization of rock masses, using a coupled DEM–DFN model. *Geophysical Journal International*. Volume 191, issue 2, p. 467-480. doi:10.1111/j.1365-246X.2012.05642.x

- Health Canada. 2010. Part IV Guidance on Human Health Detailed Quantitative Radiological Risk Assessment. Ottawa, Canada.
- Heckman, K. and J. Edward. 2020. Radionuclide Inventory for Reference CANDU Fuel Bundles. Nuclear Waste Management Organization Report NWMO-TR-2020-05. Toronto, Canada.
- Hedin, A., Johansson, A.J., Lilja, C., Boman, M., Berastegui, P., Berger, R. and Ottosson, M., 2018. Corrosion of copper in pure O<sub>2</sub>-free water? Corrosion Science. 137, pp.1-12.
- Hegger, S., Diederichs, M., Vlachopoulos, N. 2020a. Laboratory investigation of distributed fibre optic strain sensing to measure strain distribution of rock samples during uniaxial compression testing. Proceedings of EUROCK 2020. Trondheim.
- Hegger, S., Diederichs, M., Vlachopoulos, N. 2020b. Utilizing distributed fiber optic strain sensing to measure strain heterogeneity of nodular limestones during UCS testing. Proceedings of ARMA, 2020. Golden
- Hökmark H, Lönnqvist M, Fälth B, 2010. THM-issues in repository rock. Thermal, mechanical, thermo-mechanical and hydro-mechanical evolution of the rock at the Forsmark and Laxemar sites. SKB TR-10-23, Svensk Kärnbränslehantering AB.
- IAEA. 2003. "Reference Biospheres" for Solid Radioactive Waste Disposal. International Atomic Energy BIOMASS-6. Vienna, Austria.
- IAEA. 2006. Safety Requirements: Geological Disposal of Radioactive Waste. International Atomic Energy Agency Safety Requirements WS-R-4. Vienna, Austria.
- IAEA. 2020. Development of a Common Framework for Addressing Climate and Environmental Change in Post-closure Radiological Assessment of Solid Radioactive Waste Disposal. International Atomic Energy BIOMASS-6. IAEA-TECDOC-1904. Vienna, Austria
- ICRP. 2007. The 2007 Recommendations of the International Commission on Radiological Protection. International Commission on Radiological Protection Publication 103, Annals of the ICRP (W2-4). Vienna, Austria.
- ICRP. 2008. Environmental Protection: the Concept and Use of Reference Animals and Plants. ICRP Publication 108. Vienna, Austria.
- ICRP. 2013. Radiological Protection in Geological Disposal of Long-lived Solid Radioactive Waste. International Commission on Radiological Protection Publication 122, Annals of the ICRP 42(3). Vienna, Austria.
- Innocente, J., Diederichs, M., Paraskevopoulou, C., Aubertin, J. 2020. Numerical investigation of the applicability of time-dependent models. Proceedings of EUROCK 2020. Trondheim.

- INL. 2005. Damaged Spent Fuel at U.S. DOE Facilities, Experience and Lessons Learned. Idaho National Laboratory Report INL/EXT-05-00760. Idaho, USA.
- ITASCA. 2015. Long-Term Stability Analysis of APM Conceptual Design in Sedimentary and Crystalline Rock Settings. Itasca Consulting Group, Inc. report for NWMO. Nuclear Waste Management Organization Technical Report NWMO-TR-2015-27, Toronto, Canada.
- Jaquenoud, M., T.E. William, T. Grundl, T. Gimmi, A. Jakob, S. Schefer, V. Cloet, P. De Canniere, L. R. Van Loon and O.X. Leupin. 2021. In-situ X-ray fluorescence to investigate iodide diffusion in opalinus clay: Demonstration of a novel experimental approach, *Chemosphere* 269, 128674.
- Junkin, W., L. Fava, M. Cai, E. Ben Awuah. 2020. Using DFN models to improve ground control through wedge identification and hazard mapping. Extended abstract, geoconvention, May 11-13, Calgary, Canada.
- Junkin, W., E. Ben-Awuah and L. Fava. 2019a. DFN variability analysis through voxelization. Proc. ARMA 2019, 53<sup>rd</sup> US Rock Mechanics/Geomechanics Symposium, New York, USA.
- Junkin, W., E. Ben-Awuah and L. Fava. 2019b. Incorporating DFN analysis in rock engineering systems blast fragmentation models. Proc. ARMA 2019, 53<sup>rd</sup> US Rock Mechanics/Geomechanics Symposium, New York, USA.
- Junkin, W., L. Fava, E. Ben-Awuah and R.M. Srivastava. 2018. Analysis of MoFrac-generated deterministic and stochastic Discrete Fracture Network models. Proc. DFNE 2018, 2<sup>nd</sup> International Discrete Fracture Network Engineering Conference, Seattle, USA.
- Junkin W., D. Janeczek, S. Bastola, X. Wang, M. Cai, L. Fava, E. Sykes, R. Munier and R.M. Srivastava. 2017. Discrete Fracture Network generation for the Äspö TAS08 tunnel using MoFrac. Proc. ARMA 2017, 51<sup>st</sup> US Rock Mechanics/Geomechanics Symposium, San Francisco, USA.
- Jautzy, J., D. Petts, I. Clark, T. Al, R. Stern and M. Jensen. 2020. Diagenetic evolution of a sedimentary system (Michigan Basin): Insights from petrography and S-isotope micro-analysis of pyrite. *Chemical Geology* 541, 119580.
- Kachanov, M., 1987. Elastic solids with many cracks: a simple method of analysis. *International Journal of Solids and Structures*, 23(1), pp.23-43.
- Kanik, N.J. 2020. Impact of interlayer cation composition and strongly bound water on smectite  $\delta^2\text{H}$ , as determined by a modified TCEA method. M.Sc. Thesis, University of Western, Electronic Thesis and Dissertation Repository, 7472.
- Kremer, E.P., J.D. Avis, J. Chen, P.J. Gierszewski, M. Gobien, R. Guo and C.L.D. Medri. 2019. Postclosure Safety Assessment of a Canadian Used Fuel Repository. 4th Canadian

Conference on Nuclear Waste Management, Decommissioning and Environmental Restoration. Ottawa, Canada.

- Larsson J., M. Flansbjerg, N. Williams Portal, E. Johnson, F. Johansson and D. Mas Ivars. 2020. Geometrical quality assurance of rock joint replicas in shear tests – introductory analysis. ISRM International Symposium, EUROCK 2020, 14-19 June, Trondheim, Norway.
- Larsson, J. and Flansbjerg, M., 2020. An Approach to Compensate for the Influence of the System Normal Stiffness in CNS Direct Shear Tests. *Rock Mechanics and Rock Engineering*, 53(5), pp.2185-2199.
- Le Goc R., B. Pinier, C. Darcel, E. Lavoine, D. Doolaeghe, S. de Simone, P. Davy and J-R.D. Ph. 2019. Software platform for Discrete Fracture Network models. In: AGU Fall Meeting. Proceedings of AGU Fall Meeting, San Fransisco, CA, USA.
- Le Goc R., C. Darcel, P. Davy, M. Pierce and M.A. Brossault. 2014. Effective elastic properties of 3D fractured systems. Proceedings of Discrete Fracture Network Engineering, Vancouver, Canada, 2014.
- Le Goc R., P. Davy, and C. Darcel. 2015. Scaling effects on elastic properties of jointed rock mass. Proceedings of Eurock, Salzburg, Austria, 2015.
- Lemire, R.J., D.A. Palmer, P. Taylor and H. Schlenz. 2020. Chemical Thermodynamics of Iron, Part 2, Vol 13b. OECD Nuclear Energy Agency Data Bank, Eds., OECD Publications, Paris, France.
- Li, W., B. Yu, J. Tam, J.D. Giallonardo, D. Poirier, J.-G. Legoux, P. Lin, G. Palumbo and U. Erb. 2020. Microstructural Characterization of Copper Coatings in Development for Application to Used Nuclear Fuel Containers, *Journal of Nuclear Materials*. Vol. 532, p.152039.
- Liberda, K. 2020. Preliminary Radon Assessment for a Used Fuel Deep Geological Repository. Nuclear Waste Management Organization Report NWMO-TR-2019-09. Toronto, Canada.
- Lindborg, T., M.Thorne, E.Andersson, J.Becker, J.Brandefelt, T.Cabianca, M.Gunia, A.T.K.Ikonen, E.Johansson, V.Kangasniemi, U.Kautsky, G.Kirchner, R.Klos, R.Kowe, A.Kontula, P.Kupiainen, A.-M.Lahdenperä, N.S.Lord, D.J.Lunt, J.-O.Näslund, M.Nordén, S.Norris, D.Pérez-Sánchez, A.Proverbio, K.Riekki, A.Rübel, L.Sweeck, R.Walke, S.Xu, G.Smith, G.Pröhl. 2018. Climate change and landscape development in post-closure safety assessment of solid waste disposal: Results of an initiative of the IAEA. *Journal of Environmental Radioactivity*. 183: 41-83.
- Liu H-H, Rutqvist J, Zhou Q, Bodvarsson G S, 2004. Upscaling of normal stress-permeability relationships for fracture networks obeying fractional Levy motion. Elsevier Geo-Engineering Book Series Elsevier, Vol 2, 263-268. ISBN: 1571-9960.

- Liu L., S. Giger, D. Martin, R. Chalaturnyk and N. Deisman (2021 – *accepted 2020*): Stress and strain dependencies of shear modulus from pressuremeter tests in Opalinus Clay. In: Shear-Induced Pore Pressure Around Underground Excavations. *In: The 6<sup>th</sup> International Conference on Geotechnical and Geophysical Site Characterization*. Budapest.
- Liu, N., H. He, J.J Noël and D.W. Shoesmith. 2017a. The electrochemical study of Dy<sub>2</sub>O<sub>3</sub> doped UO<sub>2</sub> in slightly alkaline sodium carbonate/bicarbonate and phosphate solutions, *Electrochimica Acta* 235, 654-663.
- Liu, N., J. Kim, J. Lee, Y-S. Youn, J-G. Kim, J-Y. Kim, J.J Noël and D.W. Shoesmith. 2017b. Influence of Gd doping on the structure and electrochemical behavior of UO<sub>2</sub>, *Electrochimica Acta* 247, 496-504.
- Liu, N., Z. Qin, J.J Noël and D.W. Shoesmith. 2017c. Modelling the radiolytic corrosion of a-doped UO<sub>2</sub> and spent nuclear fuel, *Journal of Nuclear Materials* 494, 87-94.
- Liu, N., Z. Zhu, J.J Noël and D.W. Shoesmith. 2018. Corrosion of nuclear fuel inside a failed waste container, *Encyclopedia of Interfacial Chemistry*, 2018, 172–182.
- Liu, N., Z. Zhu, L. Wu, Z. Qin, J.J Noël and D.W. Shoesmith. 2019. Predicting radionuclide release rates from spent nuclear fuel inside a failed waste disposal container using a finite element model, *Corrosion Journal* 75, 302-308.
- Marty, N.C.M., P. Blanc, O. Bildstein, F. Claret, B. Cochepein, D. Su, E.C. Gaucher, D. Jacques, J.-E. Lartigue, K. U. Mayer, J.C.L Meeussen, I. Munier, I. Pointeau, S. Liu and C. Steefel. 2015. Benchmark for reactive transport codes in the context of complex cement/clay interactions, *Computational Geosciences, Special Issue on: Subsurface Environmental Simulation Benchmarks*, doi: 10.1007/s10596-014-9463-6.
- Mas Ivars D., M. Pierce, C. Darcel, J. Reyes-Montes, D. Potyondy, R.P. Young, and P.A. Cundall. 2010. The synthetic rock mass approach for jointed rock mass modelling. *International Journal of Rock Mechanics and Mining Sciences*. Volume 48, issue 2, p. 219-244. doi:10.1016/j.ijrmms.2010.11.014
- Mayer, K.U., E.O. Frind and D.W. Blowes. 2002. Multicomponent reactive transport modelling in variably saturated porous media using a generalized formulation for kinetically controlled reactions. *Water Resources Research* 38, 1174, doi: 10:1029/2001WR000862.
- Mayer, K.U. and K.T.B. MacQuarrie. 2010. Solution of the MoMaS reactive transport benchmark with MIN3P - Model formulation and simulation results, *Computational Geosciences* 14, 405-419, doi: 10.1007/s10596-009-9158-6.
- Medri, C. 2015. Non-radiological interim acceptance criteria for the protection of persons and the environment. Nuclear Waste Management Organization Report NWMO-TR-2015-03. Toronto, Canada.
- Min K-B. and L. Jing. 2003. Numerical determination of the equivalent elastic compliance tensor for fractured rock masses using the distinct element method. *International Journal of*

Rock Mechanics and Mining Sciences. Volume 40, issue 6, p. 795-816.  
doi:[http://dx.doi.org/10.1016/S1365-1609\(03\)00038-8](http://dx.doi.org/10.1016/S1365-1609(03)00038-8)

Mompeán, F.J and H. Wanner. 2003. The OECD Nuclear Energy Agency thermodynamic database project. *Radiochimica Acta*, 91: 617-622.

NEA. 2018. Metadata for Radioactive Waste Management. Report NEA# 7378. OECD Nuclear Energy Agency. Paris, France.

NEA. 2019a. Preservation of Records, Knowledge and Memory across Generations: Developing a Key Information File for a Radioactive Waste Repository. Report NEA#7377. OECD Nuclear Energy Agency. Paris, France.

NEA. 2019b. Preservation of Records, Knowledge and Memory (RK&M) across Generations: Compiling a Set of Essential Records for a Radioactive Waste Repository. Report NEA#7423. OECD Nuclear Energy Agency. Paris, France.

NEA. 2019c. Preservation of Records, Knowledge and Memory across Generations: Final Report. Report NEA#7421. OECD Nuclear Energy Agency. Paris, France.

NWMO. 2005. Choosing a Way Forward – The Future Management of Canada's Nuclear Fuel – Final Study. Toronto, Canada.

NWMO. 2010. Moving Forward Together: Process for Selecting a Site for Canada's Deep Geological Repository for Used Nuclear Fuel. Toronto. Canada.

NWMO. 2017. Postclosure Safety Assessment of a Used Fuel Repository in Crystalline Rock. Nuclear Waste Management Organization. NWMO-TR-2017-02. Toronto, Canada.

NWMO. 2018. Postclosure Safety Assessment of a Used Fuel Repository in Sedimentary Rock. Nuclear Waste Management Organization. NWMO-TR-2018-08. Toronto, Canada.

NWMO. 2019a. Implementing Adaptive Phased Management 2019-2023. Toronto, Canada.

NWMO. 2019b. RD 2019 – NWMO's Program for research and development for long term management of used nuclear fuel. Nuclear Waste Management Organization Report NWMO-TR-2019-18. Toronto, Canada.

OHN. 1994. The disposal of Canada's nuclear fuel waste: Preclosure assessment of a conceptual system. Ontario Hydro Nuclear Report N-03784-940010 (UFMED), COG-93-6. Toronto, Canada.

Packulak, TR., Ahmed Labeid, MT., Day, J.J., Diederichs, M.S. 2020. Data processing for joint normal and shear stiffness to eliminate influences of the surrounding rock and laboratory machine. ARMA, 2020. Golden

- Parmenter, A., L. Waffle and A. DesRoches. 2020. Bedrock Geology of the Revell Batholith and Surrounding Greenstone Belts. Nuclear Waste Management Organization Report NWMO-TR-2020-08. Toronto, Canada.
- Poulsen B., D. Adhikary, M. Elmoultie and A. Wilkins. 2015. Convergence of synthetic rock mass modelling and the Hoek–Brown strength criterion. *International Journal of Rock Mechanics and Mining Sciences*. Volume 80, p. 171-180
- Racette, J., A. Walker, T. Yang and S. Nagasaki. 2019. Sorption of Se(-II): Batch Sorption Experiments on Limestone and Multi-site Sorption Modelling on Illite and Montmorillonite. Proceedings of 39<sup>th</sup> Annual Conference of the Canadian Nuclear Society and 43<sup>rd</sup> Annual CNS/CAN Student Conference, Ottawa, Canada.
- Reijonen, H., T. Karvonen and J.L. Cormenzana. 2014. Preliminary ALARA dose assessment for three APM DGR concepts. Nuclear Waste Management Organization Report NWMO TR-2014-18. Toronto, Canada.
- Reijonen, H., J.L. Cormenzana and T. Karvonen. 2016. Preliminary hazard identification for the Mark II conceptual design. Nuclear Waste Management Organization Report NWMO-TR-2016-02. Toronto, Canada.
- Schardong, A., P. Breach, J. Kelly and S. Capstick. 2020. Climate Change Impacts on Climate Variables for a Deep Geological Repository (Ignace Study Area). Nuclear Waste Management Organization Report NWMO-TR-2020-04 R001. Toronto, Canada.
- Selvadurai, P.A. 2010. Permeability of Indiana limestone: experiments and theoretical concepts for interpretation of results. MEng Thesis, McGill University.
- Selvadurai, A.P.S. 2019a. A multi-phasic perspective of the intact permeability of the heterogeneous argillaceous Cobourg limestone, *Scientific Reports*, 9: 17388, <https://doi.org/10.1038/s41598-019-53343-7>.
- Selvadurai, A.P.S. 2019b The Biot coefficient for a low permeability heterogeneous limestone, *Continuum Mechanics and Thermodynamics*, 31: 939-953 [doi.org/10.1007/s00161-018-0653-7](https://doi.org/10.1007/s00161-018-0653-7).
- Selvadurai, A.P.S. 2020 (in press). On the poroelastic Biot coefficient for a granitic rock, *Geosciences*.
- Selvadurai, A.P.S., P.A. Selvadurai 2010. Surface permeability tests: Experiments and modelling for estimating effective permeability, *Proceedings of the Royal Society, Mathematical and Physical Sciences Series A*, 466: 2819-2846.
- Selvadurai, A.P.S., A. Blain-Coallier and PA Selvadurai. 2020. Estimates for the effective permeabilities of intact granite obtained from the eastern and western flanks of the Canadian Shield. *Minerals: Special Issue on Hydro-Mechanics of Crystalline Rocks*, 10(8):667.

- Selvadurai, A.P.S., S.M. Rezaei Niya. 2020. Effective thermal conductivity of an intact heterogeneous limestone, *Rock Mechanics and Geotechnical Engineering*, 12: 682-692, <https://doi.org/10.1016/j.jrmge.2020.04.001>
- Selvadurai, A.P.S., A.P. Suvorov. 2020. Influence of pore shape on the bulk modulus and the Biot coefficient of fluid-saturated porous rocks, *Scientific Reports*, 10:18959.
- Senior, N.A., Martino, T., Diomidis, N., Gaggiano, R., Binns, J., Keech, P. 2020a. The measurement of ultra low uniform corrosion rates, *Corros. Sci.* 176, 108913.
- Senior, N.A. Martino, T., Binns, J., Keech, P. 2020b. The anoxic behaviour of copper in the presence of chloride and sulphide. *Materials and Corrosion*. 72, 282-292.
- Senior, N.A., Newman, R.C., Artymowicz, D., Binns, W.J., Keech, P.G. and Hall, D.S., 2019. Communication—a method to measure extremely low corrosion rates of copper metal in anoxic aqueous media. *Journal of The Electrochemical Society*, 166(11), p.C3015.
- SKB. 2018. BIOMASS 2020: Interim report. Svensk Kärnbränslehantering AB. SKB R-18-02. Forsmark, Sweden.
- Smith, K. 2016. Update and Review of the IAEA BIOMASS-6 Reference Biosphere Methodology. Report of the first programme workshop. BIOPROTA, UK.
- Smith, K. 2017a. Update and Review of the IAEA BIOMASS Methodology. Report of the second workshop held in parallel with the first meeting of MORARIA II Working Group 6. BIOPROTA, UK.
- Smith, K. 2017b. Update and Review of the IAEA BIOMASS Methodology. Summary of the third workshop held in parallel with the first interim meeting of MORARIA II Working Group 6. BIOPROTA, UK.
- Snowdon, A, J. Sykes and S. Normani. 2020. Topography scale effects on groundwater-surface water exchange fluxes in a Canadian Shield setting. *J Hydrology*, 585 #124772. doi.org/10.1016/j.jhydrol.2020.124772
- Snowdon, A.P., S.D. Normani and J.F. Sykes. 2020 – *submitted*. Analysis of Crystalline Rock Permeability Versus Depth in a Canadian Precambrian Rock Setting. *Submitted to JGR Solid Earth*.
- Stroes-Gascoyne, S., C.J. Hamon, P. Maak and S. Russell. 2010. The effects of the physical properties of highly compacted smectitic clay (bentonite) on the culturability of indigenous microorganisms. *Appl. Clay Sci.* 47:155-162.
- Su, D., K.U. Mayer and K.T.B. MacQuarrie. 2020a. Numerical investigation of flow instabilities using fully unstructured discretization for variably saturated flow problems, *Advances in Water Resources*, 143:103673, <https://doi.org/10.1016/j.advwatres.2020.103673>

- Su, D., K. U. Mayer and K.T.B. MacQuarrie. 2020b. MIN3P-HPC: a high-performance unstructured grid code for subsurface flow and reactive transport simulation. *Mathematical Geosciences*. doi.org/10.1007/s11004-020-09898-7.
- Suzuki, S., Y. Ogawa, Y. Kitagawa, P.G. Keech, J. Giallonardo. 2020. Development of Copper–steel Composite Container for Geological Disposal Program of High–Level Radioactive Waste in Japan. *J Japan Inst. Copper*, 59:1-5.
- Tam, J., W. Li, B. Yu, D. Poirier, J.-G. Legoux, P. Lin, G. Palumbo, J.D. Giallonardo and U. Erb. 2020. Reducing Complex Microstructural Heterogeneity in Electrodeposited and Cold Sprayed Copper Coating Junctions. *Surface and Coatings Technology*. Vol. 404. p.126479.
- Tortola M., I.S. Al-Aasm and R Crowe. 2020. Diagenetic Pore Fluid Evolution and Dolomitization of the Silurian and Devonian Carbonates, Huron Domain of Southwestern Ontario: Petrographic, Geochemical and Fluid Inclusion Evidence. *Minerals* 2020, 10(2), 140; <https://doi.org/10.3390/min10020140>
- US DOE. 1994. Airborne release fractions/rates and respirable fractions for non-reactor nuclear facilities. U.S. Department of Energy DOE-HDBK-3010-94. USA.
- US DOE. 2007. Preparation of safety basis documents for transuranic waste facilities. U.S. Department of Energy, DOE-STD-5506-2007. USA.
- US DOE. 2009. Yucca Mountain Repository SAR. U.S. Department of Energy, DOE/RW-0573, Rev. 1. USA.
- Wilk, L. and G. Cantello. 2006. Used fuel burnups and power ratings for OPG owned used fuel. Ontario Power Generation Report 06819-REP-01300-10121. Toronto, Canada.
- Wilk, L. 2013. CANDU fuel burnup and power rating 2012 update. Nuclear Waste Management Organization Report NWMO TR-2013-02. Toronto, Canada.
- Vilks, P. 2011. Sorption of Selected Radionuclides on Sedimentary Rocks in Saline Conditions - Literature Review. Nuclear Waste Management Organization Report NWMO TR-2011-12, Toronto, Canada.
- Vilks, P. and T. Yang. 2018. Sorption of Selected Radionuclides on Sedimentary Rocks in Saline Conditions – Updated Sorption Values. Nuclear Waste Management Organization Technical Report NWMO-TR-2018-03, Toronto, Canada.
- Walker, A., J. Racette, J. Goguen and S. Nagasaki. 2018. Ionic Strength and pH Dependence of Sorption of Se(-II) onto Illite, Bentonite and Shale. Proceedings of 38th Annual Conference of the Canadian Nuclear Society and 42nd Annual CNS/CAN Student Conference, Saskatoon, SK, Canada, June 3-6, 2018.
- Wood. 2019. Climate Change Impacts Review and Method Development. NWMO-TR-2019-05. Toronto, Canada.

- Wren, J. C., et al. 2019. Radiation Induced Corrosion of Copper in Deep Geological Repositories – 19493. <https://www.osti.gov/biblio/23005367>.
- Wu, L., Guo, D., Li, M., Joseph, J. M., Noël, J. J., Keech, P. G., & Wren, J. C. 2017. Inverse crevice corrosion of carbon steel: Effect of solution volume to surface area. *Journal of the Electrochemical Society*, 164(9), C539–C553. <https://doi.org/10.1149/2.0511709jes>
- Wu, M, M. Behazin, J. Nam and P. Keech. 2019. Internal Corrosion of Used Fuel Container. Nuclear Waste Management Organization Report NWMO-TR-2019-02. Toronto, Canada.
- Xie, M., P. Rasouli, K.U. Mayer and K.T.B. MacQuarrie. 2014. Reactive Transport Modelling of Diffusion in Low Permeable Media – MIN3P-THcm Simulations of EBS TF-C Compacted Bentonite Diffusion Experiments. Nuclear Waste Management Organization Report NWMO TR-2014-23. Toronto, Canada.
- Xie, M., D. Su, K.U. Mayer and K.T.B. MacQuarrie. 2018. Reactive Transport Modelling Investigation of Elevated Dissolved Sulphide Concentrations in Sedimentary Basin Rocks. Nuclear Waste Management Organization Report NWMO-TR-2018-07, Toronto, Canada
- Zhu, Z., L. Wu, J.J Noël and D.W. Shoesmith. 2019. Anodic reactions occurring on simulated spent nuclear fuel (SIMFUEL) in hydrogen peroxide solutions containing bicarbonate/carbonate – The effect of fission products. *Electrochimica Acta* 320, 134546.
- Zhu, Z., J.J Noël, D.W. Shoesmith. 2020. Hydrogen peroxide decomposition on simulated spent nuclear fuel in bicarbonate/carbonate solutions. *Electrochimica Acta* 340, 135980.

**APPENDIX A: NWMO TECHNICAL REPORTS AND REFEREED JOURNAL ARTICLES**

## A.1 NWMO TECHNICAL REPORTS

Breach, P., J. Kelly and S. Capstick. 2020. Climate Change Impacts on Climate Variables for a Deep Geological Repository (South Bruce Study Area). Nuclear Waste Management Organization Report NWMO-TR-2020-09. Toronto, Canada.

Chen, J., M. Behazin, J. Binns, K. Birch, A. Blyth, A. Boyer, S. Briggs, J. Freire-Canosa, G. Cheema, R. Crowe, D. Doyle, J. Giallonardo, M. Gobien, R. Guo, M. Hobbs, M. Ion, J. Jacyk, H. Kasani, P. Keech, E. Kremer, C. Lawrence, A. Lee, H. Leung, K. Liberda, T. Liyanage, C. Medri, M. Mielcarek, L. Kennell-Morrison, A. Murchison, N. Naserifard, A. Parmenter, M. Sanchez-Rico Castejon, U. Stahmer, Y. Sui, E. Sykes, M. Sykes, T. Yang, X. Zhang. 2019. Technical Program for Long-Term Management of Canada's Used Nuclear Fuel - Annual Report 2019. Nuclear Waste Management Organization Report NWMO-TR-2020-01. Toronto, Canada.

Gobien, M. and M. Ion. 2020. Nuclear Fuel Waste Projections in Canada – 2020 Update. Nuclear Waste Management Organization Report NWMO-TR-2020-06. Toronto, Canada

Heckman, K. and J. Edward. 2020. Radionuclide Inventory for Reference CANDU Fuel Bundles. Nuclear Waste Management Organization Report NWMO-TR-2020-05. Toronto, Canada.

Liberda, K. 2020. Preliminary Radon Assessment for a Used Fuel Deep Geological Repository. Nuclear Waste Management Organization Report NWMO-TR-2019-09. Toronto, Canada.

Parmenter, A., L. Waffle and A. DesRoches. 2020. Bedrock Geology of the Revell Batholith and Surrounding Greenstone Belts. Nuclear Waste Management Organization Report NWMO-TR-2020-08. Toronto, Canada.

Schardong, A., P. Breach, J. Kelly and S. Capstick. 2020. Climate Change Impacts on Climate Variables for a Deep Geological Repository (Ignace Study Area). Nuclear Waste Management Organization Report NWMO-TR-2020-04 R001. Toronto, Canada

## A.2 REFEREED JOURNAL ARTICLES

- Briggs, S., C. Lilja and F. King. 2020. Probabilistic model for pitting of copper canisters. *Materials and Corrosion*, 72(1-2). doi.org/10.1002/maco.202011784
- Farahmand, K. and Diederichs, M.S. 2020. Calibration of the Coupled Hydro-Mechanical Properties of the Grain-Based Model for Simulating Fracture Process and Associated Pore Pressure Evolution in the Excavation Damage Zone (EDZ) Around Deep Tunnels. *Journal of Rock Mechanics and Geotechnical Engineering* 13(1). P60-83 DOI: 10.1016/j.jrmge.2020.06.006
- Forbes, B., N. Vlachopoulos, M.S. Diederichs and J. Aubertin. 2020a. Augmenting the in-situ rock bolt pull test with distributed optical fiber strain sensing. *Inter J Rock Mechanics and Mining Sciences*, 126. doi:10.1016/j.ijrmms.2019.104202
- Forbes, B., Vlachopoulos, N., Diederichs, M.S., Hyett, A.J., Punkkinen, A.P. 2020b. An in-situ monitoring campaign of a hard rock pillar at great depth within a Canadian mine. *Journal of Rock Mechanics and Geotechnical Engineering*. V12(3) p427-448. DOI:10.1016/j.jrmge.2019.07.018
- Goguen, F., A. Walker, J. Racette, J. Riddoch, S. Nagasaki. 2020. Sorption of Pd on illite, MX-80 bentonite and shale in Na–Ca–Cl solutions. *Nuclear Engineering and Technology*. doi: 10.1016/j.net.2020.09.001.
- Guerreiro, B., P Vo, D Poirier, J-G Legoux, X Zhang and J Giallonardo. 2020. Factors affecting the ductility of cold-sprayed copper coatings. *J Therm Spary Tech* 29, 630-641.
- Guo M., J Chen, C Lilja, V Dehnavi, M Behazin, JJ Noel, DW Shoesmith. 2020a. The anodic formation of sulfide and oxide films on copper in borate-buffered aqueous chloride solutions containing sulfide. *Electrochimica Acta*, 362, #137087. doi.org/10.1016/j.electacta.2020.137087
- Guo, M., Chen J., Martino T., Lilja C, Johansson A. J., Behazin M., Binns W. J, Keech P. G., Noël J. J., Shoesmith D.W. 2020b. The nature of the copper sulphide film grown on copper in aqueous sulphide and chloride solutions. *Mater. Corr.* 72(1-2), 300-307.
- Guo, R. 2020. Influence of the interval length of hydraulic packer systems on the thermally-induced pore pressure measurement in rock. *International Journal of Rock Mechanics and Mining Sciences* 135 (2020) 104500.
- Guo R., Thatcher KE., Seyedi DM., Plúa C. 2020c. Calibration of the thermo-hydro-mechanical parameters of the Callovo-Oxfordian claystone and the modelling of the ALC experiment. *International Journal of Rock Mechanics and Mining Sciences* 132 (2020) 104351.
- Guo R., Xu H., Plúa C., Armand G. 2020d. Prediction of the thermal-hydraulic-mechanical response of a geological repository at large scale and sensitivity analyses. *International Journal of Rock Mechanics and Mining Sciences* 136 (2020) 104484.

- Järvine, A.K., A.G. Murchison, P.G. Keech, M.D. Pandey. 2020. A Probabilistic Model for Estimating the Life Expectancy of Used Nuclear Fuel Containers in a Canadian Geological Repository: Effects of Latent Defects and Repository Temperature. *Nuclear Technology*, 7:1036-1058.
- Keech, P.G., Behazin, M., Binns, W.J., Briggs, S. 2020. An update on the copper corrosion program for the long-term management of used nuclear fuel in Canada. *Materials and Corrosion*, DOI: 10.1002/maco.202011763.
- Li W., Yu B., Tam J., Giallonardo J. D., Doyle D., Poirier D., Legoux J. G., Lin P., Palumbo G., Erb U. 2020. Microstructural Characterization of Copper Coatings in Development for Application to used Nuclear Fuel Containers. *J. of Nuclear Materials*. 532(15):152039.
- Martino, T., J. Chen, J.J. Noël, D.W. Shoesmith, 2020. The effect of anions on the anodic formation of copper sulphide films on copper. *Electrochim. Acta*, 331:135319.
- Selvadurai, A.P.S., A. Blain-Coallier and PA Selvadurai. 2020. Estimates for the effective permeabilities of intact granite obtained from the eastern and western flanks of the Canadian Shield. *Minerals: Special Issue on Hydro-Mechanics of Crystalline Rocks*, 10(8):667.
- Selvadurai, A.P.S., S.M. Rezaei Niya. 2020. Effective thermal conductivity of an intact heterogeneous limestone, *Rock Mechanics and Geotechnical Engineering*, 12: 682-692, <https://doi.org/10.1016/j.jrmge.2020.04.001>
- Selvadurai, A.P.S., A.P. Suvorov. 2020. Influence of pore shape on the bulk modulus and the Biot coefficient of fluid-saturated porous rocks, *Scientific Reports*,10:18959.
- Senior, N.A., Martino, T., Diomidis, N., Gaggiano, R., Binns, J., Keech, P. 2020. The measurement of ultra low uniform corrosion rates. *Corros. Sci.* 176, 108913.
- Senior, N.A. Martino, T., Binns, J., Keech, P. 2020. The anoxic behaviour of copper in the presence of chloride and sulphide. *Materials and Corrosion*. 72, 282-292.
- Snowdon, A, J. Sykes and S. Normani. 2020. Topography scale effects on groundwater-surface water exchange fluxes in a Canadian Shield setting. *J Hydrology*, 585 #124772. [doi.org/10.1016/j.jhydrol.2020.124772](https://doi.org/10.1016/j.jhydrol.2020.124772)
- Su, D., K.U. Mayer and K.T.B. MacQuarrie. 2020a. Numerical investigation of flow instabilities using fully unstructured discretization for variably saturated flow problems, *Advances in Water Resources*, 143:103673, <https://doi.org/10.1016/j.advwatres.2020.103673>
- Su, D., K. U. Mayer and K.T.B. MacQuarrie. 2020b. MIN3P-HPC: a high-performance unstructured grid code for subsurface flow and reactive transport simulation. *Mathematical Geosciences*. [doi.org/10.1007/s11004-020-09898-7](https://doi.org/10.1007/s11004-020-09898-7).
- Suzuki, S., Y. Ogawa, Y. Kitagawa, P.G. Keech, J. Giallonardo. 2020. Development of Copper–steel Composite Container for Geological Disposal Program of High–Level Radioactive Waste in Japan. *J Japan Inst. Copper*, 59:1-5.

- Tam, J., W. Li, B. Yu, D. Poirier, J.-G. Legoux, P. Lin, G. Palumbo, J.D. Giallonardo and U. Erb. 2020 Reducing Complex Microstructural Heterogeneity in Electrodeposited and Cold Sprayed Copper Coating Junctions. *Surface and Coatings Technology*. Vol. 404. p.126479.
- Tortola M., I.S. Al-Aasm and R Crowe. 2020. Diagenetic Pore Fluid Evolution and Dolomitization of the Silurian and Devonian Carbonates, Huron Domain of Southwestern Ontario: Petrographic, Geochemical and Fluid Inclusion Evidence. *Minerals* 2020, 10(2), 140; <https://doi.org/10.3390/min10020140>
- Zhu, Z., J.J Noël, D.W. Shoesmith. 2020. Hydrogen peroxide decomposition on simulated spent nuclear fuel in bicarbonate/carbonate solutions. *Electrochimica Acta* 340, 135980.